Technoeconomic Analysis : Green hydrogen production by integrating Concentrated Solar Power (CSP) & Solid Oxide Electrolyzer (SOE)

Master Thesis by
Narendran Srinivasakannan (5503248)
Delft University of Technology

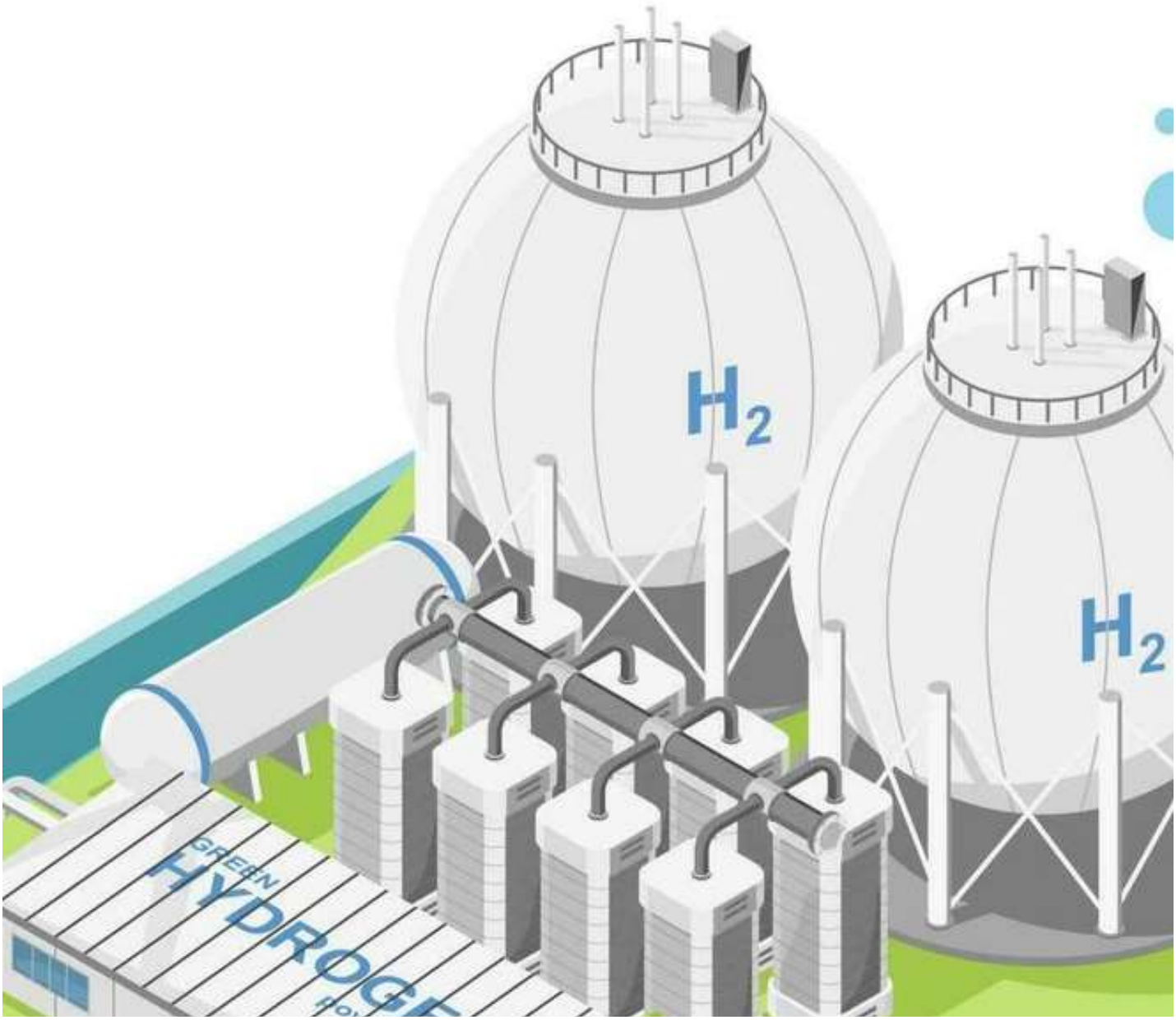

Techno-Economic Analysis: Green Hydrogen Production by Integrating Concentrated Solar Power (CSP) & Solid Oxide Electrolyzer (SOE)

By

Narendran Srinivasakannan

TU Delft Supervisor	Dr. Mahinder Ramdin
Shell Supervisor	Dr. Srikanth Santhanam, Ir. Omkar Sane
Project Duration	December,2022 – July,2023
Date of Defense	July-31-2023
MSc. Degree	Mechanical Engineering
Faculty	3ME - EFPT
University	Delft University of Technology

Contents

1 Background **11**
- 1.1 What is Green hydrogen? . . . 12
  - 1.1.1 Drivers for the green hydrogen uptake . . . 12
  - 1.1.2 Barriers for Green Hydrogen Uptake . . . 13
- 1.2 The way forward for green hydrogen . . . 13
- 1.3 Why CSP and SOEC over other technologies? . . . 13
- 1.4 Research Objective . . . 14

2 Literature Study **15**
- 2.1 History of Electrolysis . . . 15
- 2.2 Types of Electrolyzers . . . 15
- 2.3 Thermodynamics of Steam Electrolysis . . . 17
- 2.4 Fundamentals of CSP . . . 18
- 2.5 Types of CSP . . . 18
- 2.6 CSP - Technical Characteristics . . . 18
  - 2.6.1 Solar Parabolic Dish (SPD) . . . 19
  - 2.6.2 Parabolic Trough Collector (PTC) . . . 19
  - 2.6.3 Solar Power Tower (SPT) . . . 20
  - 2.6.4 Linear Fresnel Reflector (LFR) . . . 20
- 2.7 Status of the CSP . . . 21
- 2.8 Technology Selection for CSP . . . 23
- 2.9 Modelling of Systems . . . 24
- 2.10 Literature study on Solid Oxide Electrolyzer Models (SOE) . . . 25
- 2.11 Literature Study on Concentrated Solar Power (CSP) . . . 27
- 2.12 Literature Review on Integration of SOE and CSP . . . 29
- 2.13 Research gap and Thesis Outlining . . . 30

3 Conceptual process design **31**
- 3.1 Conceptual framework . . . 31
- 3.2 System level modelling . . . 32
  - 3.2.1 SOEC unit block modelling . . . 32
  - 3.2.2 CSP Unit block modelling . . . 34
  - 3.2.3 Unit block for the Combined CSP-SOE Plant . . . 37
- 3.3 Results & Discussions of the Conceptual Study . . . 38
  - 3.3.1 Identification of high impact parameters . . . 38
  - 3.3.2 Identification of suitable integration pathway . . . 38
  - 3.3.3 Effect of capacity factor on LCOH . . . 41
  - 3.3.4 Comparing the CSP-SOE system with other green hydrogen technologies . . . 43
  - 3.3.5 Analysing the system by incorporating a varying DNI profile . . . 43

4 Process Plant Design,Operation Economics **46**
- 4.1 Process Scope . . . 46
- 4.2 SOE Plant . . . 47
  - 4.2.1 SOE System Design . . . 47
  - 4.2.2 SOE Electrochemical Model, Aspen Implementation & Validation . . . 48
  - 4.2.3 SOE System - Full Load Operation . . . 52
  - 4.2.4 SOE system part load operation . . . 53

4.2.5 SOE System - Hot Standby Operation . . . 54
4.3 Hydrogen Processing Systems . . . 55
4.3.1 H2 Processing I/O Scheme . . . 55
4.3.2 Technology Selection . . . 56
4.4 Plant Operation . . . 59
4.4.1 Operation Strategy 1 - Full Load & Hot standby only . . . 60
4.4.2 Operation Strategy 2- Full Load & Part Load only . . . 61
4.4.3 Operation Strategy -3 : Full Load, Part Load Hot Standby . . . 62

5 Results & Discussion **63**
5.1 Strategy 1: Hot standby & Full Load . . . 63
5.2 Strategy - 2: Full Load & Part Load . . . 66
5.3 Strategy-3: Full Load, Part Load & Hot Standby . . . 68
5.4 Selection of suitable strategy . . . 70

6 Conclusion & Recommendations **72**
6.1 Conclusion . . . 72
6.2 Recommendations to Shell . . . 73

Preface

This thesis is the result of my pursuit of a master's degree in Mechanical Engineering at TU Delft. With a strong interest in the convergence of technology and economics, I aimed to undertake a research project that would explore not only the technical aspects but also the economic and commercial viability of a particular topic. Thus, I chose to conduct my thesis at Shell, where I had the opportunity to apply my process engineering skills.

The focus of this thesis lies in investigating the feasibility of integrating Concentrated Solar Power (CSP) and Solid Oxide Electrolyzer (SOE). In Chapter 2, the fundamentals of both SOE and CSP technologies are presented, offering the reader a comprehensive understanding of their workings. Chapter 3 encompasses a conceptual study designed to identify scenarios where this integration would make economic sense. Here, the methodology and results of the conceptual study are thoroughly discussed. Building upon the insights gained from the conceptual study, Chapter 4 delves into the development of a process plant design that meets the benchmarks established in the previous chapter. This chapter entails detailed modeling of the green hydrogen plant and explores different strategies to address intermittency issues associated with this integration.

The research presented in this thesis provides valuable insights into the conditions under which the integration of CSP and SOE becomes a viable alternative compared to existing green hydrogen technologies. Additionally, a comprehensive plant design, operational considerations, and economic analyses are provided. It is my hope that this work will contribute significantly to the growing body of research in the field of green hydrogen and expedite the transition towards sustainable energy sources.

I would like to express my gratitude to the Dr.Mahinder Ramdin from TU Delft for his guidance and support throughout this research endeavor. Furthermore, I extend my appreciation to Dr.Srikanth Santhanam and Ir.Omkar Sane from Shell for providing me with the opportunity to apply my knowledge and skills in a real-world setting. Lastly, I would like to extend my heartfelt gratitude to my parents for their unwavering support and motivation during the most challenging times. Their belief in my abilities has been the driving force behind the successful completion of my Master's program.

Abstract

This thesis presents a techno-economic analysis of integrating Concentrated Solar Power (CSP) and Solid Oxide Electrolysis (SOE) technologies for the production of hydrogen. The study begins with the development of system-level 0D models for CSP and SOE individually. These models are then combined to create a unified model for CSP-SOE integration.The Levelized Cost of Hydrogen (LCOH) is estimated and different modes of integration are explored, leading to the selection of off-grid integration as the preferred option. Sensitivity analyses are performed to assess the impact of various parameters on the system's performance, and preliminary estimates indicate that a power capacity of 195 MW for CSP and SOE is required to achieve the desired hydrogen production target. Based on the results of the basic sizing analysis, a detailed plant model is constructed, incorporating the SOE and hydrogen processing sections. The Aspen simulation software is utilized for the implementation of these sections.To address the intermittent nature of renewable energy sources, three different strategies are proposed for operating the SOE system. After careful evaluation, a strategy is selected that yields an LCOH of $4.1 per kilogram of hydrogen, with a best-case scenario of $3 per kilogram and a worst-case scenario of $5 per kilogram.

This study contributes to the understanding of the techno economic aspects of integrating CSP and SOE technologies for hydrogen production, highlighting the potential for achieving competitive costs and promoting the adoption of renewable energy-based hydrogen systems.

List of Figures

1.1 Global hydrogen demand expected to reach 210 Million tonnes by 2030 [1] 11
1.2 Green Hydrogen layout consisting of H_2O source, power source and electrolyzer stacks . . 12
1.3 Cost band of various H2 production technologies. 2050 targets require green hydrogen to match the price band of grey hydrogen.[6] 13

2.1 Technology readiness level (TRL) of different electrolyzer technologies. Solid Oxide Electrolyzer (SOE) as seen is still not as mature as Alkaline (ALK) and Proton Exchange Membrane (PEM) [9] 16
2.2 Temperature dependence of energy and voltage in electrolysis process 17
2.3 Different sections of CSP Plant 18
2.4 Concentrated Solar Power technologies and their share of commercial installations. As seen Parabolic trough have the highest no. of commercial installations and parabolic dish has the least installations. [14] 19
2.5 Concentrated Solar Power technologies and their corresponding range of LCOE values obtained from real existing plants 23
2.6 Different types of modelling as classified by [29] 24

3.1 Individual unit blocks for SOE and CSP 31
3.2 Individual unit blocks combined to give the unit block for the integrated plant 32
3.3 SOE unit block : Steam and electric power are the inputs this block resulting in production of Hydrogen & Oxygen. 32
3.4 CSP subsystems description. 3 important sections are solar energy collection, solar to thermal conversion and lastly thermal to electric conversion. 35
3.5 EPC costs for CSP with different hours of storage 36
3.6 Relationship between SM,LCOE and hours of storage as estimated by NREL 3.6 36
3.7 Sensitivity of different parameters to hydrogen costs. For CSP-SOE system the capacity factor and CSP specific CAPEX have the largest impact on economics 38
3.8 calculated LCOH values of all 3 pathways 39
3.9 LCOH sensitivity on range of CAPEX values predicted by NREL 40
3.10 Variation of different parameters as function of capacity factor 41
3.11 Comparing the current study with other green hydrogen technologies. CSP-SOE systems fare better in achieving high CF at low LCOH 43
3.12 DNI curve of Dhursar,India generated using SAM 44
3.13 Oversizing chart for systems with and without TES 44

4.1 Defined scope for the process plant design, the intake and output constraints for all three unit blocks are defined in this flow 47
4.2 Scale up of electrolyzers from cell to system and the orders of magnitude go from KW for SOE cells to MW for SOE system 47
4.3 SOE system design, an SOE system consists of electrolyzer and other equipments to satisfy the boundary constraints 48
4.4 SOE Reactor Implementation in Aspen 49
4.5 Aspen flow sheet for Hot standby mode 51
4.6 SOE System Implementation in Aspen 52
4.7 SOE Hot standby mode aspen implementation 54
4.8 Effect of Temperature, Air flow on Reactor Temperature 54
4.9 I/O scheme of H2 Processing system 55

4.10 First level separation of water from H2 stream . . . 55
4.11 Compression and purification in H2 processing scheme . . . 55
4.12 Compressor train implementation Aspen . . . 56
4.13 Selections for TSA . . . 57
4.14 Complete layout of the integrated CSP-SOE plant for hydrogen production . . . 58
4.15 Hourly DNI of Rajasthan,India . . . 59
4.16 Hour available energy production . . . 59
4.17 strategy 1 implementation for an example of DNI = 150 W/sq.m . . . 60
4.18 strategy 2 implementation for an example of DNI = 150 W/sq.m . . . 61
4.19 strategy 3 implementation for an example of DNI = 150 W/sq.m . . . 62

5.1 Power consumption of modules in different modes vs operating point . . . 63
5.2 Total power consumption of the system & power supply from CSP . . . 63
5.3 Power production from CSP plant with 10 hours of storage . . . 64
5.4 Allocation of modules into different operating modes . . . 64
5.5 Specific energy consumption of the system using strategy-1 . . . 65
5.6 LCOH when using strategy-1 . . . 65
5.7 Power consumption of modules in different modes vs operating point . . . 66
5.8 Total power consumption of the system & power supply from CSP . . . 66
5.9 Allocation of modules into different operating modes . . . 66
5.10 Specific energy consumption of the system using strategy-2 . . . 67
5.11 LCOH when using strategy-2 . . . 67
5.12 Power consumption of modules vs operation point . . . 68
5.13 Specific energy consumption using strategy-3 . . . 68
5.14 LCOH when using strategy-3 . . . 69
5.15 Allocation of modules into different operating modes . . . 69
5.16 Comparison of the strategies based on power consumption and SEC . . . 70
5.17 LCOH Sensitiviy towards changes in SOE CAPEX and CSP CAPEX . . . 71
5.18 Start up shutdown events of all 3 strategies . . . 71

List of Tables

1.1 Global Hydrogen Production Share . . . 11

2.1 Technical Characteristics of Electrolysers [10] . . . 16
2.2 Actual plant specifications of 20 of highest capacity installations . . . 22
2.3 Technology selection based on important CSP KPI . . . 23

3.1 List of assumptions made for SOE modelling . . . 33
3.2 Assumptions for CSP plant . . . 35
3.3 Detailed breakdown of the LCOH of all 3 pathways . . . 39
3.3 Detailed breakdown of the LCOH of all 3 pathways . . . 40
3.4 Different parameters as function of CF . . . 42
3.5 Comparison of systems with and without TES . . . 45

4.1 SOE System specifications . . . 48
4.2 Validation of Isothermal steam electrolysis condition . . . 50
4.3 Part Load operation validation results . . . 50
4.4 Validation results of hot standby mode . . . 51
4.5 SOE System full load specifications . . . 52
4.6 Part load system specifications . . . 53
4.7 Specifications of one compression train . . . 57
4.8 TSA Specifications . . . 57
4.9 Selection of suitable thermal energy storage . . . 58

5.1 LCOH when using strategy-1 . . . 65
5.2 LCOH when using strategy-2 . . . 67
5.3 LCOH when using strategy-3 . . . 69
5.4 LCOH of all 3 strategies . . . 70

Acronyms

ASR	Area Specific Resistance
AWE	Alkaline Water Electrolyzer
C	Capacity
CAPEX	Capital Expenditure
CF	Capacity Factor
CSP	Concentrated Solar Power
DHI	Direct Horizontal Irradiation
DNI	Direct Normal Irradiation
GHI	Global Horizontal Irradiation
IEA	International Energy Agency
IPCC	Intergovernmental Panel On Climate Change
LCOE	Levelized Cost Of Energy
LCOH	Levelized Cost of Hydrogen
LFR	Linear Fresnel Reflector
LHV	Lower Heating Value
OPEX	Operational Expenditure
P	Production
PB	Power Block
PEM	Proton Exchange Membrane
PTC	Parabolic Trough Collector
r	Rate of discounting
SH	Solar Heater
SM	Solar Multiple
SMR	Steam Methane Reforming
SOE	Solid Oxide Electrolyzer
SPD	Solar Parabolic Dish
SPT	Solar Power Tower
SR	Sweep gas Ratio
STEC	Specific Total Energy Consumption
STP	Standard Temperature & Pressure
t	Time
TES	Thermal Energy Storage
TRL	Technology Readiness Level
TSA	Temperature Swing Adsorption
U	Utilization
VRE	Variable Renewable Energy

Chapter 1

Background

Hydrogen is a versatile energy carrier used for plethora of purposes across various industrial domains. The demand for hydrogen is estimated to be 94 Million tonnes(Mt) in 2020 and is expected to grow up to 210Mt in the year 2030. The chart provided by IEA [1] well elucidates the demand for hydrogen across industries.

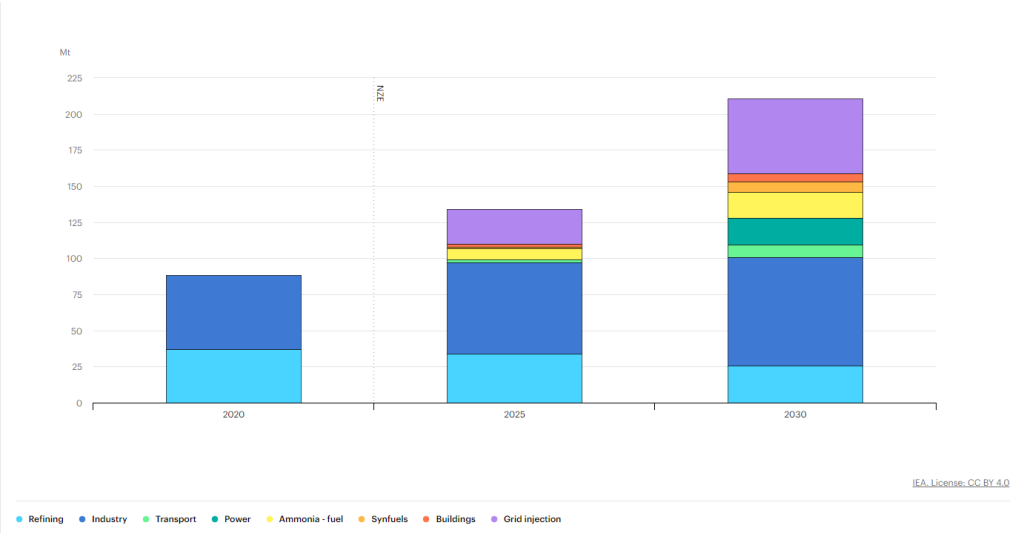

Figure 1.1: Global hydrogen demand expected to reach 210 Million tonnes by 2030 [1]

There are multiple hydrogen production technologies that contribute towards fulfilling the required demand. In order to indicate the scale of carbon emissions by these production methods, they are classified based on colours. Though there are different colours associated with hydrogen such as black hydrogen, white hydrogen, turquoise hydrogen not all the colour classifications are significant or commonly used. Grey, blue and green hydrogen have the most significance in today's hydrogen landscape. Steam Methane Reforming (SMR) is the most widely used process for hydrogen production and the hydrogen produced from this process is known as grey hydrogen. When the carbon produced via the grey hydrogen process is captured and stored instead of atmospheric release it is known as blue hydrogen. When electricity produced through renewable technologies is used to split the water via electrolysis to produce hydrogen, it is known as green hydrogen.

Table 1.1: Global Hydrogen Production Share

Method	colour	Contribution towards global demand
Steam methane Reforming (SMR)	Grey	59%
Naphtha Reformation	Grey	21%
Natural Gas + Carbon Capture	Blue	0,7%
Water Electrolysis using Renewable	Green	0,03%

The contribution of various production technologies are listed in table 1.1 using the data available from [1]. Grey hydrogen as seen in the table contributes to the majority of the hydrogen demand, Scholz [2] estimated that the carbon emissions from SMR process to be 0.44 Nm^3/Nm^3 H2 or (9.7 kg CO2/ kg H2) and this level of carbon emissions wont be sustainable with the predicted H2 demand for future. The Intergovernmental panel on climate change (IPCC) has provided a detailed special report on the necessity to restrict the increase in global average temperature to less than 1.5°C of the pre industrial times to achieve net zero emissions by 2050 [3], if these goals have to be achieved a significant transition has to be made from grey hydrogen to green hydrogen in the upcoming years.

1.1 What is Green hydrogen?

Green hydrogen can be simply understood as a hydrogen production method which utilizes electricity produced from renewable technologies to electrolyze the water, The figure 1.2 depicts the green hydrogen production layout and general equation for water electrolysis is also written down.

$$H_2O(l) \longrightarrow H_2(g) + \frac{1}{2}O_2(g) \tag{1.1}$$

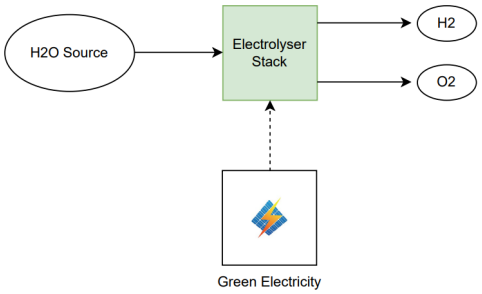

Figure 1.2: Green Hydrogen layout consisting of H_2O source, power source and electrolyzer stacks

Though other hydrogen production methods based on renewable energy such as thermochemical water splitting, photo catalysis exist, in the context of planning for net zero route, water electrolysis seems to be the most sustainable option. Technology cost of water splitting via electrolysis can be relatively low as it presents an opportunity for coupling between the synergies of different technologies [4]. The share of green hydrogen($\sim$ 0.03%) is strikingly low in comparison with the grey hydrogen ($\sim$ 80%) and this has to change considerably if the goals of net zero emissions have to be achieved.Therefore it is important to understand both the drivers and barriers to the uptake of green hydrogen.

1.1.1 Drivers for the green hydrogen uptake

There are multiple reasons as to why green hydrogen is seen as the future.The most obvious one is from the perspective of emissions, with the current rate of carbon emissions it wont be sustainable for human beings to satisfy the future hydrogen demand using grey hydrogen technologies, strong steps have to be taken towards net zero emissions. Some of the important drivers are listed below [4]

- Low cost of electricity by variable renewable energy (VRE)
- Increase in future hydrogen demand and broader application range
- Energy transition in 'Hard to Abate' sectors

Note: VRE are intermittent energy sources such as wind and solar, they are fluctuating in nature and cannot be controlled or dispatched like hydropower or geothermal.

The decreasing cost of electrolyzers, which have dropped 60% since 2010 [5], and the growing demand for hydrogen across different industries, are both positive signs for the future of green hydrogen. To facilitate this wave of interest in green hydrogen by mid 2020, 7 countries adopted net zero green house gases (GHG) emission targets in their legislation and 15 other countries provided similar legislation [4]. However, even with increased demand and suitable policies,there are barriers to overcome.

1.1.2 Barriers for Green Hydrogen Uptake

The uptake of green hydrogen faces some common challenges such as storage and transportation, but there are also unique challenges specific to green hydrogen production. These challenges are mainly related to the production stage, such as [4]

- High production cost
- Energy losses
- Lack of value recognition for Green Hydrogen

The global market in general lacks a sense of appreciation for anything green, this is because green products such as green steel, green fuel lack commercial value in the short term even though they contribute to the overall net zero emission scenario. Cost of green hydrogen production must be competitive in comparison to its grey and blue counterparts in order for it to thrive without depending too much on policies and government initiatives. Figure 1.3 providing the comparison between hydrogen production technologies is displayed [6].

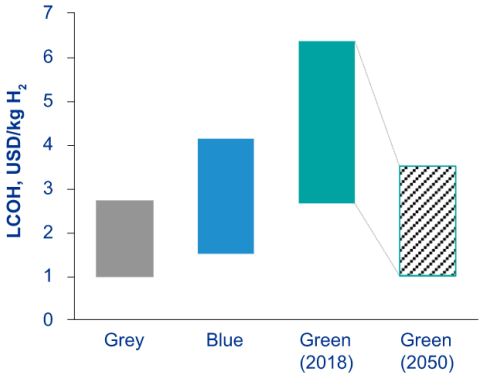

Figure 1.3: Cost band of various H2 production technologies. 2050 targets require green hydrogen to match the price band of grey hydrogen.[6]

1.2 The way forward for green hydrogen

Having understood the drivers and barriers for the uptake of the green hydrogen technology, it is important to realize studies (both technical and economical) must focus on coupling different technologies to reduce the overall cost of hydrogen. Low electricity cost of VRE should be exploited. Other forms of energy offered by renewables like thermal energy should also be exploited to bring down the overall cost of hydrogen. Different components from the green hydrogen layout such as electrolysers, green electricity source, Water source have to be studied and their synergies have to be exploited. In this work focus would be laid on the coupling of solid oxide electrolyzers (SOE) and concentrated solar power (CSP).

1.3 Why CSP and SOEC over other technologies?

CSP uses mirrors to focus sunlight onto a receiver, which then converts the energy into heat that can be used to generate electricity. CSP systems are particularly well-suited for use in regions with high levels of solar radiation. The additional advantage from CSP is its ability to provide low cost steam, this is particularly useful when electrolysis can be carried out at higher temperatures.

SOEC is an electrolyzer technology that uses a solid oxide material as the electrolyte instead of liquid or polymer electrolytes. The electricity requirement for SOE is lower than other electrolyzer technologies such as AWE and PEM. SOECs are highly efficient due to high temperature operations, making them ideal for large-scale hydrogen production. The high efficiency, the need for electricity and steam makes SOE a great candidate for integration with CSP

Overall, CSP and SOEC are chosen for their unique advantages over other solar and electrolyzer technologies. CSP offers both heat and power from solar, and SOEC offers high efficiency, high-temperature operation. Together, they can provide an efficient and reliable source of renewable energy and green hydrogen. The details of the technologies will be discussed in detail in the upcoming chapters.

1.4 Research Objective

As the way forward, it was understood the coupling and integration between variable renewable energy (VRE) and electrolyzers have to be done both technically and economically. Among the VRE, concentrating solar power is seen as an attractive option for hydrogen production via electrolysis as it has the ability to provide electrical and thermal energy. The primary motivation or initial research question of this thesis work is as follows

Will the integration of concentrating solar power and solid oxide electrolyzer to exploit the availability of thermal and electrical energy prove to be economically competitive in comparison to other green hydrogen technologies?

The initial research question can be split into further investigations as follows, the reasoning that led to raising of these questions are detailed in 2

1. *What is the business case for CSP-SOE integration in comparison with current state of the art technologies and what is the technical specification to achieve this integration?*
2. *How will the plant layout look like for the integration?*
3. *How to operate the plant efficiently to overcome the intermittency?*

Chapter 2

Literature Study

2.1 History of Electrolysis

Electrolysis as a process can be tracked back to as early as the late 1700s where it was first demonstrated by Dutch merchants J.R.Deiman and A.P.V.Troostwijk [7]. A century later towards the late 1800s the industrial scale water electrolysis was developed and continued to grow till early 1900s where close to 400 industrial scale electrolysers were under operation in 1902 [8]. Gradually the interest in hydrogen production using H_2O electrolysis diminished as SMR process provided hydrogen at a cheaper price. Having understood the environmental impacts of SMR process and the need for energy transition, once again interest is renewed in H_2O electrolysis for hydrogen production.

2.2 Types of Electrolyzers

Different applications demand different type of electrolyzers, the main established methods for H_2O electrolysis are

- Alkaline Water Electrolyzers (AWE)
- Proton Exchange Membrane Electrolyzers (PEM)
- Solid Oxide Electrolyzers (SOE)

Among the the current three type of electrolysers AWE are the most commercially installed. This is because they have a long history of deployment in the industry for Chlor-Alkali process for Chlorine gas production. However for exclusively producing hydrogen both AWE and PEM are at the same commercial maturity with a rating of TRL9 according to IEA .The SOE technology however is in the demonstration stage with good promise for future having a TRL4 commercial maturity rating, Large scale projects such as Norsk-efuel which is estimated to deploy 25MW SOE electrolyser [9].The figure depicting the TRL levels for three elctrolyser technology is visualized by IEA.

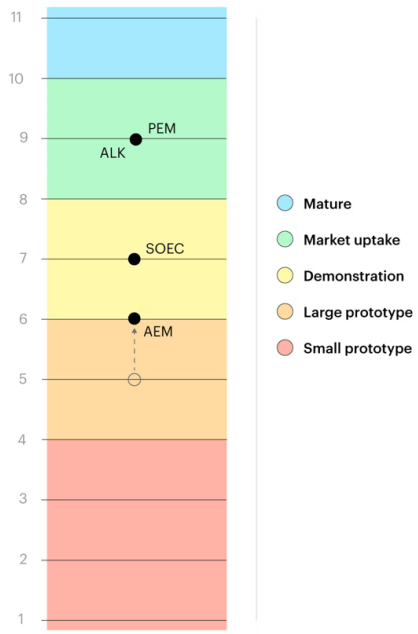

Figure 2.1: Technology readiness level (TRL) of different electrolyzer technologies. Solid Oxide Electrolyzer (SOE) as seen is still not as mature as Alkaline (ALK) and Proton Exchange Membrane (PEM) [9]

Discussing the complete details of all the electrolyser technologies is out of scope for this section as well as the report; However,the technical characteristics are discussed in a concise manner.

Parameters	**Units**	**AEC**	**PEMEC**	**SOEC**
Electrolyte	NA	Aq.potassium hydroxide	Polymer membrane	Yttria stabilised Zirconia
Cathode	NA	Ni,Ni-Moalloys	Pt,Pt-Pd	Ni/YSZ
Anode	NA	Ni,Ni-Coalloys	RuO2 ,IrO2	LSM /YSZ
Current density	A/cm^2	0.2-0.4	0.6-2.0	0.3-2.0
Cell voltage	V	1.8-2.4	1.8-2.2	0.7-1.5
Voltage efficiency	% HHV	62-82	67-83	<110
Cell area	m^2	<4	<0.3	<0.01
Operating Temp.	C	60-80	50-81	650-1000
Operating Pressure	bar	<30	<200	<25
Production Rate	m^3/hour	<760	<40	<40
Stack energy	KWh(el) m^3/H2	4.2-5.9	4.2-5.5	>3.2
System energy	KWh(el) m^3/H2	4.5-6.6	4.2-6.6	>3.7
Gas purity	%	>99.5	99.99	99.9
Lower dynamic range	%	10 – 40	0 -10	>30
System Response	NA	Seconds	Milliseconds	Seconds
Cold-starttime	min	<60	<20	<60
Stack Lifetime	hour	60,000-90,000	20,000-60,000	<10,000
Maturity	NA	Mature	Commercial	Demonstration
CapitalCost	Euros/KWel	1000-1200	1860-2320	>2000

Table 2.1: Technical Characteristics of Electrolysers [10]

In this thesis work the focus would be on solid oxide electrolysers. From the technical characteristics we can clearly see that the solid oxide technology significantly lacks the commercial maturity and also does not show promising stack lifetime at the moment, solid oxide electrolysers also have slow response time which mandates the need for careful integration between renewable power sources which are very intermittent in nature. However an interesting attribute of solid oxide technology is the lower energy requirement and its ability to operate at higher temperatures. This is a huge benefit for the electrolysis process as a portion of energy required to carry out the process can be supplied as thermal energy. To understand this in detail we look into the thermodynamics of the the electrolysis process in the next section.

2.3 Thermodynamics of Steam Electrolysis

The thermodynamics of hydrogen production via steam is determined primarily by the global reaction

$$\mathrm{H_2O(g)} \longrightarrow \mathrm{H_2(g)} + \frac{1}{2}\mathrm{O_2(g)} \tag{2.1}$$

The total energy requirement of this reaction comprises of electrical and thermal contributions. They can be described by the following temperature dependant thermodynamic indicators. $\Delta H(T)$ is representative of the total energy requirement and $\Delta G(T)$, $T\Delta S(T)$ are for electrical and thermal contributions respectively.

$$\Delta H(T) = \Delta G(T) + T\Delta S(T) \tag{2.2}$$

Hydrogen production via water/steam electrolysis is an endothermic process till 2250°C as the $\Delta H(T)$ stays positive [11]. From the reaction it can also be seen one mole of reactants give 1.5 moles of product which implies the change in entropy is positive, this dictates the $T\Delta S(T)$ term to stay positive. The $\Delta G(T)$ term also stays positive meaning the reaction is non-spontaneous. The relationship between the energy requirement and the temperature is an interesting one as it gives rise to optimal design spaces. The following graph depicts the relationship figure 2.2.

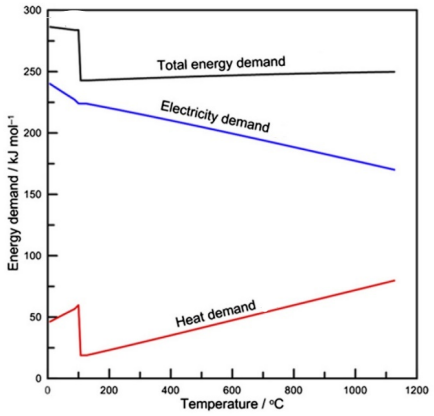

(a) Energy Requirement vs Temperature [12]

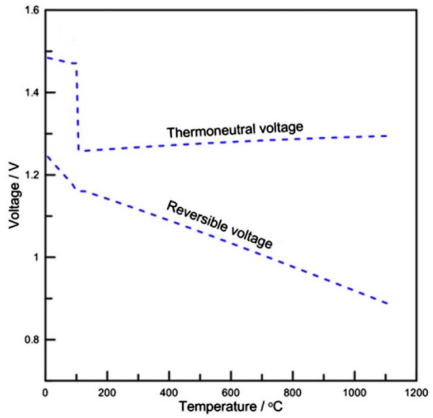

(b) Voltage Requirement vs Temperature [12]

Figure 2.2: Temperature dependence of energy and voltage in electrolysis process

Important thermodynamic voltages can be described using the the Gibbs energy and the enthalpy of the reaction.

$$E_{\text{rev}} = \frac{\Delta G(T)}{nF} \tag{2.3}$$

$$E_{\text{tn}} = \frac{\Delta H(T)}{nF} \tag{2.4}$$

Here n represents the number of electrons transferred in the reaction i.e n=2, F = 96,485 C/mol is the Faraday's constant. At standard temperature and pressure the E_{rev}= 1.23 V and E_{tn} = 1.48 V. However it is important to note that these thermodynamic voltages are also function of temperature and is depicted in figure 2.2. From the graphs it could be noted that at higher temperatures the portion of thermal energy contribution to the overall energy requirement increases, this is economically highly beneficial as the cost of thermal energy is much lesser than the cost of electricity. Using SOEC provides an opportunity to utilise this thermodynamic advantage.

Based on the Cell voltage (E_{cell}) 3 modes of operation are possible for the considered electrochemical operation.

- $E_{\text{cell}} < E_{\text{rev}}$: The reaction does not occur
- $E_{\text{rev}} < E_{\text{cell}} < E_{\text{tn}}$: Extra heat is required to operate the reaction (Endothermic)
- $E_{\text{tn}} < E_{\text{cell}}$: The reaction occurs with production of excess heat (Exothermic)

With the thermodynamic advantage of high temperature operations justified, a source of low cost heat or steam would drive the performance of SOEC operations in a positive way. For this purpose the integration of SOEC systems with concentrating Solar Power (CSP) would be studied in this thesis work.

2.4 Fundamentals of CSP

A concentrated solar power plant utilizes the solar energy to produce electricity. Solar radiation consists of 3 components - 1. direct radiation, 2. diffused radiation and 3. reflected radiation. CSP plants utilize the direct normal irradiation (DNI) to heat up a heat transfer fluid which is used to produce steam to run a turbine-generator system. Several components exists in the CSP plant which enable this solar to electric conversion, to understand the system from a zoomed out manner we focus on 3 different sections in a CSP plant.

- Solar Field
- Thermal Integration Region
- Power Block

The solar field in a typical CSP plant consists of mirrors, receivers, collectors, HTF pumps, tracking systems and so on. Thermal integration unit consists of heat exchanger systems, heat storage applications and finally the power block consists of turbine, generator, and other balance of plant applications.

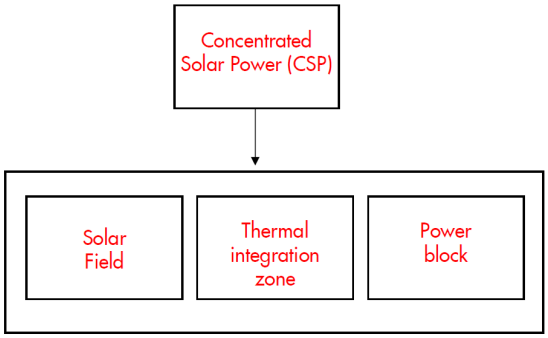

Figure 2.3: Different sections of CSP Plant

2.5 Types of CSP

In Industry predominantly 4 types of CSP plants are found and they are classified based on the type of collectors that they use. The 4 types of CSP plants are

- Solar Parabolic Dishes (SPD)
- Parabolic Trough Collectors (PTC)
- Solar Power Tower (SPT)
- Linear Fresnel Reflectors (LFR)

Among the 4 technologies PTC is the commercially most adopted followed by SPT and LFR. The SPD technology is relatively less established with only less than 1 % of existing commercial plants using it, However the SPD promises highest solar to electric efficiency among all the technologies [13] and high operating temperatures. The figure 2.5 depicts the fundamental structure of the technologies along with their installation ratios.

2.6 CSP - Technical Characteristics

The 4 different CSP technologies offer different technical capabilities and depending on the project requirement an appropriate technology is chosen. The characteristics of the different CSP technology is discussed individually highlighting the important specifications using the data compiled by [13].

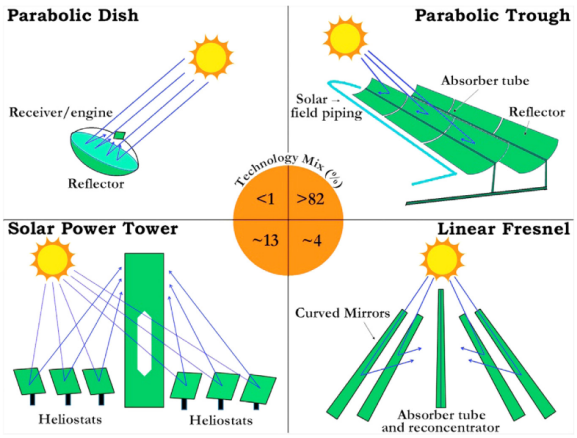

Figure 2.4: Concentrated Solar Power technologies and their share of commercial installations. As seen Parabolic trough have the highest no. of commercial installations and parabolic dish has the least installations. [14]

2.6.1 Solar Parabolic Dish (SPD)

The SPD-CSP systems operates on the principle of point focusing, a parabolic dish is used to concentrate the solar radiation onto a receiver at focal point. At this focal point a Stirling/Brayton engine is placed of efficient power conversion. The SPD systems have high concentration ratios 2000 and the working fluid can operate in temperatures and pressures of 700 °C [15] and 200 bar. A single unit of SPD can have power generation capacity of 0.01MW- 0.5MW [16]. The SPD-CSP systems also provide a solar-electric efficiency of 25%-30% [17]and this is highest of all the 4 technologies. One additional advantage of SPD-CSP is the flexibility with respect to land availability as it does not require the need to have level land. The SPD-CSP systems are not however very mature from a commercial standpoint. The only commercial and operational system is in Tooele at the Tooele Army Depot in Utah,United States.

Features

- High Efficiency as a result of direct power conversion in the dish using Stirling cycle which is not present in other CSP technologies.
- Geographical flexibility is relatively better as it can be installed in remote locations and different terrains.
- High cost of investment and operation as large number of dishes are required to generated same amount of electricity as other CSP systems.
- There are not many existing CSP plants which use dish technology, this means the reliability of these technologies still remain unproven.

2.6.2 Parabolic Trough Collector (PTC)

PTC are commercially the most well established CSP technology, more than 80 % [14] of the plants that are operational have employed PTC. PTC have several troughs aligned parallel to each other in order to collect and concentrated heat onto a HTF. The hot HTF is used to produce steam which is then used to drive a turbine-generator system to produce electricity. The parallel troughs are aligned in North-South direction for best tracking. The HTF are usually molten salts (Proportions of Sodium Nitrate and Potassium Nitrate) and the typical working temperature is around 400 °C, and the maximum operating temperatures reaches 550 °C [18], the maximum working temperature is limited by the HTF. PTC can also be combined with heat storage options to produced electricity during non-sunshine hours. Overall PTC are a commercially reliable option as there is abundant data available from the pre-existing plants. The capacity of operational PTC plants vary from 10-200MW. Globally there are 81 different installations of the PTC-CSP plants around the globe [19].

Features

- Commercially well established and reliable technology, more than 80% of the existing plants use PTC.
- The technology can be scaled to various different capacities and has proven to be reliable.
- Fragility of the parabolic trough collectors pose an issue as they are susceptible to strong winds.
- Due to the nature of the technology very high concentration ratios cannot be obtained. The typical concentration ratios are in the order of 100s [14]

2.6.3 Solar Power Tower (SPT)

The SPT technology has a tall central tower where the receiver is located, flat mirrors surrounding the tower focuses the solar radiation onto the tower. Owing to large concentration ratios the operating temperature of the solar field reaches a maximum of 600 °C. SPT technology in combination with heat storage options are capable of achieveing high Capacity factors (CF). SPT technology however is cost intensive investment options as it requires a high capital expenditure per meter squared of area. SPT can provide capacities from 10-150 MWe, In order to reduce the financial risk SPT with >30MWe capacity are usually hybridized [20]. SPTs are also commercially mature with option of thermal storage and around 32 of the existing CSP plants have employed SPT [21].

Features

- Commercially well established and reliable technology, most number of existing installations after PTC.
- The technology is robust and provides very high concentration ratios as high as 1000 [14]
- SPT demands large land areas in flat terrain with high water availability. Largest installed SPT plant occupies 14 Km^2 of land area [21]
- There is high financial risk for SPT owing to its high initial capital investment. The cost per KW for some for some of the existing plant is as high as 18000$ [21]

2.6.4 Linear Fresnel Reflector (LFR)

In LFR technology flat mirrors are used to focus solar radiation onto piping which is placed on the focal line for these mirrors. These piping carry feed water which gets converted into steam after absorbing the solar radiation. LFR like PTC provides capacity ranging from 10-200MWe and their operating temperatures ranges from 250-390 °C, the solar-electric efficiency is estimated to be 8-10% [22]. A well organized and optimised LFR plant is capable of producing low values of Levelized Cost Of Electricity (LCOE). LFR offer simplistic receiver design with stationary absorbers however this also means LFR have low optical efficiency

Features

- LFRs have simplistic design which leads to reduced cost. LFRs have some of the lowest Cost/KW values that are as low as 2900$/KW. [23]
- The technology has been proven to be reliable for different capacities.
- Similar to PTC, LFR systems are fragile. Therefore, careful maintenance is mandatory. [21]
- Similar to PTC, LFR systems cannot achieve very high concentration ratios. The concentration ratio achieved through LFR is on the order of 100s [21]

Depending on the the constraints imposed on the CSP plant such as geography, land availability, capital availability selection of the appropriate technology is made. If a reliable robust operation is preferred PTC shall be selected, if reliable operations at high temperature is required SPT is chosen, when the project demands simplistic design and lower expenditure LFR are chosen. SPD installation is limited and there is only one operational plant even though SPD promises high conversion efficiency.

A co-generation CSP plant is capable of producing both heat and electricity. The availability of steam and electricity from a single plant makes it a very attractive option to be integrated with electrolyzer plants. The solid oxide electrolyzer plant as we discussed requires both thermal and electrical energy, integration of CSP and SOE is worthy of investigation as there is a potential to produce hydrogen at reduced cost. Literature study will be performed on modelling and design of SOE Plants, CSP plants and works which have researched the possible integration between them will also be discussed.

2.7 Status of the CSP

The number of CSP installations are steadily increasing globally, this is primarily due to the economic and technical benefits CSP plants provide over other solar technologies. The projections for CSP is optimistic and 11% of the total global electricity production is expected to be satisfied via CSP by the year 2050 [24]. Like we discussed in the previous section, CSP works by concentrating the solar radiation onto a heat transfer fluid which is used to generated electricity. For a CSP 3 main subdomains are present - Solar collection fields, Thermal energy storage/exchange unit and power block. Among the available 4 technologies for solar collectors, Parabolic trough is the most utilized technology in existing plants followed by solar power towers. Even though Solar power dish (SPD) offers the highest solar-electric conversion there is only one existing plant that is still operational. LFR technology like described in the literature offers low cost/KW and this is validated by some of the existing plants. It is important to note that all technologies except for solar power dish have commerically proven thermal energy storage systems.The most common thermal energy storage technology used was two-tank molten salt system, and as of today the highest hours of storage for CSP which has been installed is 17.5 hours [25]. Regarding the power block most of the CSP installations globally have used Steam Rankine cycle, the other alternative to steam rankine cycle was organic rankine cycle which was installed in 5 plants and operates with good reliability, the latest installation that uses organic rankine cycle was the Aalborg CSP plant in Denmark which was constructed in the year 2016 which has a 5.5MW capacity [26]. Stirling power cycle is used globally in only one plant, this is also the only plant globally which employs SPD [27].

SolarPACES is a society which has been formed by a network of international researchers and industry experts for the development and technology push of concentrated solar power. Solarpaces have compiled the data of all/most of the existing CSP plants globally [28]. Using the data compiled by solarPACES a table is reported which contains select details of the 20 largest installations of CSP globally 2.2. The largest installed CSP plant is located in UAE with a capacity of 600MW. From the table it can also be noted the cost/KW is lower in Asian countries such as India and China. The reason for high capital investment in Europe, Americas and Australia is not clearly explained however it can be attributed to high real estate cost and higher operational costs.

The data compiled by [28] is highly valuable as it provides insights into the technical and economic numbers from existing plants of different capacity scales, though the compilation contains lots of important specifications, details regarding capacity factor of these plants are not known. However, the data collected should be extremely helpful when performing modelling as these numbers can either be set as target numbers and also as figures of limit.

Table 2.2: Actual plant specifications of 20 of highest capacity installations

S.no	Power	Country	MW Capacity	Tech	Year	Total Cost (Million USD2020)	Cost/KW (USD2020)	LCOE(USD2020)	Power cycle	TES(hrs)
1	Noor	UAE	600	PTC	2018				Steam Rankine	11
2	Ivanpah	USA	377	SPT	2010	2339.89	6206.6	0.19	Steam Rankine	
3	Mojave	USA	280	PTC	2011	1701.74	6077.6	0.24	Steam Rankine	
4	Solana	USA	250	PTC	2010	2161.06	8644.3	0.2	Steam Rankine	6
5	Genesis	USA	250	PTC	2010	1292.79	5171.2	0.19	Steam Rankine	
6	NOOR	Morocco	200	PTC	2015	1119.2	5596	0.16	Steam Rankine	7
7	NOOR	Morocco	160	PTC	2013	1214.26	7589.1	0.28	Steam Rankine	3
8	NOOR	Morocco	150	SPT	2017	877.05	5847	0.15	Steam Rankine	7
9	Dhursar	India	125	LFR		366.24	2929.9	0.11	Steam Rankine	
10	Ashalim	Israel	121	SPT	2015	854.66	7063.3	0.23	Steam Rankine	
11	Atacama	Chile	110	SPT	2021				Steam Rankine	17.5
12	Crescent	USA	110	SPT	2011	1032.24	9384	0.18	Steam Rankine	10
13	Ashalim	Israel	110	PTC	2015	1017.45	9249.6	0.21	Steam Rankine	4.5
14	Noor	UAE	100	SPT	2018				Steam Rankine	15
15	Redstone	South Africa	100	SPT	2021					12
16	Shouhang	China	100	SPT	2016	458.15	4581.5	0.08	Steam Rankine	11
17	CSNP	China	100	PTC	2017	421.98	4219.8	0.1	Steam Rankine	10
18	Jinta	China	100	SPT	2022					9
19	Xina	South Africa	100	PTC	2014	895.36	8953.6	0.2	Steam Rankine	5.5
20	Kathu	South Africa	100	PTC	2016	917.86	9178.6	0.16	Steam Rankine	5

2.8 Technology Selection for CSP

In this work the CSP plant would be used as a black box and therefore for technology selection a simple comparison table is used. The collection technologies are compared on the basis of few important KPIs for the CSP plant.

Table 2.3: Technology selection based on important CSP KPI

	PTC	SPT	LFR
Commercial Maturity	+	+	+
Area Requirement	+	-	+
Efficiency	+	++	-
Investment cost	+	-	++
LCOE	-	+	++
Score	**3**	**2**	**5**

The table indicates LFR as a good choice based on the KPIs compared. When it comes to green hydrogen production cost is an important factor and reduced plant efficiencies can be disregarded if there is large reduction in costs without performance dip. Using the data available from [28] a comparison on

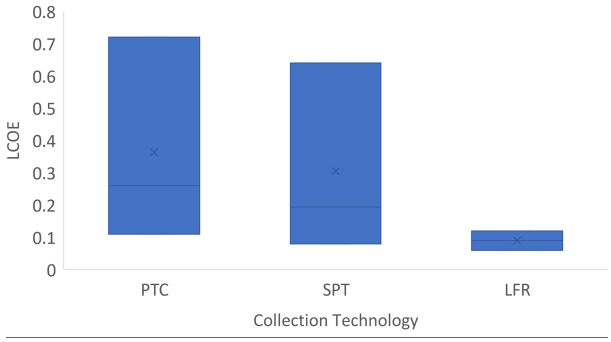

Figure 2.5: Concentrated Solar Power technologies and their corresponding range of LCOE values obtained from real existing plants

the LCOE values were made and it is clear that the LFR technology provides the cheapest LCOE. Since power price is an important parameter in the green hydrogen production LFRs are preferred. It must be noted for a serious technology selection on CSP detailed engineering decisions must be made and for this thesis it would be out of scope.

2.9 Modelling of Systems

Modelling of systems can be done in different ways depending on the requirement and the stage at which the design is being done. Figure 2.6 shows the various commonly used modelling methods classified on different basis. Emperical and semi empirical models are predominantly used in cases of computational modelling where the full physical understanding of the phenomenon is not required. Phenomenological models use the underlying physics to model the systems. Models can also categorized by the dimensions considered such as OD,1D,2D and 3D. Our task here is to describe the system and the plant in general and therefore for our work level based modelling approach is most suitable i.e system level, macroscopic level and microscopic level. [29] has reviewed different models of SOEC and all the models studied were categorized according to figure 2.6

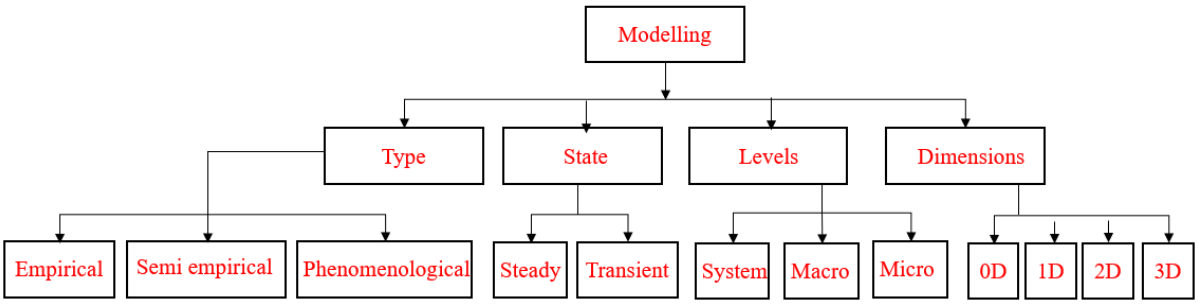

Figure 2.6: Different types of modelling as classified by [29]

System level modeling is a method of modeling complex systems by taking a high level view and solving the more manageable components. These components are then modeled individually and the interactions between them are analyzed to understand the behavior of the overall system. In level based modelling approach, system level modelling is the first design level.This is also the stage where different parameters and subsections are studied for their sensitivities and most impactful parameters are identified.

Macroscopic modeling is a method used to simulate and predict the behavior of systems at a large scale. It involves using mathematical equations and computer simulations to describe the flow of energy, mass, and other relevant quantities through the system. The goal of macroscopic modeling is to understand the overall behavior of the system and how it is affected by different factors such as operating conditions, design, and control systems. For a SOE this could mean the goal is to predict the performance of the SOE under different operating conditions and to identify ways to improve its efficiency and reduce costs. This is typically done using computer simulations, which take into account factors such as the operating temperature, the pressure, the flow rate of the reactants and the current density. The model will also consider the thermodynamic and kinetic behavior of the materials and the interactions between the different components of the SOE. For a CSP the goal is to predict the performance of the plant under different operating conditions and to identify ways to improve its efficiency and reduce costs. This is typically done using computer simulations, which take into account factors such as the weather, the design of the plant, and the control system.

Microscopic modelling consists of doing analysis at a micro-level for one or many of the subs domains in the system. For SOE it could mean concentrating on the cermet electrode behavior to improve the system behaviour, for CSP it could mean understanding different phenomenons of the CSP solar collectors to improve the system performance. The relevance of microscale modelling during a feasibility study is limited and therefore these type models are ignored.

2.10 Literature study on Solid Oxide Electrolyzer Models (SOE)

Across literature the most commonly adopted way of modelling the SOE was macroscopic approach, this involves using Faraday's law, Buttler-Volmer equation, Ohms Law and gas transport theories. The main idea in this approach is to estimate the operating cell voltage by first calculating the reversible potential and summing it with over potentials due to concentration, Ohmic resistance and activation. Microsopic modelling were used to improve the accuracy of the simulation/modelling by considering the micro-structure of the cermet electrode, these do not typically classify the over-potentials rather carryout charge and mass balance at each electrode. The relevance of micro level models for our research is not much and for this reason literature that used microscopic-models were avoided.

The focus of this research would be to understand the process in a system level to identify the critical parameters. To enable this macro level/ OD models are most useful,the literature was also studied for macro level models for Solid oxide Hydrogen electrolysis and models which incorporated the balance of plant in addition to the electrolyzer stacks were preferred as these models tend to give better picture of the plant operations.

S.No	*Year*	*Title*	*First Author*	*Abstract*	*Inference*
1	*2007*	*Energy and exergy analysis of hydrogen production by solid oxidesteam electrolyzer plant*	*Meng Ni*	*Energy/Exergy analysis on steam electrolysis plant done, waste heat recovered, SOE stack was identified to be major source of exergy destruction, efficiency as fucntion of operating parameters were studied.*	*Macroscopic electrochemical model was used*
2	*2007*	*Can high temperature steam electrolysis function with geothermal ehat?*	*J.Sigurvinsson*	*SOE was integrated with waste hear from geothermal, Technoeconomics was studied, system was optimised using genetic algorithms*	*Macroscopic Model, Overpotentials were estimated by linearized models which were validated against experiments*
3	*2018*	*Modeling and performance optimization of a solid oxide electrolysis systemfor hydrogen production*	*Abdullah A. AlZahrani*	*1MW SOE System with and without hydrogen storage was proposed,System is assumed to operate without external heat,Energy and Exergy study was conducted,Exergy destruction was investigated, Optimisation was done to improve efficiency.*	*Macroscopic Electrochemical model was used, Influence of operating conditions on power demand,Exergy/energy destructions. Energy and exergy efficiency as optimized. Economics was not studied*

4	*2018*	*Flowsheet-based model and exergy analysis of solid oxide electrolysiscells for clean hydrogen production*	*Karittha Im-Orb*	*Userfriendly SOE model was developed in ASPEN Plus, parametric analysis on operating parameters, energy and exergy efficiency was optimized*	*Macroscopic electrochemical model was used,Relationship between overpotenital,energy demand,efficiency versus temperature.Process modeler Aspen plus was used*
5	*2018*	*Techno-economic analysis of hydrogen production by solid oxideelectrolyzer coupled with dish collector*	*Amin Mohammadi*	*SOE is integrated with Solar dish collector,Efficiency and economica analysis were performed.*	*Macroscopi Electrochemical Model was used, Levelized cost of hydrogen estimated. System performance vs solar dish collector*
6	*2020*	*Solar hydrogen production: Techno-economic analysis of a parabolic dish-supported high-temperature electrolysis system*	*Luca Mastropasqua*	*SOEC was integrated with parabolic solar dish, SOEC efficiency was estimated, LCOH was estimated*	*Electrochemical model was custom built in Aspen custom modeler,1D Macroscopic model was used to estimate stack performance.*
7	*2022*	*Techno-economic analysis and Monte Carlo simulation of green hydrogen production technology through various water electrolysis technologies*	*Dohyung Jang*	*Technoeconomics of different electrolyser technogies - Unit cost, Net present value, LCOH were estimated*	*Macroscopic Model was used, ASR Method was used to estimate operating cell voltage, Process modeler EBSILON was used*

The references for the literature in the table are [30–36] respectively. From the literature review it was understood the modelling approach towards SOEC stack + system have largely been on the macroscopic basis and focus has primarily been on optimizing the energy efficiency of the system. However the issue is no standard approach for defining the efficiency has been established in literature, this makes it very difficult to compare the efficiency of different system models available in literature. The initial design level in a process plant modelling would be to estimate the specifications of the system from a high level view. These specifications will have to be then used to define the system boundaries on which macroscopic modelling must be performed. However all the models have avoided this multilevel design approach and have directly proceeded with macroscopic modelling.

2.11 Literature Study on Concentrated Solar Power (CSP)

Concentrated solar power (CSP) systems use mirrors or lenses to concentrate sunlight and convert it into thermal energy, which is then used to generate electricity. CSP systems can be classified into four main types: parabolic trough, linear Fresnel, Parabolic Dish and central receiver.

There are different approaches to model CSP systems, including mathematical models, experimental methods and simulation tools. Mathematical models for CSP systems typically include the modeling of the solar collector, the thermal energy storage system, and the power generation system. These models can be used to simulate the performance of the system under different operating conditions and can be used to optimize the system design. Experimental methods involve conducting experiments on real CSP systems and measuring the performance under different operating condition. The System Advisor Model (SAM) is a widely used simulation tool for modeling concentrated solar power (CSP) systems. It can be used to model the performance of CSP systems under different operating conditions, optimize the system design, estimate the economic and financial performance of CSP systems and model the performance of CSP systems with thermal energy storage. SAM is a free, open-source software developed by the US National Renewable Energy Laboratory (NREL) and it is a reliable tool to model CSP systems.

The larger picture of the thesis is to build an integrated concentrated solar powered solid oxide electrolyzer using a top down approach i.e to first design the integration from a system level and then perform a detailed modelling. This has been considered through out the literature review process and among the literature studied the most relevant works are reported as a showcase for the different modelling techniques available.

The literature on CSP predominantly focused on performance modelling and optimisation of one of the subsections of the CSP or on developing new methodologies/techniques to improve the subsections of the CSP. However, many of these studies lacked justifications relating to subsection's efficacy on a system level ; a top down modelling approach is extremely crucial as it identifies and improves the subsections that improve the efficiency at system level and improve the plant economics. Few of the subsections that were focused in the literature are modelling and alternatives of thermal storage, power cycles and heat transfer systems. The initial phase of this thesis will focused on system level modelling to identify the crucial parameters and these parameters/subsections will be designed and improved in the second phase of the work. To enable this focus was placed on works that performed technical/economic modelling at system level. It was noticed many of the system level models were on case study format which checked the feasibility of CSP plant in a particular geography and few of the relevant works are reported.

S.No	*Year*	*Title*	*First Author*	*Abstract*	*Inference*
1	*2013*	*An analysis of the costs and opportunities for concentrating solar power inAustralia*	*Hinkley.J*	*Estimates on expected costs of Trough and Tower technologies in Austtralia, Efficiency improvement,Performance comparison between trough and tower*	*Cost reduction opportunity identification,Loss quantification, Technology bsuggestion for Australia*
2	*2018*	*Technical feasibility of a sustainable Concentrated Solar Power in Moroccothrough an energy analysis*	*Bouhal.T*	*Thermal performance was assessed for CSP in Morocco. Physical model was developed and simulations were performed in different regions of Morocco*	*Physical Model for CSP, Thermal performance modelling of CSP system, Geography selection for CSP in Morocco*

3	*2020*	*Optimization and techno-economicassessment of concentrated solarpower(CSP)in South-Western Africa:A cases tudy on Ghana*	*Agyekum. EB*	*Technonoeconomic performance evaluation was performed on 2 locations in Ghana*	*Lvelized cost of electricity was estimated at 2 locations,Optimal Solar Multiple was estimated,Solar Tower were suggested as the technology suitable for Ghana*
4	*2022*	*Design of a 100 MW concentrated solar power Linear Fresnel plant inRiyadh, Saudi Arabia: A comparison between molten salt and liquidsodium thermal energy storage*	*Barqi.A.S*	*Feasibility study of constructing 100MW CSP Linear Fresnel Solar Power in Riyadh,Saudi Arabia*	*2 Heat transfer fluids were studied, High capacity factors (~90%) were achieved, Saudi Arabia is concluded to have high potential for CSP*

The literature on CSP system level performance evaluation in specific geographies [37–40] are of high value as they highlight the performance and economic metrics in a straightforward manner. One of the biggest constraints for a CSP plant is the selection of geography, the literature has several case studies which have studied the performance of CSP in different geographies in a thorough manner. The geography specific details and performance can be derived from these literature and the simulation done with the use of software like SAM are very helpful during the feasibility study of CSP plants.

2.12 Literature Review on Integration of SOE and CSP

The integration of solid oxide electrolyzers (SOEs) and concentrated solar power (CSP) has been studied as a potential way to efficiently store excess solar energy in the form of hydrogen. This technology involves using the high temperature steam and electricity generated by CSP to drive the electrolysis process in the SOE, which splits water into hydrogen and oxygen.

Modeling of systems that integrate solid oxide electrolyzers (SOEs) and concentrated solar power (CSP) can be done using a variety of different approaches, depending on the specific goals of the model and the level of detail required. One common approach is to use mathematical models to simulate the performance of the SOE and CSP components separately, and then to combine these models to predict the overall performance of the integrated system. These models can include equations that describe the thermodynamic and electrochemical processes that occur in the SOE and CSP, as well as the heat and mass transfer processes that occur between the two components.

S.No	*Year*	*Title*	*First Author*	*Abstract*	*Inference*
1	*2014*	*Optimal integration of a solid-oxide electrolyser cell into a direct steamgeneration solar tower plant for zero-emission hydrogen production*	*J.S.Bermejo*	*Energetic analysis on integration of SOEC unit into solar tower plant.Different configurations have been studied for efficient integration.*	*different integration strategies were proposed, Strategies to reduce penalities on the solar plant are discussed, Oxygen co-production discussed.*
2	*2017*	*Techno economic design of a solid oxideelectrolysis system with solar thermal steamsupply and thermal energy storage for thegeneration of renewable hydrogen*	*Seitz.M*	*Solar thermal receiver integrated with solid oxide electrolyzer and thermal energy storage is optimized to minimize the Levelized cost of Hydrogen (LCOH)*	*LCOH of the system is estimated and domains of cost reduction possibilities are listed.*
3	*2018*	*Techno-economic analysis of hydrogen production by solid oxideelectrolyzer coupled with dish collector*	*Amin.M*	*Dish collector is used to provide energy to SOEC .Compressed air energy storage system has been used to produce electricity.Efficiency and LCOH are estimated.*	*Efficiency of electrolyzer and power cycle are estimated, LCOH is estimated. Design parameters impacting efficiency and LCOH are identified.*
4	*2020*	*Solar hydrogen production: Techno-economic analysis of a parabolic dish-supported high-temperature electrolysis system*	*Luca Mastropasqua*	*SOEC was integrated with parabolic solar dish, SOEC efficiency was estimated, LCOH was estimated*	*Electrochemical model was custom built in Aspen custom modeler,1D Macroscopic model was used to estimate stack performance.*

The existing studies have a common way of approaching the integration, the systems are individually modelled and one of the subsections of the systems is looked into deeply and optimized to provide a low LCOH value. Though the existing approach is useful and effective to a certain degree a strong justification on why a particular subsystem is chosen for optimization is lacking. A top down approach is needed in this case where different layers of design and integration yield different points of focus. The studies tabulated are [34, 35, 41, 42] respectively.

2.13 Research gap and Thesis Outlining

From the literature study it was identified for CSP-SOEC Integration, modelling has been carried out to improve the performance and economics by focusing on one or many particular subsystems. Though this results in improved efficiency in some cases, the degree of impact of the chosen subsystem or design parameters relative to other parameters are unknown. As indicated in figure 2.6 different models have to be adopted at different stages of design. There is a need to first perform a system level modelling from a high level to identify the most impactful subsystems/design parameters. These parameters must then be set as targets for plant integration and detailed modelling of the plant must be done based on this.This multilevel approach will be implemented across 3 phases in this thesis, each and every phase would be used to answer the following sub questions respectively.

1. *What is the business case for CSP-SOE integration in comparison with current state of the art technologies and what is the technical specification to achieve this integration?*
2. *How will the plant layout look like for the integration?*
3. *How to operate the plant efficiently to overcome the intermittency?*

The mentioned sub questions can be answered during the different levels of modelling, The inferences from these modelling phases can be combined and the primary research question below can be answered.

Will the integration of concentrating solar power and solid oxide electrolyzer to exploit the availability of thermal and electrical energy prove to be economically competitive in comparison to other green hydrogen technologies?

Chapter 3

Conceptual process design

3.1 Conceptual framework

The integration of Solid Oxide Electrolyzers (SOE) and Concentrated Solar Power (CSP) involves combining two different technologies to create a more efficient system for producing clean energy. To better understand how these technologies can work together, a conceptual framework is needed to understand the different components of the system and how they interact.

The first step in developing conceptual process design is to define separate unit blocks for SOE and CSP. This involves creating models for each technology that capture their individual characteristics and behavior. These models will serve as the building blocks for the overall system model.The SOE model will include factors such as Material consumption, energy consumption. This model will provide insight into the efficiency and performance of the SOE under different operating conditions.The CSP model, on the other hand, will include factors such as the size of solar field, the efficiency of the heat transfer system. This model will provide insight into the efficiency and performance of the CSP under different operating conditions 3.1.

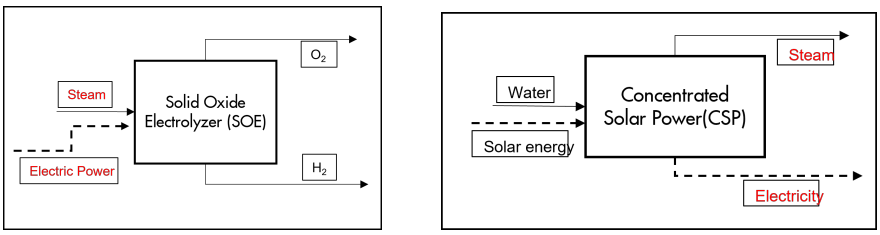

(a) SOEC unit block (b) CSP Unit block

Figure 3.1: Individual unit blocks for SOE and CSP

Once these individual models have been developed, they can be combined to create a single OD and efficiency-based system level model 3.2. This model will provide a holistic view of how the SOE and CSP interact and how the overall system performs. The system level model will take into account factors such as the amount of solar energy available, the efficiency of the SOE in converting that energy into hydrogen or other products, and the efficiency of the CSP in providing the required heat. It will also consider other factors such as the cost and availability of materials, the maintenance requirements of the system. By combining these individual models into a system level model, it is possible to gain a more complete understanding of the potential benefits and limitations of integrating SOE and CSP technologies.

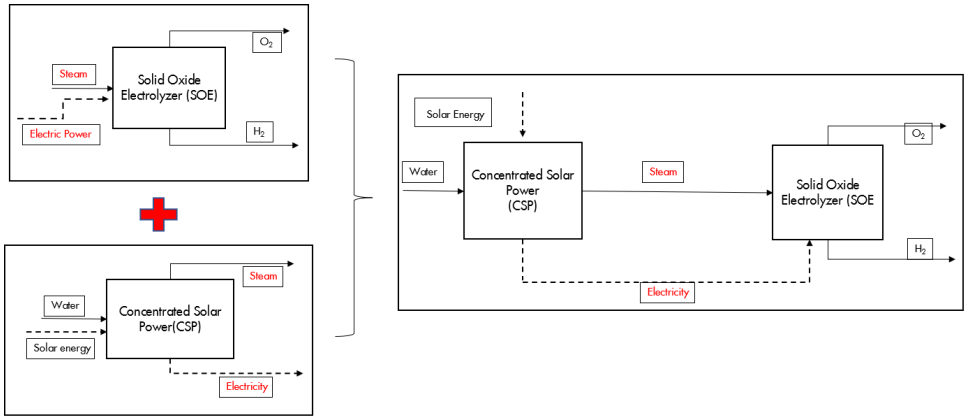

Figure 3.2: Individual unit blocks combined to give the unit block for the integrated plant

Overall, the framework of integrating SOE and CSP technologies provides a powerful tool for optimizing the design of the system, identifying areas of high impact, it can also be used as a tool to identify where the performance is most/least efficient give us areas of improvement and focus.

3.2 System level modelling

The focus of this modeling will be on a high level to provide an overview of the system's functionality and its translate them to obtain economic indicators. The modeling will involve identifying the key inputs, processes, and outputs of each unit block. Once the unit blocks have been modeled individually, they will be integrated into a single model to simulate the overall system's performance. The purpose of simulating the integrated system is to identify the critical pathways and bottlenecks in the system and determine the key parameters that impact its overall performance and economics. The findings from this modelling stage will be used to define realistic targets for the subsequent stages for the project.

3.2.1 SOEC unit block modelling

The task here is to create a 0D, efficiency based system level model that would be able to give first level estimations on the energy requirement,material requirement,CAPEX, OPEX for a fixed hydrogen production. The economic data obtained from these models would be used to predict the Levelized cost of hydrogen (LCOH).

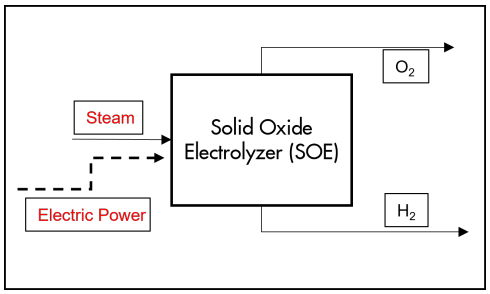

Figure 3.3: SOE unit block : Steam and electric power are the inputs this block resulting in production of Hydrogen & Oxygen.

Figure 3.3 visualizes the SOE as a unit block, the inputs necessary for the system are steam and electric power and the outputs are H2 and O2. In order to make estimates on the energy and material requirement the specific energy requirement of this block will be assumed and the material requirement would be estimated through simple mass balance by adopting steam utilisation factor. Sweep gas is used in high temperature electrolysis to remove the oxygen produced and avoid buildup on the anode side. SOE systems built and experimentally verified by different institutes such as KIT,Sunfire,DLR,and FZJ were studied to understand the specifications of SOE systems [43–46]. The specifications that were assumed for modelling of SOE system is listed in the table 3.1

Table 3.1: List of assumptions made for SOE modelling

1	H2 production/day	tonnes	100
2	Daily hours of production	Hours	24
3	Hours of operation/Year	Hours	8760
4	LHV of H2	MJ/Kg	119.96
5	System total energy requirement (STEC)	KWh/Kg	39
6	Steam Utilisation factor	-	0.8
7	Sweep gas ratio (Air)	-	2
8	Mw of Hydrogen	Kg/mol	0.002
9	Mw of Oxygen	Kg/mol	0.032
10	Mw of Air	Kg/mol	0.029
11	Mw of Steam	Kg/mol	0.018
12	Capex/KW(Total)	$/KW	1000
13	Lang Factor		2
14	Power Price	$/KWh	0.09
15	Maintainence OPEX	$/KW/Year	155
16	Cost of LP Steam	$/tonne	38

Estimations on Energy Requirement

The efficiency for high temperature electrolysis process can be defined by the following simple equation

$$\eta = \frac{\dot{m_{H2}} \times \text{LHV} \times 1000}{E_{in}} \tag{3.1}$$

where

η - Efficiency of the process

$\dot{m_{H2}}$ - mass flow rate of hydrogen at outlet (Kg/s)

LHV - Lower heating value of hydrogen (MJ/kg)

E_{in} - Power provided to the system (KW)

now the equation can be be re-written to obtain the System Total Energy consumption (STEC) (Note for our calculations we have assumed a value for STEC)

$$\text{STEC(KWh/kg)} = \frac{E_{in}}{\dot{m_{H2}} \times 3600} = \frac{\text{LHV} \times 1000}{\eta} \tag{3.2}$$

The Power requirement C_{SOE} (MW) for the SOE plant can now be estimated using the STEC (KWh/Kg)

$$\text{C}_{\text{SOE}}\text{(MW)} = \frac{\text{STEC} \times \dot{m_{H2}} \times 3600}{1000} \tag{3.3}$$

Estimations on Material Requirement

Sweep gas (air) ratio (SR) and Steam utilisation factor (U) are two important parameters when it comes to the estimation of the material requirement. The values for these parameters are assumed and is listed in the table 3.1, their definitions are listed below.

$$\text{SR} = \frac{n_{O_2}, in}{n_{O_2}, produced} \tag{3.4}$$

$$\text{U} = \frac{n_{H2O,reacted}}{n_{H2O,feed}} \tag{3.5}$$

The reaction which dictates the process is

$$\text{H}_2\text{O(g)} \longrightarrow \text{H}_2\text{(g)} + \frac{1}{2}\text{O}_2\text{(g)} \tag{3.6}$$

From this reaction we can see that one mole of H_2O gives one mole of H_2 and half a mole of O_2, once the mole flow of the substances are estimated the mass flow rate can also be easily obtained as it is just the product of mole flow rate and molecular weight (Kg/mol).The mole flow rate of hydrogen gas produced at the outlet can be obtained from the below equation.

$$\dot{m_{H2}}, produced = \dot{n_{H2}}, produced \times M_w \tag{3.7}$$

We know that the mole flow of hydrogen is same as the mole flow of the steam inlet and the mole flow of Oxygen is half that of the mole flow of hydrogen. Using this we can estimate the mass flow of steam and sweep gas required.

$$\dot{m_{H_2O}}, feed = \frac{\dot{n_{H2O}}, reacted \times M_w, steam}{U} \tag{3.8}$$

$$\dot{m_{air}} = \dot{n_{O_2}}, produced \times M_w, air \times \mathrm{SR} \tag{3.9}$$

where

$\dot{n_{O_2}}, in$ - Number of moles of oxygen in the sweep gas (mol/s)

$\dot{n_{O_2}}, produced$ - Number of moles of oxygen produced (mol/s)

$\dot{n_{H2O}}, reacted$ - Number of moles of steam utilized (mol/s)

$\dot{n_{H2O}}, feed$ - Number of moles of steam in feed (mol/s)

M_w - Molecular weight (kg/mol)

$\dot{m_{air}}, in$ - mass flow of sweep gas (Kg/s)

$\dot{m_{O_2}}, produced$ - mass flow of oxygen produced (Kg/s)

$\dot{m_{H2O}}, produced$ -Mass flow of steam (Kg/s)

$\dot{m_{H2}}, produced$ -Mass flow of hydrogen produced/Target Hydrogen production (Kg/s)

Economic modelling

The levelized cost of hydrogen (LCOH) is a widely used economic indicator in the energy industry to assess the cost competitiveness of different hydrogen production pathways. It takes into account all capital and operational expenses, including financing costs, providing a comprehensive understanding of the actual cost of producing hydrogen. The LCOH is defined below as follows

$$\mathrm{LCOH} = \frac{\mathrm{CAPEX} + \frac{\sum_{n=1}^{t} \mathrm{OPEX}}{(1+r)^t}}{\frac{\sum_{n=1}^{t} P}{(1+r)^t}} \tag{3.10}$$

$$\mathrm{CAPEX} = \mathrm{C_{SOE}} \times \mathrm{CAPEX/KW} \tag{3.11}$$

$$\mathrm{OPEX} = (\mathrm{C_{SOE}} \times \mathrm{O\&M\ OPEX/KW}) + (\frac{\dot{m_{H2O}} \times 3600 \times \mathrm{hours} \times \mathrm{Steamcost}}{1000}) + \mathrm{Power(KWh)} \times \mathrm{Power\ price} \tag{3.12}$$

where

CAPEX - Total CAPEX cost of electrolyzer ($)

OPEX - Total OPEX of electrolyzer unit per year ($/year)

P - Hydrogen production/ year (Kg)

t - Year

r - Discount rate (%)

3.2.2 CSP Unit block modelling

Goal here is to establish a 0D system level model which is capable of estimating the specifications of the CSP plant in a high level, the model for a fixed power block duty and geography should be capable of estimating the solar field area, storage hours, CAPEX,OPEX and LCOE for the CSP plant.The basic unit block representation for the CSP plant can be seen in figure 3.1 The inlet energy and material streams are solar energy and water respectively. The output energy and material streams are electricity and steam respectively. In order to describe a model for this system we have to understand the energy conversion at different subsystems in the CSP plant. Figure 3.4 describes the different subsystems in the CSP plant.

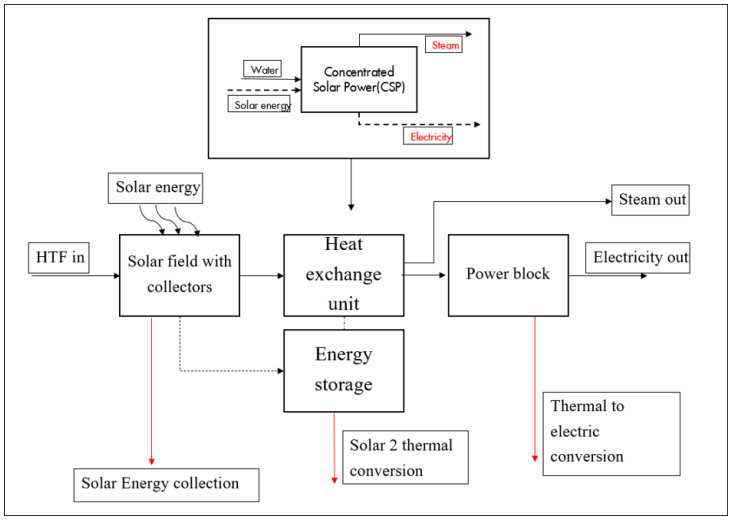

Figure 3.4: CSP subsystems description. 3 important sections are solar energy collection, solar to thermal conversion and lastly thermal to electric conversion.

The general working of the CSP plant can be understood as follows with help of figure 3.4.Solar field with solar concentrators collects the solar energy by means of a heat transfer fluid (HTF), this HTF produces steam in the heat exchange unit which is used to drive a turbine-generator system in the powerblock. The flow of energy is determined by the efficiency at every stage, 3 main efficiencies are used to describe the process 1.Solar to thermal efficiency, 2. Thermal to electric efficiency and 3. Solar to electric/ round trip efficiency. The solar energy available is determined by the geography of the plant predominantly and it should also be understood it is an instantaneous value, due to the intermittency with the solar energy there is a capacity factor (CF) associated with the plant. In some cases CSP plant would employ energy storage in which excess energy from the solar field is stored in the form of heat. This energy is used to produce steam and eventually electricity during hours of low sunshine.Addition of energy storage system would increase the hours of operation of the CSP plant.

$$\text{CF} = \frac{\text{Energy Output (KWh)}}{\text{Hours} \times \text{Name plate capacity (KWh)}} \tag{3.13}$$

Using the description of our system we can develop 0D models which are capable of estimating the area of solar field required, over sizing of the solar field required when storage is incorporated and other economic parameters like CAPEX, OPEX and LCOE. To make these estimations certain assumptions have to be made and they are listed in the following table.

Table 3.2: Assumptions for CSP plant

1	Solar to thermal conversion - η_{s2t}	-	0.6
2	Thermal to electric conversion - η_{t2e}	-	0.34
3	Solar to Electric conversion - η_{s2e}	-	0.20
4	OPEX costs	$ /KW-thermal Year	7

It should be noted the Solar-electric conversion is the product of solar-thermal and thermal-electric conversion.The values for these conversion were obtained from [47]. The values for OPEX were obtained from the targets for 2030 set by US department of energy under sun-shot initiative of 2011 [48]. The assumptions for specific CAPEX ($/ KW) is not straightforward, the current values prescribed by agencies like NREL,IRENA only provide the value for a particular plant size with storage. Even though this may be representative for plants of that size, for economic estimations we need our specific CAPEX values to scale with hours of energy storage. This is necessary because solar field would be oversized as a function of hours of storage, for this purpose the relationship between CAPEX and hours of storage was estimated using a tool provided by shell and is represented as a figure 3.5.

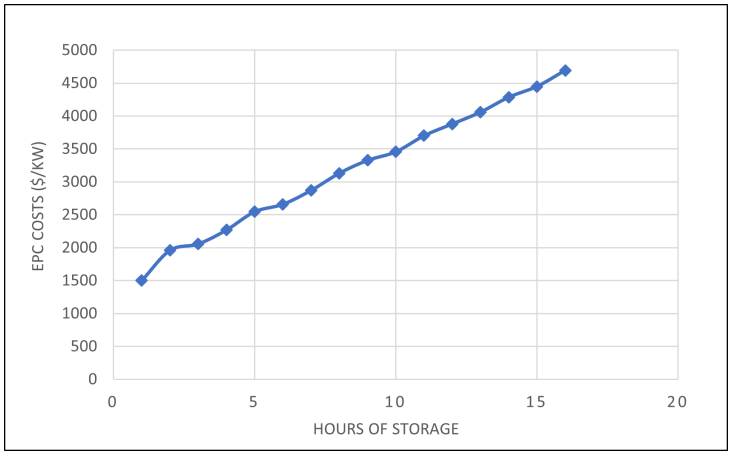

Figure 3.5: EPC costs for CSP with different hours of storage

As the hours of storage increases we notice the CAPEX ($/KW) also increases, this is because as we increase the hours of storage the field will have to be oversized accordingly to capture enough solar energy. The factor at which the field is oversized is represented by a parameter known as Solar Multiple (SM). SM has to be chosen carefully as high SM would lead to over-sizing the field more than necessary. When hours of storage for the plant is fixed, there is an optimal SM value which gives the lowest Levelized cost of electricity (LCOE). In our calculations we adopt this SM value. This relationship is represented by curve provided by NREL in figure 3.6.

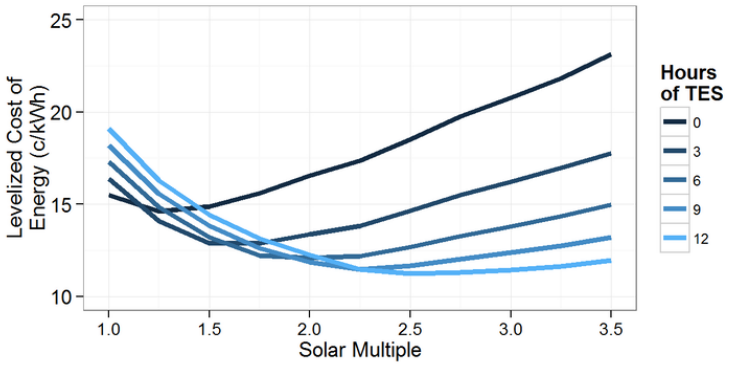

Figure 3.6: Relationship between SM,LCOE and hours of storage as estimated by NREL 3.6

Estimating the energy requirements

Let $\mathrm{C_{CSP}}$ be the duty of the CSP plant in MW. By using the assumptions from the table 3.2 we can estimate the energy requirement from the Solar field to heat exchange unit and from the heat exchange unit to Power block $\mathrm{PB_{th}}$ and Solar Heater (SH)

$$\mathrm{PB_{th}(MW_{th})} = \frac{\mathrm{C_{CSP}}}{\eta_{t2e}} \tag{3.14}$$

Now in addition to the thermal energy supply to the power block a portion of the thermal energy is used to produce steam (150 °C). The thermal energy requirement for this solar heater is given by the following equation.

$$\mathrm{SH(MW_{th})} = \dot{m} C_{pw} \Delta T \tag{3.15}$$

These thermal energy requirements has to be supplied by the solar field, using this we can estimate the amount of Solar energy that has to be collected in our solar field.

$$\text{Solar Energy} = \mathrm{SM} \times \frac{\mathrm{PB_{th}} + \mathrm{SH}}{\eta_{s2t}} \tag{3.16}$$

Additionally using this solar energy we can also estimate the area of the solar field required in a simple way using the DNI $(\mathrm{W/m^2})$ of the location.

$$\text{Area} = \frac{\text{Solar Energy}}{\text{DNI}} \tag{3.17}$$

Economic Estimations

Levelized Cost of Electricity (LCOE) is a frequently used parameter to estimate the cost of electricity produced in project economics. It takes into account all capital and operational expenses, including financing costs, providing a comprehensive understanding of the actual cost of producing electricity and acts as a parameter of comparison between various different technologies.

$$\text{LCOE} = \frac{\text{CAPEX} + \frac{\sum_{n=1}^{t} \text{OPEX}}{(1+r)^t}}{\frac{\sum_{n=1}^{t} P}{(1+r)^t}} \tag{3.18}$$

$$\text{CAPEX} = \text{C}_{\text{CSP}} \times \text{CAPEX/KW} \tag{3.19}$$

$$\text{OPEX} = \text{Solar Energy} \times \text{O\&M OPEX}(\$/\text{KW})) \tag{3.20}$$

where

CAPEX - Total CAPEX cost of CSP Plant ($)

OPEX - Total OPEX of CSP unit per year ($/year)

P - Electricity production/ year (KWh)

t - Year

r - Interest rate (%)

3.2.3 Unit block for the Combined CSP-SOE Plant

To create a comprehensive OD system level model for the CSP-SOE system, we utilize the unit block model developed for both SOE and CSP in the previous section. This allows us to combine the two models and understand the performance of the integrated CSP-SOE plant. Using a similar approach as the SOE model, we calculate the financial indicators of the combined system, such as the levelized cost of electricity (LCOH).

$$\text{LCOH} = \frac{\text{CAPEX} + \frac{\sum_{n=1}^{t} \text{OPEX}}{(1+r)^t}}{\frac{\sum_{n=1}^{t} P}{(1+r)^t}} \tag{3.21}$$

The CAPEX and OPEX values are estimated as follows

$$\text{CAPEX} = \text{CAPEX}_{\text{CSP}} + \text{CAPEX}_{\text{SOE}} \tag{3.22}$$

$$\text{OPEX} = \text{OPEX}_{\text{CSP,O\&M}} + \text{OPEX}_{\text{SOE,O\&M}} \tag{3.23}$$

CAPEX - Total CAPEX cost of the plant ($)

OPEX - Total Maintenance costs of the plant unit per year ($/year)

P - Hydrogen production/ year (Kg)

t - Year

r - Interest rate (%)

3.3 Results & Discussions of the Conceptual Study

High-level analysis of the CSP-SOE integration was made using the system level model outlined in the previous section. This analysis provided insights into several critical aspects, including identifying the parameters with the highest impact on the system's performance, determining the most suitable integration pathway, identifying optimal operation points, and evaluating the economics of the system. In this section, we will discuss these insights in detail, and the final results of this concept study will be carried over to the engineering phase.

3.3.1 Identification of high impact parameters

To better understand the performance and economics of the CSP-SOE system, it is crucial to identify the parameters that have the most significant impact. To achieve this,a sensitivity analysis was conducted on selected parameters that affect the unit cost of hydrogen. The unit cost of hydrogen was calculated by dividing the total expenditure and operational costs by the total amount of hydrogen produced over the analysis period and a similar unit cost model for electricity production from CSP was also used in terms of ($/KWh). Since the primary objective of this exercise was to identify the parameters with the highest impact on hydrogen cost,a simple unit cost model would be sufficient. Different parameters were varied by 30% both positively and negatively, the effect of these changes on the unit cost of hydrogen ($/Kg) and electricity ($/KWh) are studied and is represented as a table in the figure. 3.7. The base case values of all these parameters can be found in tables 3.1 and 3.2

Sensitivity analysis on unit cost of hydrogen from SOE ($/Kg)

Parameter(Change)	-30%	-25%	-20%	-15%	-10%	-5%	Base	5%	10%	15%	20%	25%	30%
Power Price ($/KWh)	2.22	2.28	2.34	2.40	2.46	2.52	2.58	2.65	2.71	2.77	2.82	2.88	2.94
O&M (Million $/Year)	2.38	2.41	2.44	2.48	2.52	2.55	2.58	2.62	2.66	2.69	2.72	2.75	2.78
Steam Cost($/Tonne)	2.45	2.47	2.49	2.52	2.54	2.56	2.58	2.61	2.63	2.65	2.67	2.69	2.71
CAPEX($/KW)	2.52	2.53	2.54	2.55	2.56	2.57	2.58	2.60	2.61	2.62	2.62	2.63	2.64

Sensitivity analysis on unit cost of electricity from CSP ($/KWh)

Parameter(Change)	-30%	-25%	-20%	-15%	-10%	-5%	Base	5%	10%	15%	20%	25%	30%
Capacity Factor	0.08	0.07	0.07	0.06	0.06	0.06	0.05	0.05	0.05	0.05	0.05	0.04	0.04
CAPEX($/KW)	0.04	0.04	0.05	0.05	0.05	0.05	0.05	0.06	0.06	0.06	0.06	0.07	0.07
OPEX($/KW/Year)	0.05	0.05	0.05	0.05	0.05	0.05	0.05	0.06	0.06	0.06	0.06	0.06	0.06

Sensitivity analysis on unit cost of hydrogen from CSP-SOE ($/Kg)

Parameter(Change)	-30%	-25%	-20%	-15%	-10%	-5%	Base	5%	10%	15%	20%	25%	30%
CSP CAPEX($/KW)	2.68	2.74	2.80	2.86	2.91	2.97	3.03	3.09	3.20	3.26	3.26	3.32	3.38
CF	3.26	3.22	3.18	3.14	3.11	3.07	3.03	2.99	2.92	2.88	2.88	2.84	2.80
Power Price ($/KWh)	2.88	2.91	2.93	2.96	2.98	3.00	3.03	3.05	3.10	3.13	3.13	3.15	3.18
CSP OPEX($/KW/Year)	2.94	2.96	2.97	2.99	3.00	3.02	3.03	3.04	3.07	3.09	3.09	3.10	3.12
SOE CAPEX($/KW)	2.96	2.97	2.98	3.00	3.01	3.02	3.03	3.04	3.06	3.07	3.07	3.09	3.10
Steam Cost($/Tonne)	2.98	2.99	3.00	3.00	3.01	3.02	3.03	3.04	3.06	3.06	3.06	3.07	3.08

Figure 3.7: Sensitivity of different parameters to hydrogen costs. For CSP-SOE system the capacity factor and CSP specific CAPEX have the largest impact on economics

3 tables are shown in the figure, first figure is the sensitivity analysis on cost of hydrogen produced from a standalone SOE plant, the second table represents the sensitivity on cost of electricity produced from a CSP plant based on different parameters and the third table represents the sensitivity on unit cost of hydrogen produced from a combined CSP and SOE plant. The table represents this impact for various parameters and ones with highest impact are on top of the table and vice versa. It can be seen that for the combined plant CSP CAPEX and Capacity factor (CF) play a huge role in the cost of hydrogen.

3.3.2 Identification of suitable integration pathway

The basic hypothesis which suggests CSP-SOE integration is beneficial than standalone SOE is that a standalone SOE system consumes electricity from the grid and this contributes to a big chunk of the

hydrogen cost. Having said this, the selection of pathway for integration is not trivial and requires some analysis before proceeding. For this reason 3 scenarios are studied and compared against each other.

- Standalone SOE Plant : This is standalone SOE plant with connection to the electricity grid, this system is used as a reference case for comparison of the other two system.
- On grid CSP + SOE system : This is CSP + SOE system with connection to the electricity grid, this system uses the electricity produced by the CSP to run the SOE plant and grid electricity is only used in hours where the solar energy is not enough to run the system. This also means that the dependence on power provided by the electricity grid is still present which reflects in the increased OPEX costs. In this case the effect of electricity prices are even more prominent, this is because CSP plants are typically installed in remote locations and grid electricity in remote locations are costlier owing to lack of infrastructure. [49]
- Off grid CSP + SOE system : This is CSP + SOE system with no connection to the grid. However, this system employs thermal energy storage options to over come the intermittency of the solar radiation. It should be noted that incorporation of storage would mean that the solar field would have to be oversized to capture the solar energy required by the thermal storage system. This addition of solar field also means there is addition to the CAPEX of the system.

The comparison of these 3 pathways would be on the basis of the LCOH,certain assumptions have been made to make the comparison of these three pathways, this is important because parameters such as capacity factor (CF) have large impact on the LCOH and operating the 3 plants at different capacity factors would not lead to a like to like comparison. For this reason all three pathways are assumed to be operating at 70% capacity factor i.e the plants are capable of producing hydrogen only 70% of the time. The hydrogen production of all these pathways are fixed to 100 tonnes/day. CSP plant on its own can power the SOE unit only 30% of the time and to achieve a CF of 0.7 electricity has to be purchased from the grid for rest of hours or energy storage of equivalent number of hours has to be employed for the on grid and off grid pathways respectively. These calculations have also been taken into the account. The LCOH values for all 3 pathways have been shown in the figure and the breakdown of the number has been reported in the table.

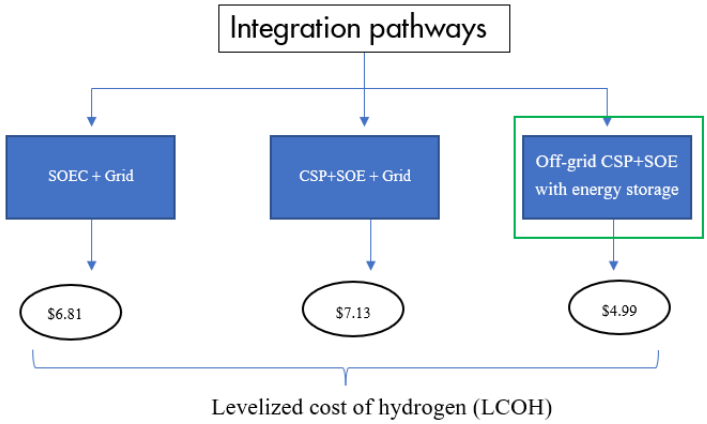

Figure 3.8: calculated LCOH values of all 3 pathways

Table 3.3: Detailed breakdown of the LCOH of all 3 pathways

S.No	Parameters	Unit	SOE+GRID	CSP+SOE+GRID	CSP+SOE
1	Daily H2 Production (Yearly Average)	tonnes	100	100	100
2	SOE Power requirement	MW	232	232	232
3	CSP electric duty	MW	-	232	232
4	Plant CF	-	0.7	0.7	0.7
5	CSP power (%)	-	-	40%	100%
6	Grid Power (%)	-	100%	60%	-

Table 3.3: Detailed breakdown of the LCOH of all 3 pathways

S.No	Parameters	Unit	SOE+GRID	CSP+SOE+GRID	CSP+SOE
7	SOE CAPEX	Million $	464	464	464
8	SOE OPEX/year	Million $	205	162	36
9	CSP CAPEX	Million $	-	450	896
10	CSP OPEX/year	Million $	-	12	18
11	Total CAPEX	Million $	464	915	1360
12	Total OPEX/year	Million $	205	174	54
13	LCOH	$/kg	6.8	7.13	4.99

From the figure 3.8 it can be seen that off grid system has the lowest LCOH values among the three pathways. The table 3.3 breaks down the calculation of these LCOH numbers and provides more detail. It can be seen all three pathways operate at same capacity factor and hydrogen production rate, this imposes a power requirement for the SOE and the CSP plant in our system is matched to provide this energy to the SOE. The contribution of CSP and grid for hydrogen production is also reported for the on-grid system. As mentioned previously the electricity costs for the on-grid CSP-SOE system is higher than the usual and the value is assumed to be 0.18 $/KWh [28] and it can be seen the purchase of grid electricity has increased the OPEX of this system in comparison with off grid. In case of the off grid system the high capacity factor is achieved by employing energy storage and the consequence of this is the increased CAPEX costs. In this case achieving high capacity factor by spending money on CAPEX is more beneficial than spending money on the OPEX yearly. However, it should be mentioned the market of CSP is changing rapidly and this means the specific CAPEX costs ($/KW) could change quickly as well. NREL has predicted a range of specific CAPEX values of the CSP [50] and along with a range of CAPEX values for SOE provided by shell, a sensitivity chart was made to see the behaviour of LCOH at different price positions. It can be seen from the sensitivity chart LCOH values as low as (4$/Kg) are possible if

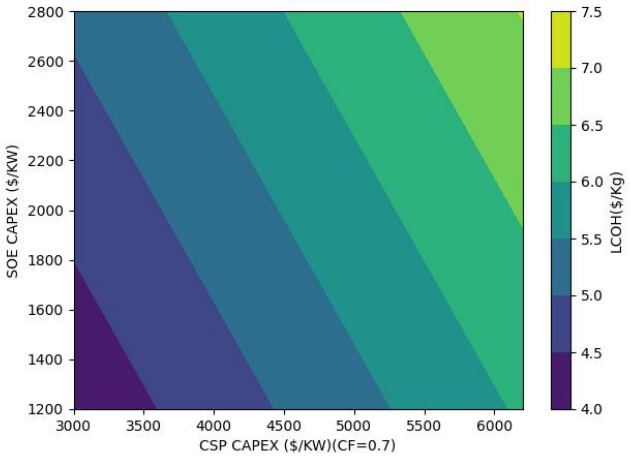

Figure 3.9: LCOH sensitivity on range of CAPEX values predicted by NREL

there is cost reduction in CAPEX values of CSP and SOE. General consensus across industry is that the CAPEX values for CSP and SOE are going to decrease and throughout history the power prices from the grid have always increased every decade. Considering this off grid CSP-SOE integration is the selected pathway and further investigations will be carried out.

3.3.3 Effect of capacity factor on LCOH

As seen from the the figure 3.7 it is clear how much of an impact CF has on the LCOH, in the previous analysis of determining the suitable pathway the CF was fixed to get like to like comparison. In this analysis, by fixing the the production to 100 tonnes/day all the other parameters are varied as function CF, finally the LCOH is also mapped out as a function of CF. In the CSP-SOE integration, the selection of operating CF is not trivial. At lower CF to achieve 100 tonne production all the equipment are oversized than in comparison to operation at higher CF, putting it simply at lower CF we have high SOE power consumption and therefore to match the requirement we need CSP system capable of producing that much power. To achieve high CF however the solar resource (Solar Resource : Solar energy collected in the solar field) has to be increased in order to cater to the demands of thermal energy storage systems, which implies an additional costs due to field over-sizing and addition of thermal energy storage equipment.A trade off has to be obtained after looking into the behavior of these parameters as a function capacity factors (CF).

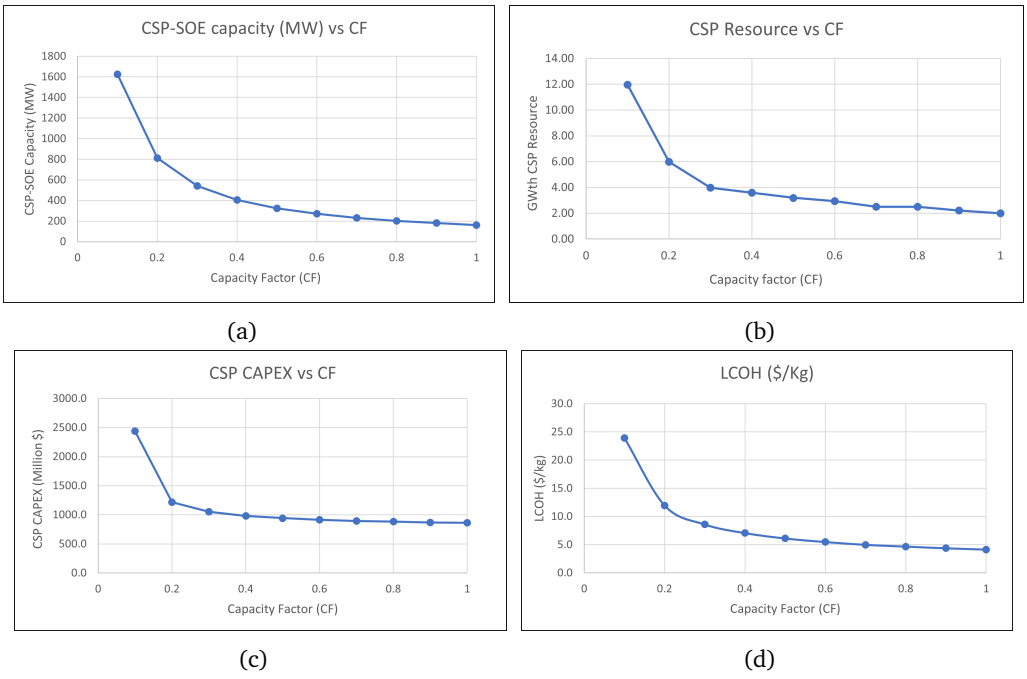

Figure 3.10: Variation of different parameters as function of capacity factor

It can clearly be seen from the figure that low capacity factors imposes high energy requirement from the SOE/CSP due to large over-sizing of the SOE plant to maintain 100 tonne/day of production, this means at lower CF more and more energy has to be captured in the solar field which increases the size of all equipments in the CSP plant leading to high capacity of CSP and SOE. The interesting observation here is that even at higher CF the CSP CAPEX continues to reduce, this is counter intuitive as we expect the cost of adding thermal energy storage to increase the CAPEX significantly. However,this trend is not observed and this is attributed to the low thermal energy storage costs. If a costlier energy storage option is employed this trend will be observed. This goes to show the benefit of operating at high capacity factors, it can also be seen from the LCOH curve the benefit of improving the CF is much better at lower CF than at higher CF i.e the LCOH reduction for increase in CF is diminishing. For this reason we choose the CF value at which the LCOH curve starts to flatten, therefore a target CF of 70% is taken as optimal. The details of all breakdown of the LCOH curve is reported in the table 3.4.

Table 3.4: Different parameters as function of CF

CF	SOE MWp	CSP MWp	CSP Resource (GWth)	H2 Prod (Mt/year)	LCOH ($/Kg)	CSP CAPEX (M$)	SOE CAPEX (M$)	SOE OPEX (M$)	CSP OPEX (M$)
0.1	1625.0	1625.0	12.0	36.5	23.9	2437.5	3250.0	251.9	83.8
0.2	812.5	812.5	6.0	36.5	12.0	1218.8	1625.0	125.9	41.9
0.3	541.7	541.7	4.0	36.5	8.6	1050.8	1083.3	84.0	27.9
0.4	406.3	406.3	3.6	36.5	7.1	983.1	812.5	63.0	25.1
0.5	325.0	325.0	3.2	36.5	6.1	942.5	650.0	50.4	22.3
0.6	270.8	270.8	2.9	36.5	5.5	915.4	541.7	42.0	20.5
0.7	232.1	232.1	2.5	36.5	5.0	896.1	464.3	36.0	17.6
0.8	203.1	203.1	2.5	36.5	4.7	881.6	406.3	31.5	17.5
0.9	180.6	180.6	2.2	36.5	4.4	870.3	361.1	28.0	15.5
1.0	162.5	162.5	2.0	36.5	4.1	861.3	325.0	25.2	14.0

3.3.4 Comparing the CSP-SOE system with other green hydrogen technologies

The LCOH vs CF curve acts as good performance indicator for the off grid CSP-SOE system, along with this different performance data points were collected from the literature and were reported. Among the various data points collected from the literature reliable mentions of the CF values were missing and in these cases values of CF for the particular region were adopted from different studies(Ex. For the Guajira Wind park there are no mentions of official CF values, however there are studies that report the CF values of a wind park in that region). The only study which had mentions of LCOH values as function of capacity factor was the Shell/TNO study which analysed the integration AWE+PV+Battery electric storage system-BESS(in the study, the LCOH were obtained as function hours of energy storage used) . When we compare our CSP+SOE system with this particular study, the benefit of CSP+SOE is clear at high capacity factors. CSP+SOE systems provide low cost green hydrogen production at high capacity factors and the benefit of CSP-SOE over PV-Alkaline takes place at capacity factors greater than 0.35 as the crossover can be observed from the graph. The studies and the data points were obtained from [51–55]

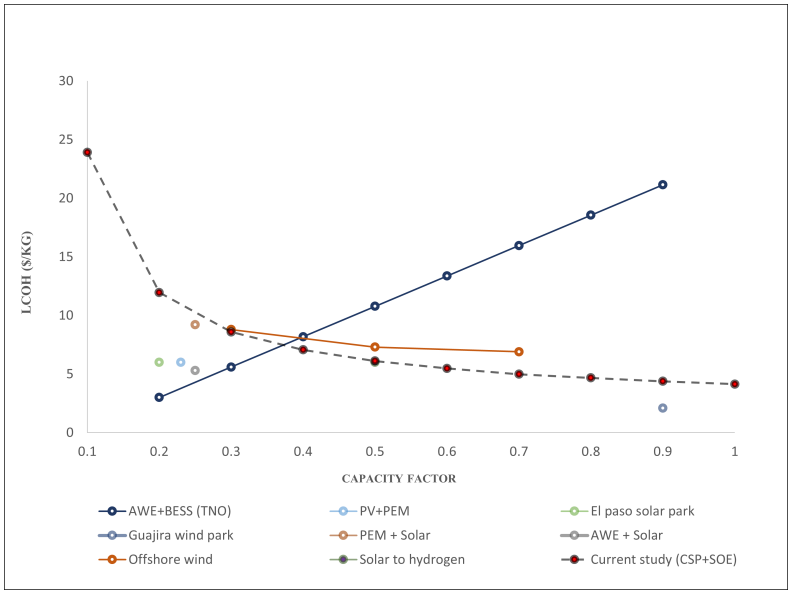

Figure 3.11: Comparing the current study with other green hydrogen technologies. CSP-SOE systems fare better in achieving high CF at low LCOH

3.3.5 Analysing the system by incorporating a varying DNI profile

In the subsection 3.2.2 CSP unit-block has been described on the basis of solar Energy, it is important to understand the solar energy and its utilisation. The solar energy from the sun comes in 3 different 1. Direct Normal Irradiation (DNI), Global Horizontal Irradiation (GHI), 3. Direct Horizontal Irradiation (DHI), the CSP technology is capable of utilizing only the DNI component of the DNI component of the solar irradiation (W/m^2) [56]. The geography dictates the DNI and it is higher in regions that are closer to the equator, DNI is also impacted by the elevation of a particular geography as at higher elevation there is lesser scattering of the solar energy by atmospheric hindrances. The distribution of DNI has been mapped out by many different sources and the Global Solar atlas is a reliable reference [57].The evaluation of site for CSP plant has set of detailed practices primarily based on the solar resource categorisation [50] and this procedure is well established in literature and industry guidelines. The selection of geography for CSP is a separate work by itself and in this study India has been selected as the geography due to the several factors that include cost-effectiveness, good hydrogen landscape, suitable governmental policies and interest's of shell business in that region. All the analysis done up till this point has incorporated a constant value for DNI and in this analysis a varying DNI curve of a location of Dhursar in Rajasthan,India will be used.Obtaining the DNI values of this particular region was not straightforward and this DNI curve was generated using the open source System Advisor Model (SAM) provided by NREL.

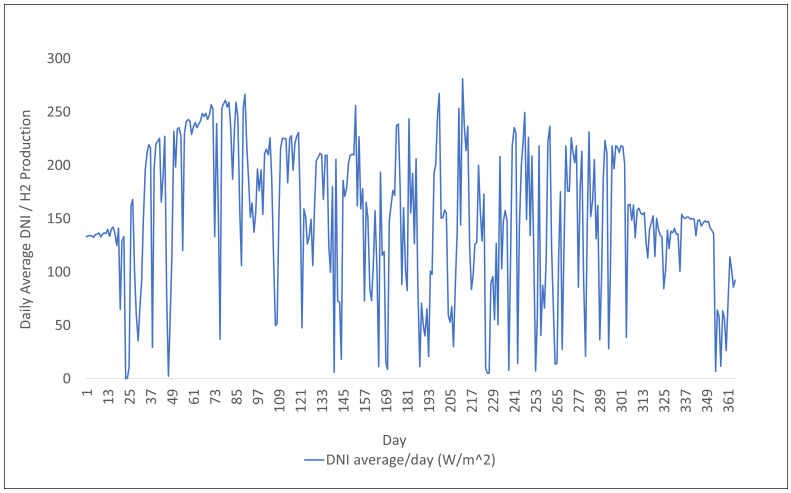

Figure 3.12: DNI curve of Dhursar,India generated using SAM

In this analysis, for a fixed production of 100 tonnes/day the CSP-SOE system is sized using the DNI profile for Dhursar as shown in the figure 3.12. Approach taken here is as follows first a design point DNI was calculated for this particular region. The design point DNI is simply the average DNI values for all the sunshine hours, this approach is taken as it resembles a DNI value which is closer to the actual DNI values during operation [56]. Using this Design point DNI the system solar field requirements and other equipments sizing was made. This is done primarily to make estimates for the area of the solar field required to achieve target production. This design when tested with the varying DNI profile instead of design DNI the system does not yield 100 tonnes/day of hydrogen, From this design point the system is resized to achieve 100 tonnes per day of hydrogen production. Resizing is based on two parameters CSP Resource (GWth) and SOE capacity (MWe), CSP resource is simply the solar energy collected in the area. For a fixed geography increasing or decreasing the CSP resource means increasing or decreasing the solar field area. The Oversizing chart is made for two cases without energy storage and with thermal energy storage(TES)capable of achieving 0.7 CF. It can be seen that curves all have

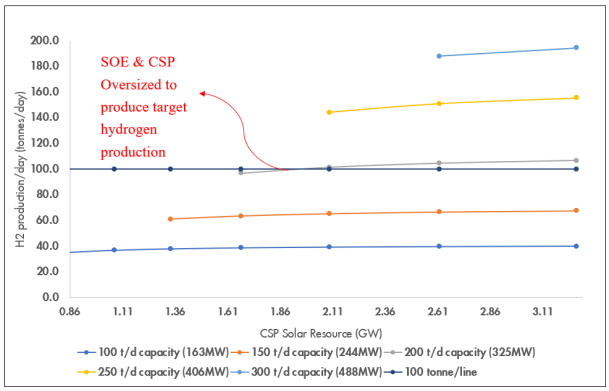

(a) Oversizing chart of system without TES

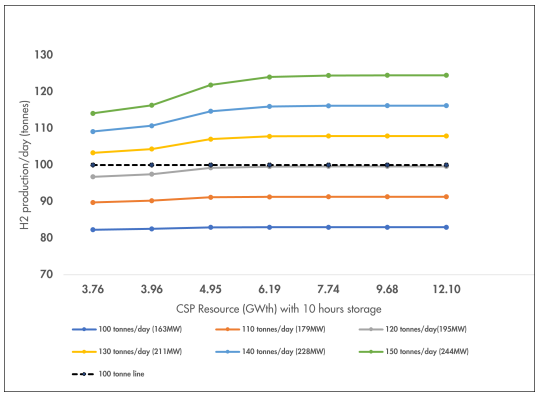

(b) Overizing chart of system with TES

Figure 3.13: Oversizing chart for systems with and without TES

different starting point and all the curves flatten at some point. The starting point (Ordinate) is dictated by the CSP resource employed. Flattening of these curves is determined by the SOE capacity, after some point it does not matter to what extent the solar field is overbuild (increasing solar resource) the system would be incapable of producing more hydrogen as the SOE capacity becomes limiting. For both the systems the the design point to achieve 100 tonne per day of hydrogen production can be obtained from these curves. For a system without TES the we need CSP resource of 1.90 GWth and SOE production capacity of 200 tonnes/day (325MW), for a system with TES we need CSP resource of 6.32GWth and SOE production capacity of 120 tonnes/day (195MW). The economics of building a system at these design point is reported in the table.

Table 3.5: Comparison of systems with and without TES

Parameter	System with TES	System without TES
Target H2 production	100	100
SOE CAPACITY (MWe)	195	325
CSP CAPACITY (MWe)	195	325
SOE CAPEX ($/Kg)	1.0	1.7
CSP CAPEX ($/Kg)	1.8	1.3
SOE OPEX ($/Kg)	0.8	1.4
CSP OPEX ($/Kg)	0.3	0.4
Total LCOH ($/Kg)	3.9	4.8

Chapter 4

Process Plant Design,Operation Economics

In the previous chapter basic sizing has been done to achieve the required capacity of the plants for target hydrogen production, In this chapter the detailed process and plant design is done to realize the specifications established in the conceptual study.

4.1 Process Scope

The general anatomy of a chemical manufacturing plant typically consists of six process section, starting from raw material storage and ending with product storage and sales [58]. Although our green hydrogen plant is not a conventional chemical plant, we can employ a similar approach as outlined by [58], with certain modifications. It is important to note that certain aspects, such as waste management and byproduct monetization, are not incorporated into our plant design. However, recycling of wastewater is assumed to be part of the process.

Here 3 sections of the plant are defined and using these 3 sections the scope of the plant design is defined.

1. Power & Feed Production : This is essentially our CSP plant which produces the required power and feed (steam) for our plant
2. Reactor : This is our SOE plant, which converts the LP steam from our CSP plant to hydrogen (wet)
3. Separation & Purification: This is our H2 processing system and here the low pressure wet hydrogen is converted to high pressure dry hydrogen of required purity.

The design choices for the plant are influenced by the quality requirements of the end user and therefore it is important to begin the scope definition from the end. Hydrogen has a very low volumetric density at ambient pressure and temperature, which necessitates pressurization of the hydrogen. Currently, large-scale hydrogen storage is carried out either underground in salt caverns (at 200 bar) or in existing natural gas pipelines (at 20-30 bars) [59]. In the case of this hydrogen production plant, the assumed end users are refueling stations. Typically, hydrogen refueling stations receive hydrogen at a pressure of 30 bar [60] with a dew point ranging from -60 to -90 °C [61]. Therefore, the delivery constraints for our H2 processing system are dry pressurized hydrogen at 30 bar with a moisture level of 0.1 ppmv. The intake constraint for H2 processing is water saturated wet hydrogen. The CSP plant is assumed to extract water at STP to produce the feed for the reactor, feed is at 3 bar and 150 °C. The figure 4.1 also represents the decided scope.

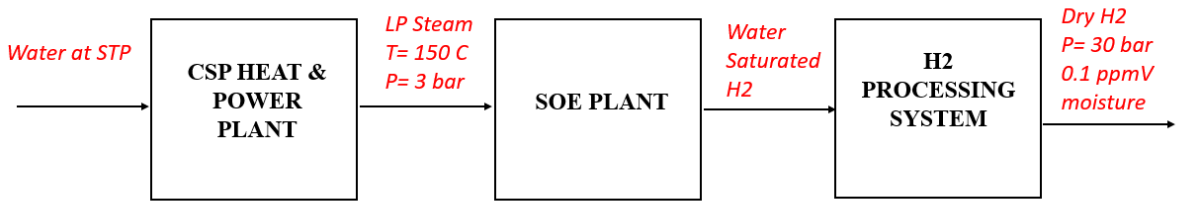

Figure 4.1: Defined scope for the process plant design, the intake and output constraints for all three unit blocks are defined in this flow

4.2 SOE Plant

Electrolyzer plants utilize a modular design, combining cells into stacks, stacks into modules, and modules into systems. This modular approach offers scalability, flexibility, and efficient operation in hydrogen production. It enables easy expansion or reduction of the system size, offers simplified maintenance, and optimized resource utilization. The individual cells within the stacks operate independently but collectively produce higher hydrogen output. Modules integrate multiple stacks, providing improved system integration and control. Multiple modules are combined to form complete electrolyzer systems. The architecture of SOE is demonstrated in the figure 4.2. For this work the focus will be on module and system level.

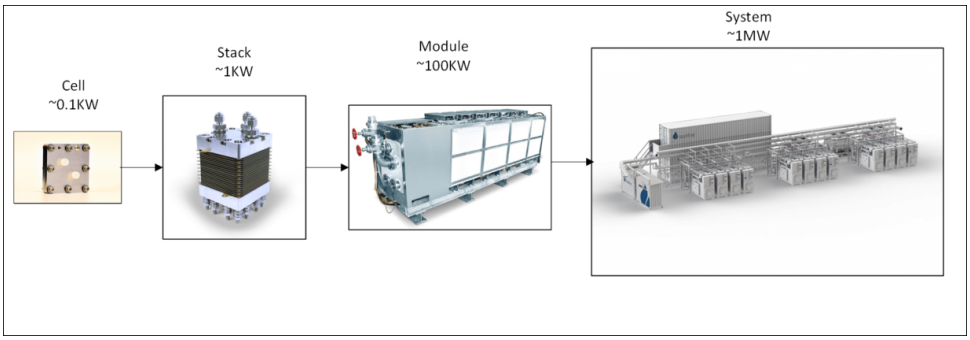

Figure 4.2: Scale up of electrolyzers from cell to system and the orders of magnitude go from KW for SOE cells to MW for SOE system

4.2.1 SOE System Design

From our target parameters 3 our task is to build a plant of $\sim$ 200MW. This would require collection of SOE systems to achieve a plant size of $\sim$ 200MW. Since the TRL of the SOE technology is still not at commercial level, in order to build SOE systems we will have to rely on designs from existing demonstration projects and adopt a similar approach. Green Industrial Hydrogen project (GrInHy) demonstrates the integration of steam electrolyzer developed by Sunfire with an industrial process (Salzgitter Flachstahl GmbH) [62].This provides us with a starting point and the SOE systems in this work are inspired by the Sunfire-HyLink systems. The SOE system design for our work is shown in the figure 4.3 There are two input streams to our SOE system, the first stream is the feed stream which takes in LP steam from the CSP plant, second stream is air from ambient which is blown to the SOE using a blower, the purpose of the air here is to act as a sweep gas. Two heat exchangers facilitate the pre heating of the input streams using the outgoing product gas. Two more heaters are used to bring the input streams to the operating temperature of the SOE reactor. Coolers downstream of the reactor is used to cool the hot air down to less than 100 °C and the hydrogen stream to saturation temperature.The specifications of the system is listed in the table.4.1

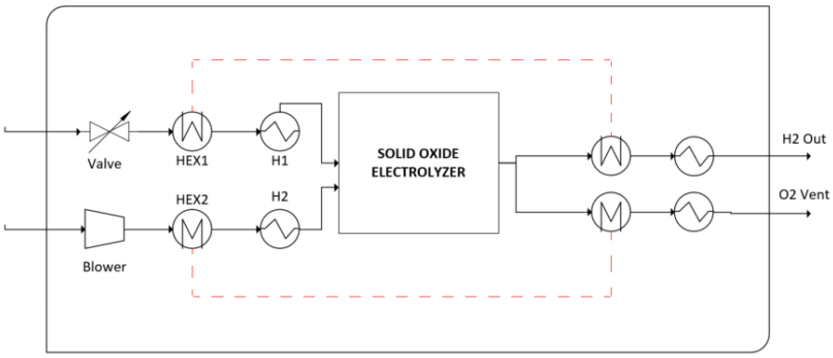

Figure 4.3: SOE system design, an SOE system consists of electrolyzer and other equipments to satisfy the boundary constraints

Table 4.1: SOE System specifications

S.No	Parameter	Specification
1	Power Consumption	20 MW
2	Inlet feed conditions	150 °C, 3 bar
3	H_2 side Outlet	wet H_2 , 300 mbar-gauge
4	O_2 side outlet	<100 °C, Exhausted

4.2.2 SOE Electrochemical Model, Aspen Implementation & Validation

The governing chemical equation for the electrolysis process is:

$$\mathrm{H_2O(g)} \longrightarrow \mathrm{H_2(g)} + \frac{1}{2}\mathrm{O_2(g)} \tag{4.1}$$

The Nernst equation can be used to estimate the the Nernst potential of the electrolysis system, this is the minimum voltage that has to be provided for the reaction to occur [63].

$$E_N = |E^\circ| + \frac{RT}{2F} ln(\frac{P_{H2}\sqrt{P_{O2}}}{P_{H_2O}}) \tag{4.2}$$

$$E^\circ = \frac{\Delta G^\circ}{2F} \tag{4.3}$$

Temperature dependant relation for Gibbs energy has been adopted from [64]

$$\Delta G^\circ = 246000 - 54.8.T \tag{4.4}$$

It should be noted that the Nernst potential estimated using the Nernst equation only valid in open circuit, when the circuit is completed i.e there is production of hydrogen due to irreversibility additional voltage has to be provided to account for the losses. The irreversibilities are usually classified into 3 over potentials

- Ohmic Over potential : Over potential due to resistance in the electrolyte or materials used.
- Activation Over potential : Over potential needed to overcome the energy barrier for a reaction to occur as described by the Buttler-Volmer equation.
- Concentration Over potential: Over potential caused by slow diffusion or mass transfer of reactants/products near the electrode, affecting reaction kinetics.

The current commercial option for the solid oxide electrolyte (SOE) is the planar Electrolyte-supported cell (ESC). It is constructed using a thick electrolyte that supports thin electrodes. The electrolytes consist of solid ceramics, specifically Yittrium-stabilized zirconia, which exhibit high ionic conductivity and low electrical conductivity. Consequently, there is a significant Ohmic overpotential in comparison to

activation and concentration overpotential. As a result, the activation and concentration overpotential can be disregarded, and the resistance due to Ohmic overpotential can be considered solely as a function of temperature. To quantify the losses resulting from resistance, a lumped temperature-dependent resistance term known as Area Specific Resistance (ASR) is utilized. Correlations for the ASR were obtained from the DLR test rig and subsequently employed to estimate the ASR values [64].

$$V_{cell} = E_N + E_{loss} \tag{4.5}$$

$$E_{loss} = j.ASR \tag{4.6}$$

where j is the current density and the current for the SOE is given by the following formula, where U is the steam utilisation factor.

$$I_{SOE} = U_f.2.F.n\dot{H_2}O \tag{4.7}$$

The power required for SOE operation is given by

$$P_{SOE} = V_{cell}.I_{SOE} \tag{4.8}$$

The heat of the process is described by

$$\dot{Q_{SOE}} = \Delta\dot{H}_{rxn}.\dot{n_{H2}} - P_{SOE} \tag{4.9}$$

The SOE implementation has been made in aspen based on the electrochemical model described, The Power of the SOE has been calculated using a calculator block. Rstoic reactor (B1), separator block (B3) have been used to carry out the reaction and imitate an electrolyzer. Rstoic (B1) has been considered because for our system the stoichiometry of the reaction is known and kinetics of the reaction is not considered. The flow sheet has been shown in the figure 4.4

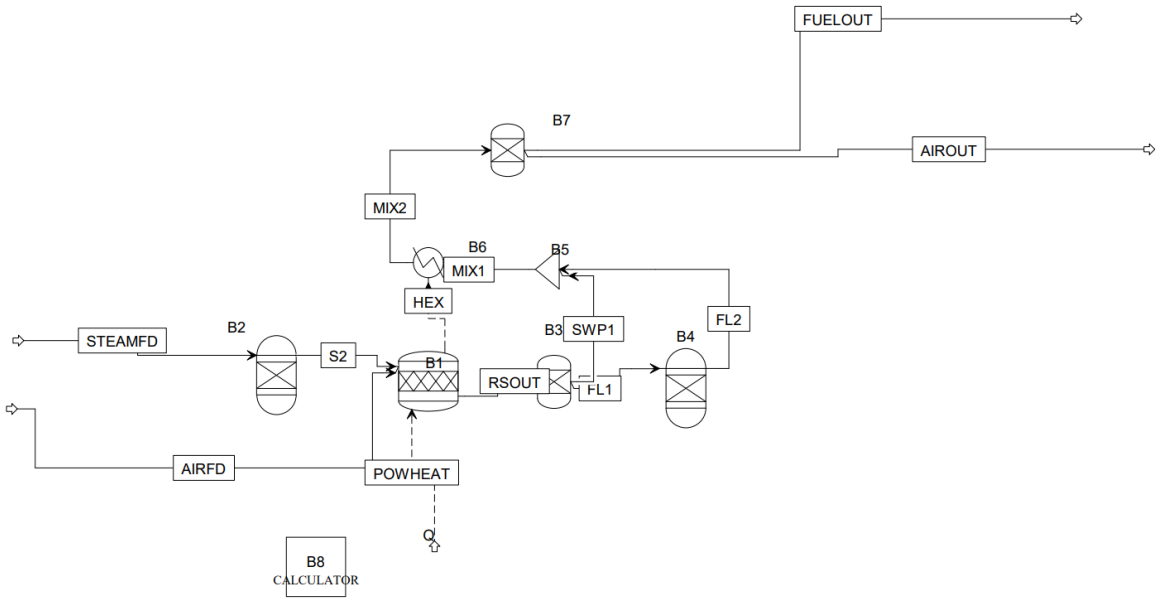

Figure 4.4: SOE Reactor Implementation in Aspen

The internal heat exchange in the SOE system has been mimicked by heater (B6), which extracts heat from the reactor. Additionally, two Gibbs reactors (B2, B4) have been incorporated into the Aspen model to enable co-electrolysis. Gibbs reactors were selected due to the requirement for chemical equilibrium calculations in co-electrolysis mode. However, this study focuses solely on steam electrolysis only. German Aerospace Center (DLR) studied the operation strategies for MW scale electrolysis system based on the DLR's SOEC test rig GALACTICA. Experiments and simulations were used to obtain set of stationary operating points for 3 different modes of operation 1. Full load Isothermal operation, 2. Part Load and 3. Hot standby mode [65].

- Full Load : This operation indicates the SOE system is the producing hydrogen at its full capacity, the inlet and outlet stream temperature in this mode is same and therefore this mode is considered also to be isothermal
- Part Load : Here the hydrogen production is not at full capacity rather reduced to a certain set point, in this case unless mentioned otherwise part load indicates 50% of the design hydrogen production. It should be noted hydrogen production is reduced by reducing the feed supplied.
- Hot Standby : In this mode no hydrogen is being produced, the power consumed by the system is used to maintain the reactor closer to the operating temperature.

The isothermal operation point obtained by [65] was used to validate the electrochemical model and aspen implementation.The results of the validation of isothermal operation point is listed in the table 4.2.

Table 4.2: Validation of Isothermal steam electrolysis condition

S.No	Parameter	Units	OP2 - Isothermal (Design Load)		
			Paper	Model	% var.
1	Reactant Conversion	-	0.7	0.7	NA
2	H2 inlet mole fraction	-	0.1	0.1	NA
3	H2O inlet mole fraction	-	0.9	0.9	NA
4	Air Inlet flow	g/s	12.1	12.1	NA
5	Inlet flow (calculated using the data provided in ref.paper)	mol/s	0.411	0.411	NA
6	Feed Inlet temperature	C	830	830	NA
7	Air Outlet temperature	C	830	830	0%
8	O2 outlet mole fraction	-	0.4	0.4	0%
9	Power	KW	64.3	64.35	0%

In order to overcome situations of scarce energy production, SOE typically have other operational modes apart from full load isothermal operation. One such operation mode is the previously mentioned chemical part load operation, in this mode instead of producing hydrogen at nominal production the hydrogen production is reduced to utilize the available power. DLR [65] has published the stationary operating points for the part load operations as well. It should be noted that when the SOE is operated in part load, the heat addition from the internal losses reduces due to reduction in current density which thereby reduces the reactor temperature. This means upstream of the reactor bigger air heater must be installed to provide higher flow-rate of sweep gas. Another method of maintaining the reactor temperature is by adjusting the inlet temperature, however this is not recommended as this leads to non uniform temperature at the reactor which damages the stacks [65]. The aspen model is also validated for this operation mode and the results are listed in the table 4.3.

Table 4.3: Part Load operation validation results

S.No	Parameter	OP3 - Part Load		
		Paper	Model	% var.
1	Reactant Conversion	0.7	0.7	NA
2	H2 inlet mole fraction	0.1	0.1	NA
3	H2O inlet mole fraction	0.9	0.9	NA
4	Air Inlet flow (g/s)	73.8	73.8	NA
5	Inlet flow (calculated using the data provided in ref.paper) (mol/s)	0.22792	0.22792	NA
6	Feed Inlet temperature (°C)	830	830	NA
7	Air Outlet temperature (°C)	797	816	2%
8	O2 outlet mole fraction	0.23	0.23	0%

Since SOE operate at temperatures as high as 800 °C, to have a cold shut down every time there is scarce power production is unrealistic and also risky as high temperature non uniformity could damage the cells. To counter this issue, SOE are operated in hot standby i.e during scarce power production situations higher flow rates of hot sweep gas is supplied to keep the reactor close to the operating temperature (upto a minimum of <50 K from operating temperature). The aspen model is also validated for this mode and the results are reported in the table 4.4. In order to simulate one minor change has to be made to the aspen file, an additional heater to mimic the heat loss to the ambient has to be added. It should also be noted that during hot standby mode the steam feed is replaced with nitrogen, this is

done in order to prevent the cathode side oxidation during standby conditions. The modified aspen file is shown in the figure 4.5.The details of the calculation of part load and hot standby power consumption for our system are calculated in the following subsections.

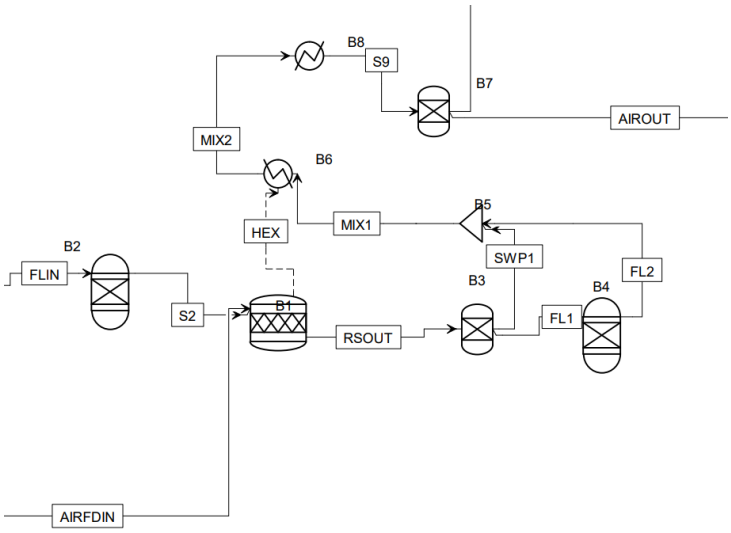

Figure 4.5: Aspen flow sheet for Hot standby mode

Table 4.4: Validation results of hot standby mode

S.No	Parameter	Hot standby		
		Paper	Model	% var.
1	Reactant Conversion	0.7	0.7	NA
2	H2 inlet mole fraction	0.05	0.05	NA
3	N2 inlet mole fraction	0.95	0.95	NA
4	Air Inlet flow (g/s)	21.5	21.5	NA
5	Power	-	-	NA
6	Form gas Inlet flow (calculated using the data provided in ref.paper) (mol/s)	2	2	NA
7	Feed Inlet temperature (°C)	830	830	NA
8	Air Outlet temperature (°C)	797	797	0%
9	O2 outlet mole fraction	0.21	0.21	0%

4.2.3 SOE System - Full Load Operation

The implementation shown in figure 4.4 was the aspen implementation of the reactor alone. A SOE system as described in figure 4.3 consists of feed pre-treatment system and after coolers. Now using the SOE reactor developed in aspen the balance of system is built around the reactor. The schematic of the SOE system is demonstrated using the figure 4.6.

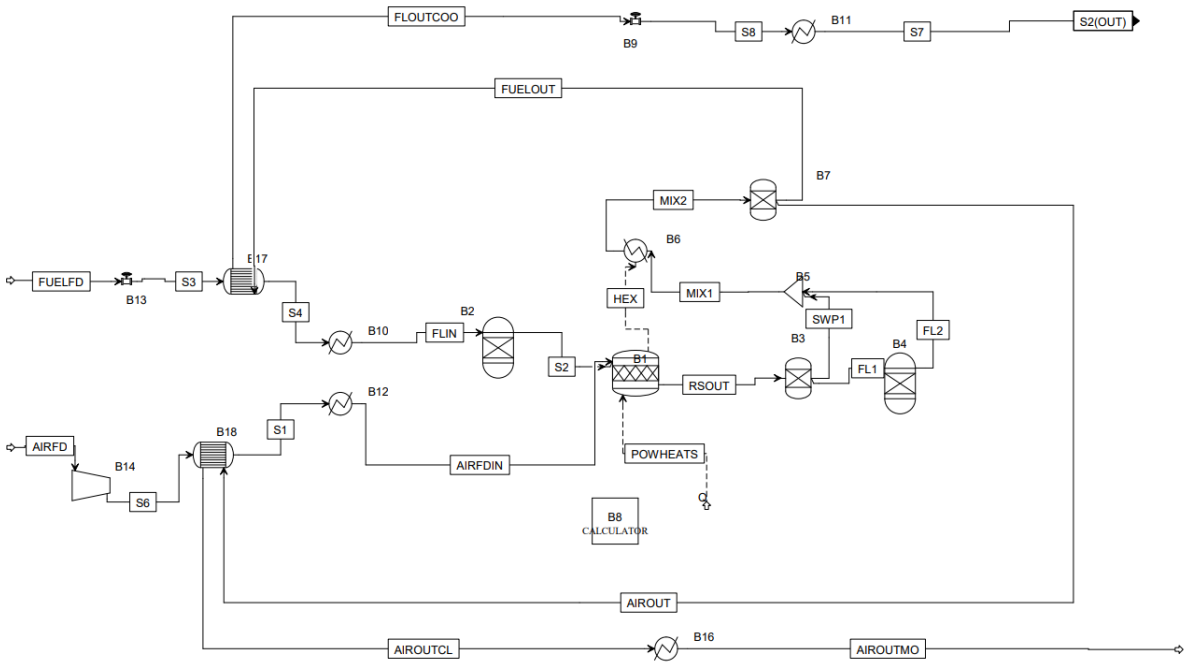

Figure 4.6: SOE System Implementation in Aspen

The FUELFD line carries the fuel in this case steam, the steam feed is preheated using the hot product gas and later heated to the reactor operating temperature using a heater (B10). It can be noted a valve is present in the steam feed line, this is used to control the pressure of the LP steam from the CSP plant. The Air side line uses a blower pass air to the reactor, a similar approach of pre heating using product gas and heating to operating temperature using a heater (B12) is used. Downstream of the electrolyzer coolers are used to reduce the temperature of the air to less than 100 °C and the temperature of hydrogen stream to saturation. The system power consumption comprises of all the electrical power consumption, here electrical power consumers are the electrolyzer stack, air blower and since the heaters are run electrically their power consumption is also included. Of this the major electrical consumption is for the reactors followed by the heaters.

Table 4.5: SOE System full load specifications

Parameter	Units	full load
Tin	C	800
Tout	C	800
HB10	KW	1380
Hb12	KW	996
Air blower	KW	200
Pstack	KW	16000
Ptotal	MW	18.576
P -AC	MW	20
Steam feed in	Kg/hr	6052
Air feed in	Kg/hr	10627
H2 prod	Kg/hr	542.5

4.2.4 SOE system part load operation

The SOE system part load design is the similar to the full load operation, the chemical part loading here happens by reduction of the input steam feed. This reduction in steam feed also reduces the the current density which results in the cell voltage below thermal neutral operation. Operating below thermal neutral voltage pushes the system into endothermic mode and results in outlet product gas temperatures less than the operating temperature of the cell.

$$V_{cell} = V_N + J.ASR \tag{4.10}$$

This is the cell voltage under nominal conditions, it should be noted that the cell voltage in this case is designed for isothermal operation. When chemical part loading happens the current density reduces. Considering a set point of 50 % for part loading, the cell voltage results in

$$V'_{cell} = V_N + (J/2).ASR \tag{4.11}$$

$$V'_{cell} = V_{cell} - (J/2).ASR \tag{4.12}$$

The part load operation becomes endothermic since the cell voltage is less than that of thermal neutral. As a result, the duty of the electric heaters upstream of the reactor increases for two reasons. Firstly, the product gas is unable to heat the input streams to the same high temperature as in nominal operation. Additionally, maintaining the reactor temperature requires a higher airflow, leading to increased power consumption by the blower and also the heaters.

Table 4.6: Part load system specifications

Parameter	Units	part load
Tin	C	830
Tout	C	760
HB10	KW	787
Hb12	KW	3800
Air blower	KW	590
Pstack	KW	7020
Ptotal	MW	12
P -AC	MW	13
Steam fd in	Kg/hr	3026
air fd in	Kg/hr	31267
H2 prod	Kg/hr	271

4.2.5 SOE System - Hot Standby Operation

In the Hot standby operation mode, there is no hydrogen being produced and the reactor is maintained close to the operating temperature by either increasing the flow-rate of the hot air or by increasing the inlet feed stream temperature, in most cases it is a combination of both the methods. In order mimic the heat loss of the reactor in the hot standby mode, a heater is used to mimic this behaviour. An analysis

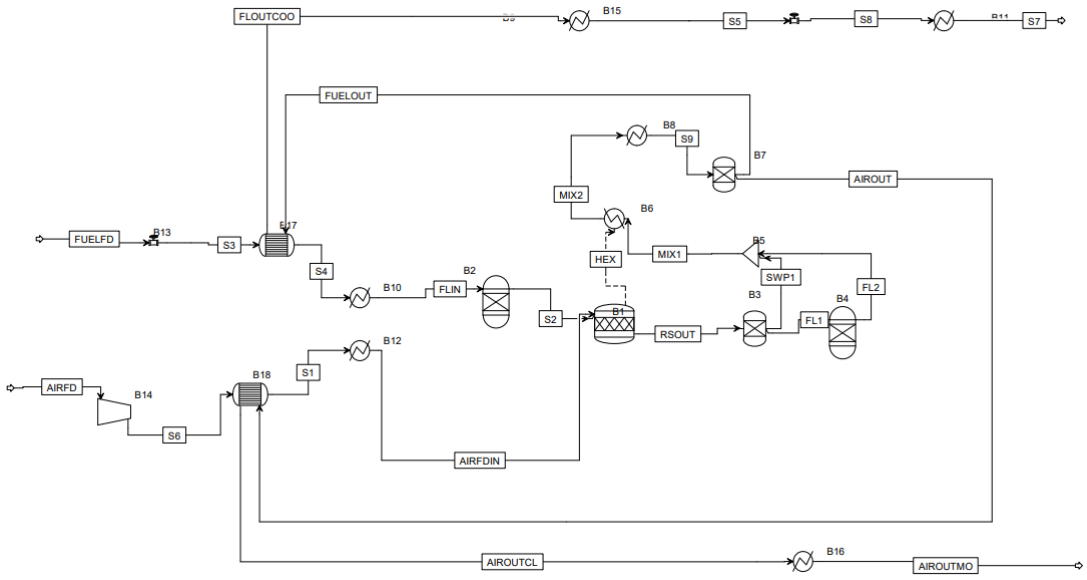

Figure 4.7: SOE Hot standby mode aspen implementation

was done in the SOE system to evaluate how much consumption is required to keep the system in hot standby, the air flow rate and inlet feed temperature is varied to see the reactor temperature. The target would be to have the lowest power consumption and have the reactor outlet temperature as close to the operating temperature of the system. The first figure in the 4.8 represents the effect of air flow and feed inlet temperature on the reactor temperature, it can be seen that as inlet temperature affects the reactor temperature positively and the effect of air flow rate diminishes at some point while the power consumption increases linearly with increasing air flow rate. For this reason higher inlet temperatures were preferred to increase the working reactor temperature. In this case a relative air flow of 1 and inlet air temperature of 810 °C was selected which led to power consumption of 1.8MW.

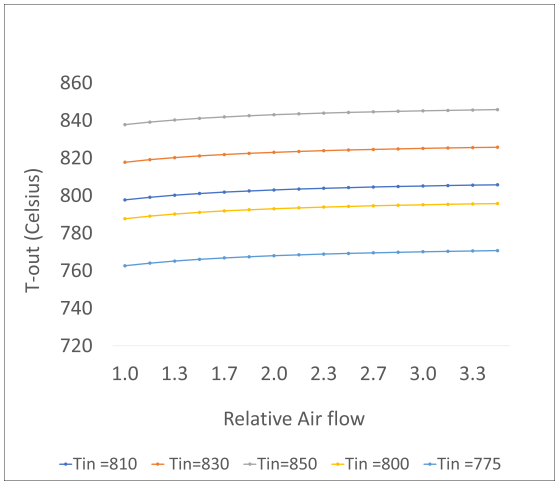

(a) Effect of Temperature and airflow on reactor temperature

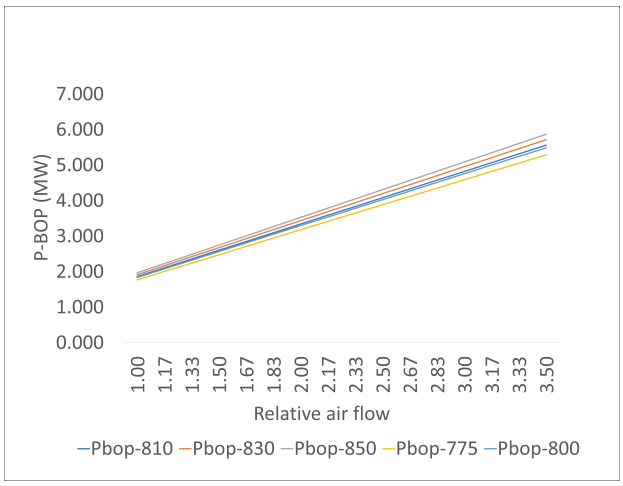

(b) Power Consumption as function of air flow

Figure 4.8: Effect of Temperature, Air flow on Reactor Temperature

4.3 Hydrogen Processing Systems

As discussed in the process scope there is a quality gap between the hydrogen that comes out of the electrolyzer and the hydrogen to be delivered. H2 processing system is designed to close the gap and get the wet hydrogen from the electrolyzer to required delivery quality and pressure. In this section the H2 processing system is explained using I/O schemes.

4.3.1 H2 Processing I/O Scheme

The water content in the hydrogen stream coming out of the electrolyzer is 0.27 by mole fraction, this value is obtained from our aspen implementation. The outlet constraint from our H2 processing scheme would be our delivery quality constraints and this is represented in the first i/o scheme.

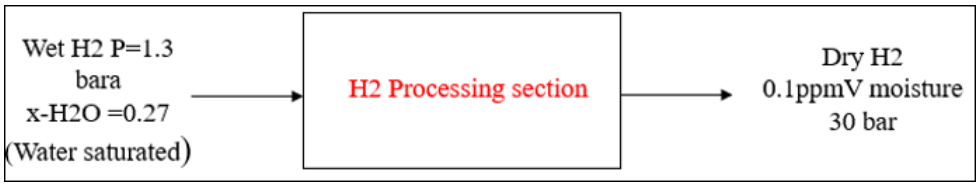

Figure 4.9: I/O scheme of H2 Processing system

Since the stream is water saturated, the unreacted water can be removed by cooling and condensation and subsequently passing it through a vapour liquid separator. It can be noted that after this step majority of the water is removed and water content in current stream is reduced by lot.

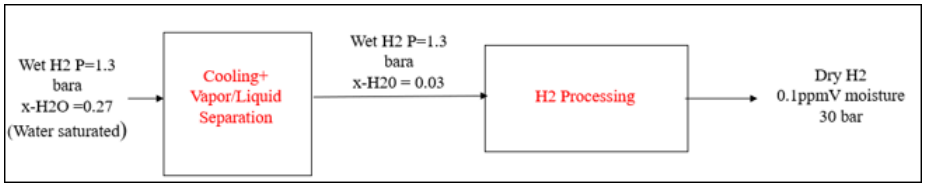

Figure 4.10: First level separation of water from H2 stream

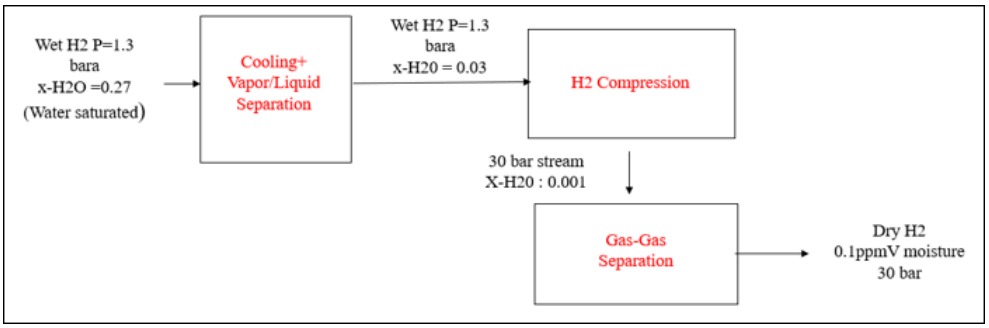

Figure 4.11: Compression and purification in H2 processing scheme

The following step would be to compress the H2 stream and pass it through a gas-gas separation block to purify it to the required quality.

4.3.2 Technology Selection

One of the important technology selections that has to be made in this section is for the gas-gas separation i.e the hydrogen drying. The available options at this moment are discussed briefly

- Membrane Separation : Membrane separation utilizes a selectively permeable membrane that allows the passage of hydrogen molecules while blocking impurities like moisture. The process is based on the size and permeability differences between the hydrogen molecules and other components. While membrane separation can be effective for certain applications, it may not be as suitable for drying hydrogen gas to very low moisture levels. [66]
- Pressure Swing Adsorption (PSA): PSA relies on the adsorption and desorption properties of a solid adsorbent material, such as activated carbon or zeolite, to remove impurities from the hydrogen gas. The process involves cyclically pressurizing the feed gas and then depressurizing it through adsorption beds. While PSA can effectively remove impurities, it may not be as efficient in drying the hydrogen gas as there is pressure loss and also hydrogen loss.
- Temperature Swing Adsorption (TSA): It employs a solid adsorbent material, typically activated alumina or molecular sieves, which selectively adsorbs moisture from the hydrogen gas. The process involves two alternating steps: adsorption and desorption. In the adsorption step, the moist hydrogen gas passes through the adsorbent bed, where water molecules are adsorbed onto the surface. In the desorption step, the temperature is increased to release the trapped moisture, regenerating the adsorbent material for subsequent cycles. Unlike PSA it does not involve pressure loss during desorption phase and can be effective for integration when process heat is available.
- Glycol Dehydration : Glycol dehydration involves the use of a liquid desiccant, typically a glycol such as triethylene glycol (TEG) or diethylene glycol (DEG), to absorb moisture from the gas stream. This method has been widely used for NG dehydration at large scales. However fuel cell grade hydrogen requires very low moisture levels that this method is incapable of providing and also glycolcontamination is an issue.

Temperature swing adsorption (TSA) has been selected as it provides an efficient way for H2 drying and also provides opportunities for integration. For compressors Reciprocating type has been selected as they offer high pressure ratios and other compressors such as centrifugal are mechanically limited for hydrogen compression [59]. The Compression has been implemented in aspen, reciprocating compressors have a turn down of close to 50 % and for this reasons two parallel compressor trains designed for 50 % of the flow rate are used. In addition to turn down improvement use of two compressor trains add redundancy to our system. As per industry recommendations a inter stage temperature increase was restricted to 150 °C. The Aspen implementation of the compression is show in the figure 4.12 it can be seen a combination of compressor, inter cooler and separator is used to implement the multistage compression. Separator is used to collect the water that gets dropped out during the compression process.

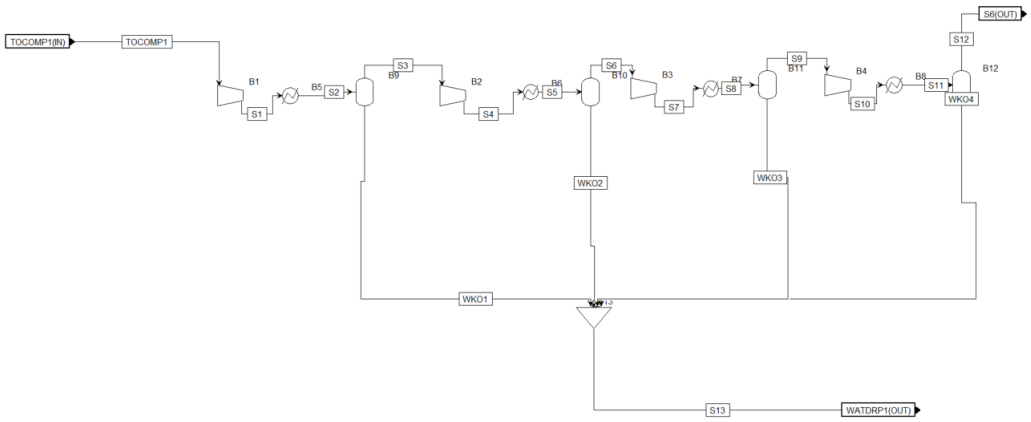

Figure 4.12: Compressor train implementation Aspen

The separators used both after every compression stage and also during the initial Vapour/Liquid separation is usually a Knockout pot. Knockout pots are vertical/horizontal vessels that rely on gravity settling to separate the entrained liquid droplets/mists from the gas stream. Often they use knitted stainless steel pads to improve the separation vessel performance, low pressure drops and separating efficiency of 99% can be expected [67]. The design of knockout pots are well established and detailed design methodologies have been provided by [68] and [69].

The specifications of the one compressor train is listed in the table, the specifications were obtained as result of simulation in Aspen 4.7.

Table 4.7: Specifications of one compression train

S.No	Parameter	Value	Units
1	Pin	1	bar
2	Pout	30	bar
3	stages	4	-
4	Net Power Required	5	MW
5	Mass flow rate	3533	Kg/hr.
6	Compression Energy	1.4	KWh/Kg

For H2 stream drying, the desiccant can be selected on the basis of the outlet water dew point requirements. The selection process is straightforward and depending on the outlet dew point requirement the selection can be made. Here in this case since a dew point requirement of less than -40 °F is required for this reason molecular sieve has been chosen and the sieve pore opening has to be larger than the molecule nominal size, for this reason 3A type zeolite is chosen 4.8.

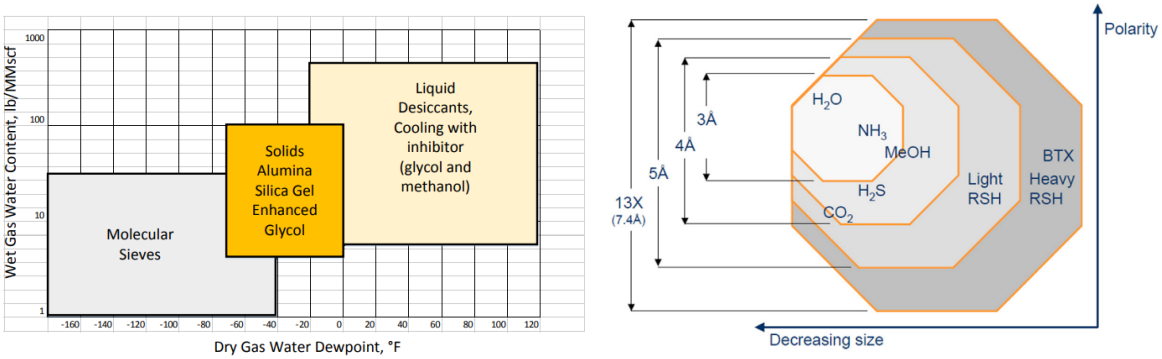

(a) Gas hydration technology selection [70]

(b) Molecular Sieve selection chart [71]

Figure 4.13: Selections for TSA

Table 4.8: TSA Specifications

Parameter	Specification	Unit
Vessel pressure	30.4	bar
Vessel regeneration temperature	330	C
vessel Diameter	1.5	m
vessel height	6.7	m
weight of molecular sieves (all vessels)	15369	kg

TSA Columns have been sized according to standard design procedures [72] and the specifications of the TSA column is listed in the table 4.8, it should be noted that standard two column arrangement with 12 hour cycle time is assumed and 1/16 extrudate type molecular sieve is used as adsorbent is used for the column. The design calculations to estimate the diameter was made using the Ergun equations, this is done by assuming a pressure drop per unit length and. The equation relates pressure drop to superficial velocity. Here B and C are Ergun constants and μ and ρ are viscosity and density of the wet gas.

$$\frac{\Delta P}{L} = B.\mu.V + C.\rho.V^2 \tag{4.13}$$

Once the maximum superficial velocity (V) has been obtained, diameter is obtained using volumetric flow-rate and max. superficial velocity. The height of the column is estimated by calculating the length of mass transfer zone and saturation zone [72]. The calculated height must be no less than the inside diameter or 6 feet, whichever is greater.

Finally, the comprehensive layout of the plant is presented in the figure 4.14 comprising of CSP section, SOE section and H2 processing section. CSP section plays a pivotal role as it consists of advanced Solar Collectors designed to efficiently capture abundant solar energy. The primary purpose of this energy capture is to satisfy the multifaceted needs of power production, steam generation, and energy storage systems.Within the CSP plant, an intricate arrangement of heat exchange units and power blocks are present. After evaluation of the existing CSP plants, steam rankine has been selected as the thermodynamic cycle for power block. The decision is backed by its proven commercial maturity and reliable performance.

Table 4.9: Selection of suitable thermal energy storage

S.No	Parameters	2 tank direct	2 tank indirect	single tank thermocline
2	TES Medium	Molten Salts	Molten Salts	Ruths tank
3	HTF Medium	Molten Salts	Thermal Oil	Water
4	Max T from field	++	+	-
5	Storage (hours)	++	++	- -
6	Commercial Maturity	+	++	-
7	Cost	-	- -	++
9	**Score**	**4**	**3**	**-**

Furthermore, the selection process for the thermal energy storage system was carried out based on the existing thermal energy storage technologies, taking into account various factors and considerations and is represented in figure 4.9. As a result of this exercise 2 tank direct systems were chosen.

On the other hand, the SOE plant plays a critical role in the overall system, comprising ten individual SOE systems, each with 20 MW capacity and these systems can be operated flexibly by using appropriate operation strategy. The H2 processing section comprises a Gas-Liquid separator, 2 compression trains, and TSA column. These components work to produce hydrogen while ensuring high purity and quality. It's worth noting that the energy requirements for the compressor and TSA column are efficiently met by the CSP plant.

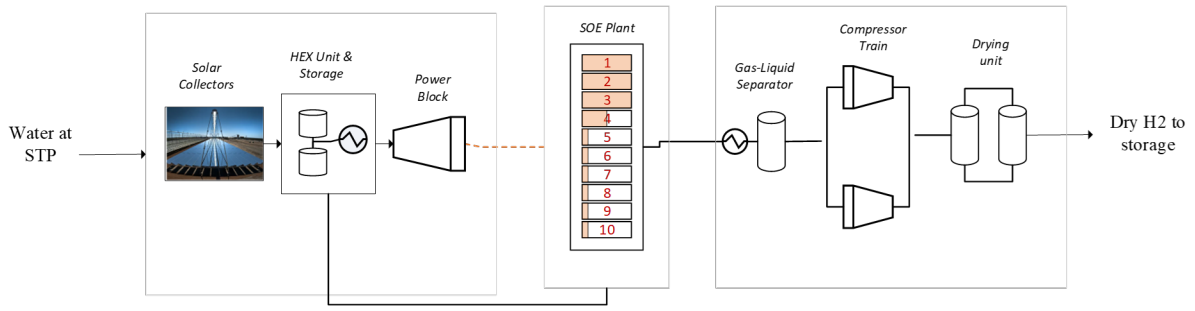

Figure 4.14: Complete layout of the integrated CSP-SOE plant for hydrogen production

4.4 Plant Operation

To develop strategies for the modular plant, it is necessary to study the power production at an hourly time step. This will enable a detailed analysis of how the modules can be operated during each hour. The power requirement for the SOE plant is approximately 200 MW, and to achieve this capacity, 10 modules of 20 MW each are needed. The DNI profile of the selected geography (Rajasthan,India) is visualized in the following figure 4.15, the DNI is taken for one single year and is discretized on hourly basis.

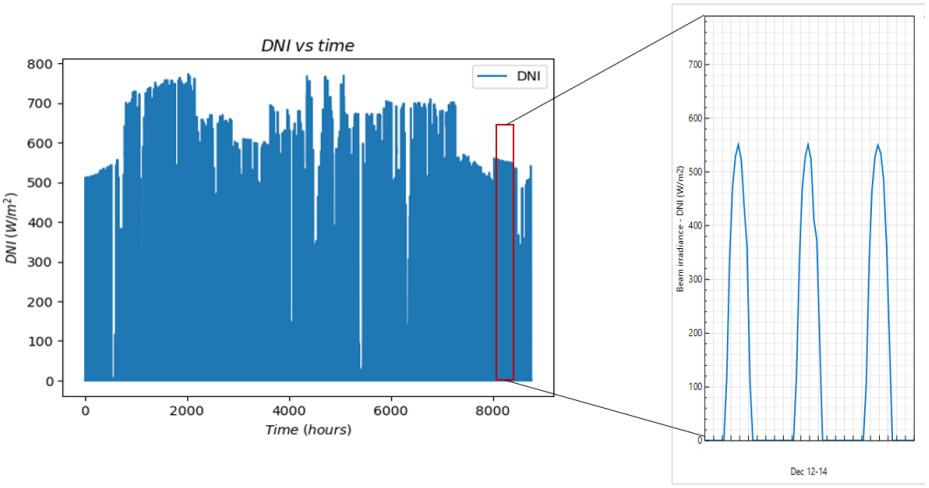

Figure 4.15: Hourly DNI of Rajasthan,India

From the DNI it can be calculated the amount of solar energy collected at each and every hour by the plant, in the figure 4.16 a dotted line is drawn which represents the solar energy required to run the power block which would be enough to satisfy the requirements of SOE plant. The peaks above this line are excess solar energy at every and this can be stored in the form heat. The second figure 4.16 represents the thermal energy that is available for storage at each and every hour. The average of the available thermal energy comes close to 600MWth and the capacity of the energy storage is designed for this value and for 10 hour discharge.

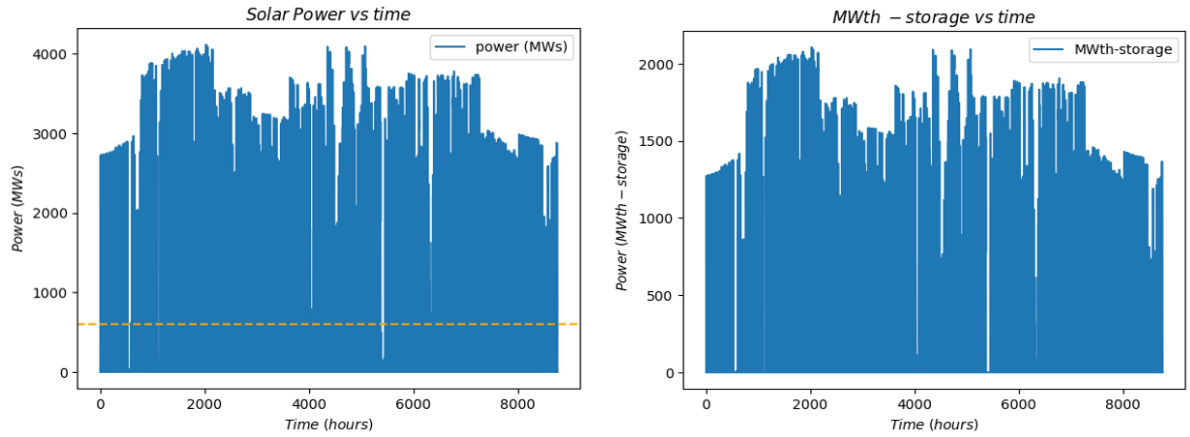

(a) Solar energy collected every hour

(b) Available thermal energy for storage

Figure 4.16: Hour available energy production

The CSP plant experiences hours of low energy production despite having storage capacity. To prevent plant idleness and shutdown, smart operation strategies are essential. The plant's SOE module offers three distinct operating modes: full load, part load, and hot standby. Each module needs to be operated differently during periods of scarce energy production. To address this challenge, three distinct strategies are proposed.

4.4.1 Operation Strategy 1 - Full Load & Hot standby only

In this strategy, in order to overcome the intermittency problem the modules are operated in two modes - full load and part load only. Whenever energy availability is scarce, certain rules are followed and a number of modules are operated in full load and a number of modules are operated in part load. whenever the power from CSP is less than the minimum power requirement all modules go into shutdown, here the minimum power requirement is the product of hot standby power consumption and the total number of modules. Whenever the power from CSP is more than sum of of minimum power and full load module power, the number of modules in full load and hot standby can be calculated using the following rule. Note that the fraction is round down to the closest whole number.

$$n_{fl} = (\frac{p_{csp} - p_{min}}{p_{fl}}) \tag{4.14}$$

$$n_{hs} = n_{total} - n_{fl} \tag{4.15}$$

when the power from CSP is more than the minimum power but less than the sum of minimum power and full load module power, all modules go into hot standby. Additionally when the power from CSP is equal to the product of full load power and number of modules all the modules are run in full load.

Let us consider a hour where the DNI = 150 W/sq.m and this results in power of 95 MW, in this scenario the strategy results in 7 modules being in full load and 3 modules in hot standby.

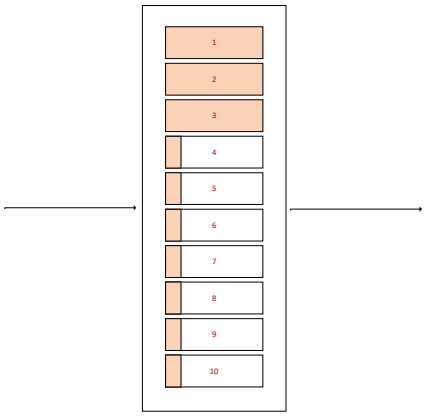

Figure 4.17: strategy 1 implementation for an example of DNI = 150 W/sq.m

4.4.2 Operation Strategy 2- Full Load & Part Load only

The benefit of strategy 1 is that it makes sure there is always enough energy for all the modules to go into hot standby before choosing modules to be operated in full load, the disadvantage is there is no hydrogen production whenever we choose to operate certain modules in hot standby. To counter this challenge a different approach is taken, only full load and part load modes are chosen to over come the intermittency. The disadvantage of this mode however is that there are more shutdown and start up of modules when using this approach. When the power from CSP is less than the minimum power all modules go into shutdown, here minimum power is equal to the part load power of an individual module. Whenever the power from CSP is more than sum of of minimum power and full load module power, the number of modules in full load and part load can be calculated using the following rule. Note that the fraction is round down to the closest whole number.

$$n_{fl} = (\frac{p_{csp}}{p_{fl}}) \tag{4.16}$$

$$n_{pl} = \frac{p_{csp} - n_{fl}.p_{fl}}{p_{pl}} \tag{4.17}$$

$$n_{sd} = n_t - nfl - n_{pl} \tag{4.18}$$

when the power from CSP is more than the minimum power but less than the sum of minimum power and full load module power, number of modules going to full load will be zero and number of modules in part load is defined by the following rule

$$n_{pl} = \frac{p_{csp}}{p_{pl}} \tag{4.19}$$

$$n_{sd} = n_t - n_{pl} \tag{4.20}$$

Let us consider an example where the DNI=150 W/sq.m and this results in a power production of 95MW, use of this strategy results in 4 modules being in full load, 1 module in part load and 5 modules being shutdown for this particular hour.

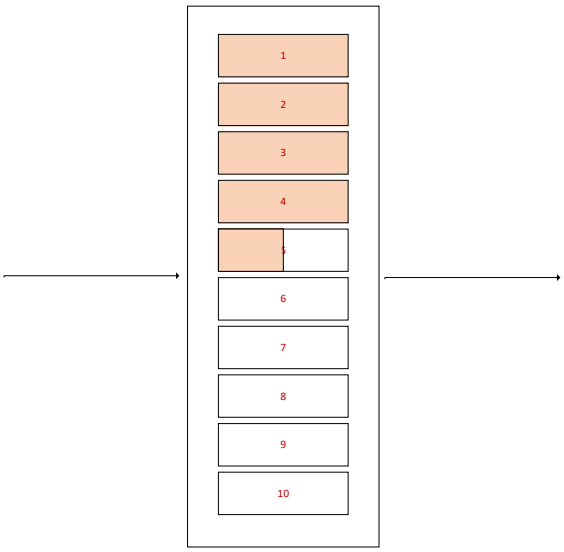

Figure 4.18: strategy 2 implementation for an example of DNI = 150 W/sq.m

4.4.3 Operation Strategy -3 : Full Load, Part Load Hot Standby

This strategy aims to combine the benefit of both strategy 1 and 2, before estimating number of modules to be put in full load and hot standby enough power is allocated for all modules to be in hot standby.Whenever the power from CSP is less than the minimum power requirement all modules go into shutdown, here the minimum power requirement is the product of hot standby power consumption and the total number of modules.Whenever the power from CSP is more than sum of of minimum power and full load module power, the number of modules in full load and hot standby can be calculated using the following rule. Note that the fraction is round down to the closest whole number.

$$n_{fl} = \frac{p_{csp} - p_{min}}{p_{fl}} \tag{4.21}$$

$$n_{pl} = \frac{p_{csp} - n_{fl}.p_{fl} - p_{min}}{ppl} \tag{4.22}$$

$$n_{sd} = n_t - nfl - n_{pl} \tag{4.23}$$

when the power from CSP is more than the minimum power but less than the sum of minimum power and full load module power, number of modules going to full load will be zero and number of modules in part load is defined by the following rule, whenever the power from csp is equal to product of number of modules and full load power all modules are run in full load.

$$n_{pl} = \frac{p_{csp} - p_{min}}{ppl} \tag{4.24}$$

$$n_{sd} = n_t - n_{pl} \tag{4.25}$$

Let us consider an example where the DNI=150 W/sq.m and this results in a power production of 95MW, use of this strategy results in 4 modules being in full load, 1 module in part load and 5 modules being shutdown for this particular hour.

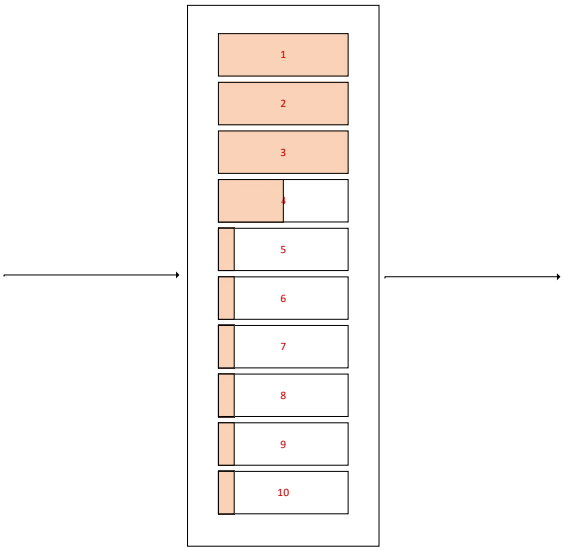

Figure 4.19: strategy 3 implementation for an example of DNI = 150 W/sq.m

Chapter 5

Results & Discussion

The results of all 3 strategies are explored here, initially the plant behavior for each and every strategy with respect to operation point is explored and as an extension from this the plant operation is explored for a DNI distribution. The Levelized cost of Hydrogen (LCOH) is estimated for all three strategies.

5.1 Strategy 1: Hot standby & Full Load

In order to understand the effect of strategy on the system, first series of values are studied against the operation point(i.e from 0-100 % power supply from CSP). To begin with the number of modules going into to different operating modes (here, Hot standby & Full Load) is studied and as expected the number of modules in hot standby decreases when the power supplied from CSP increases, the vice versa happens for modules in full load. This can be seen in the following figure 5.1 where the power consumed by modules in full load increases and that by modules in hot standby decreases as the power supplied from CSP increases.

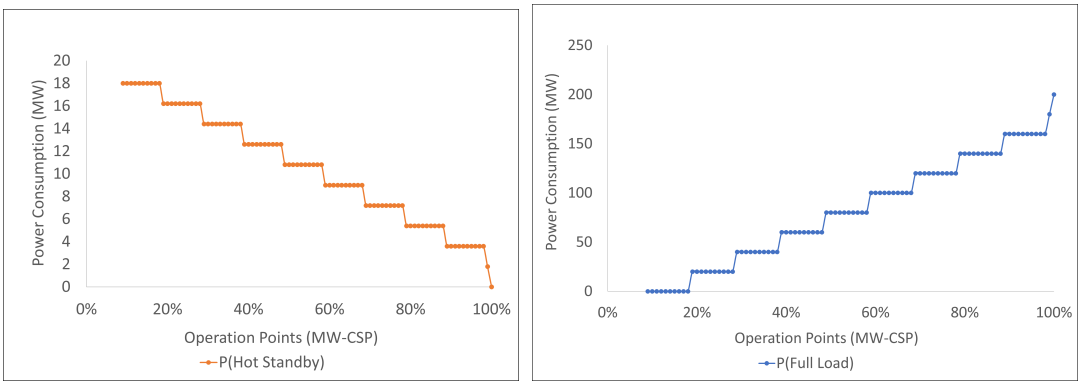

(a) Power Consumption of modules in Hot standby (b) Power Consumption of modules in full load

Figure 5.1: Power consumption of modules in different modes vs operating point

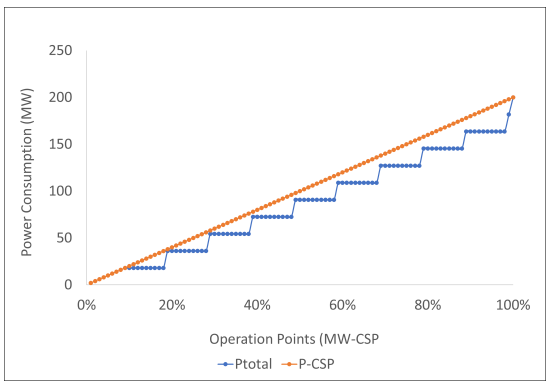

Figure 5.2: Total power consumption of the system & power supply from CSP

The power consumption plots display a stepped curve, this is because of the way in which rules have been defined for the strategy. It can be noted from the rules for all values of power supply greater than the cutoff power a minimum power is reserved for putting all the modules in hot standby (This is done to prevent shutdown of modules above the cutoff power) and this results in the stepped graph. The figure 5.2 shows the total power consumption of the plant with respect to the operating point.The blue line indicates the total power consumption and the orange line indicates the power provided by the CSP at different operating points.The gap between the two lines indicate the un-utilized power, in principle the area has to be minimal. The plant was simulated using the DNI profile of Rajasthan and module allocation, hydrogen production were studied. The DNI data is recorded at a hourly frequency this means for each and every hour a decision has to be made for all 10 modules on which operating mode the module has to enter, this split of this decision is represented using the figure 5.4 and the varying DNI profile is shown in the figure 5.3. It should also be noted the storage is designed in such a way to produce power for 10 hours a day during hours of low sunshine.

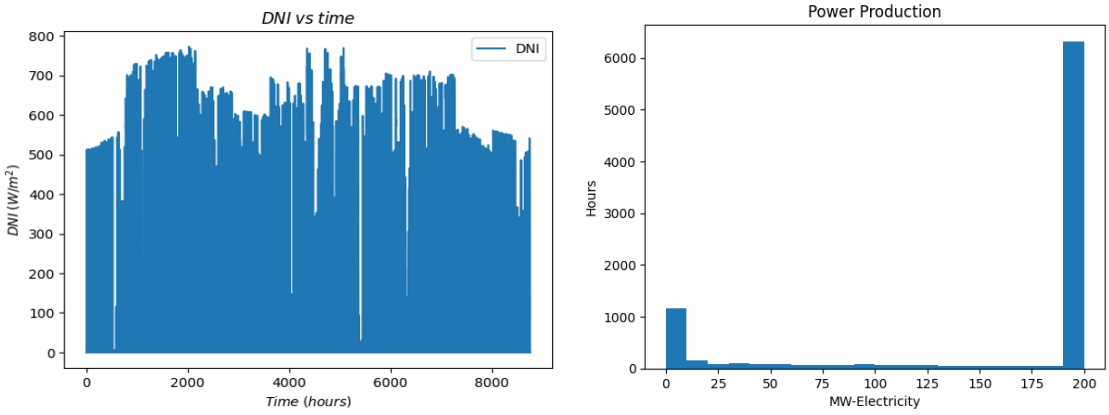

(a) DNI distribution per year

(b) Power production from CSP

Figure 5.3: Power production from CSP plant with 10 hours of storage

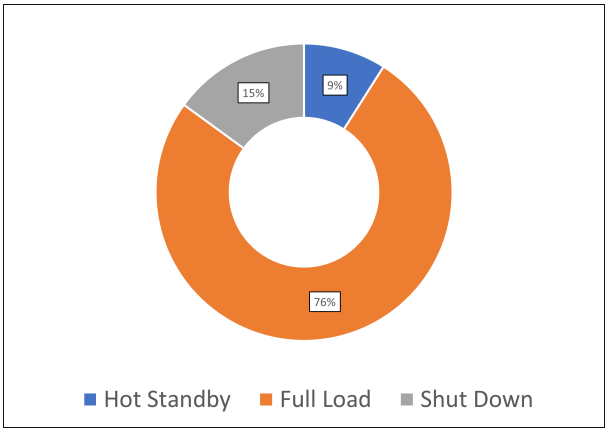

Figure 5.4: Allocation of modules into different operating modes

The figure 5.4 represents the allocation of modules to different operating modes, every hour 10 decisions have to be made to put the modules in different operating modes. It can be seen that for majority of the selection the modules go into full load operation and during hours of scarce energy production modules are put in hot standby. When the power produced is less than the minimum power requirement the modules are shut down and it happens 15 % of the selection.

The specific energy consumption 5.5 of this strategy is also obtained for this particular strategy, this is a good indicator of the performance of our SOE plant.The Specific energy consumption at a plant level is very high at low operation points and it reduces and flattens as we move towards higher operating regions. The stepped curve is once again due to the power reservation made for hot standby and it can be noticed whenever the SEC curve has a step down the power consumption by the modules in full load takes a step up, this indicates the allocation of power towards useful process (here hydrogen production).

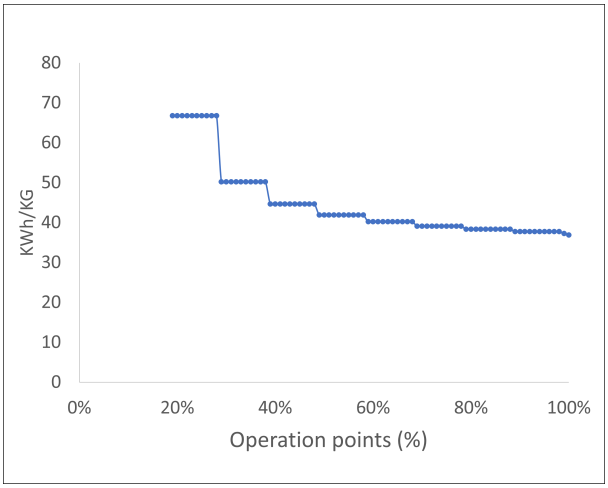

Figure 5.5: Specific energy consumption of the system using strategy-1

Figure 5.6: LCOH when using strategy-1

Table 5.1: LCOH when using strategy-1

Cost Component	Cost/Kg
SOE CAPEX	$1.043
CSP CAPEX	$1.917
SOE O&M	$0.857
CSP O&M	$0.290
Compression CAPEX	$0.015
Compression O&M	$0.08
Dehydration CAPEX	$0.002
Dehydration O&M	$0.001
LCOH	$4.134

Additionally using the hydrogen production from simulation the LCOH is also calculated and the split of it is reported in the figure 5.6 and table 5.1, it can be observed that the major cost component in the system is due to CAPEX of SOE and CSP and the Dehydration column has the least cost addition to the LCOH. It should also be noted all the plant is electrically & thermally self sufficient, this means the

electricity required for compressors in addition the SOE and the thermal energy required for regeneration of the TSA column is supplied by the CSP plant.

5.2 Strategy - 2: Full Load & Part Load

For strategy two the same parameters are studied once again with respect to the operation point, the relationship between the power consumed and the operation point is represented by the figure 5.7. We can see for the part load power consumption there is cyclic jump and the amplitude remains the same and corresponds to power consumption of one module in part load, this indicates that whenever a scenario is such that part loading happens it happens only to maximum of one module. As for the full load power consumption we notice a stepped increase and in this case the stepping happens when the power supplied from the CSP is integral multiple of the power consumption of module in full load.In the figure 5.8 blue curve represents the total power consumption at each stage and orange curve indicates the power supplied from the CSP, we can note that this strategy is able to track the power curve from CSP better than strategy-1.

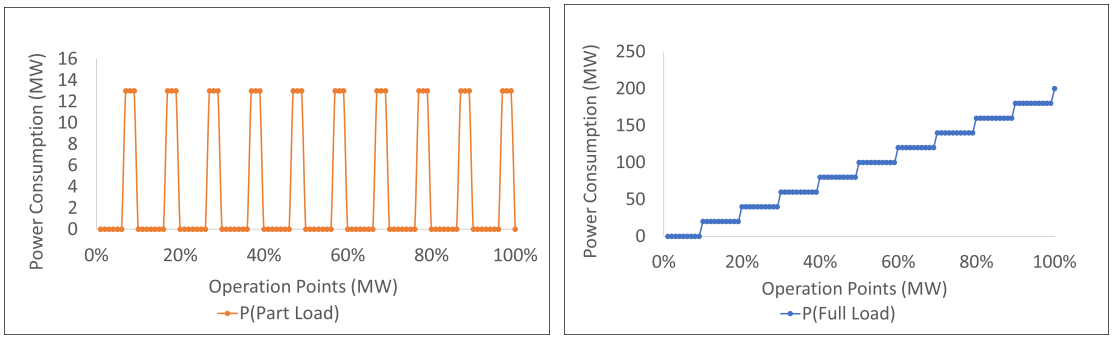

(a) Power Consumption of modules in part load (b) Power Consumption of modules in full load

Figure 5.7: Power consumption of modules in different modes vs operating point

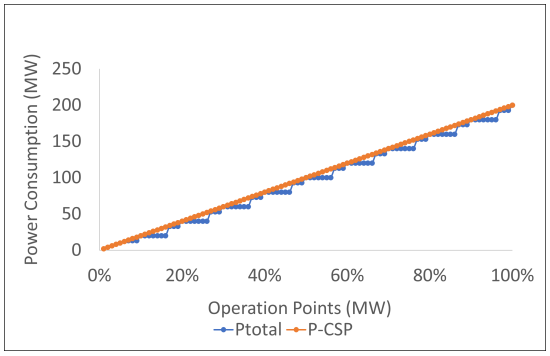

Figure 5.8: Total power consumption of the system & power supply from CSP

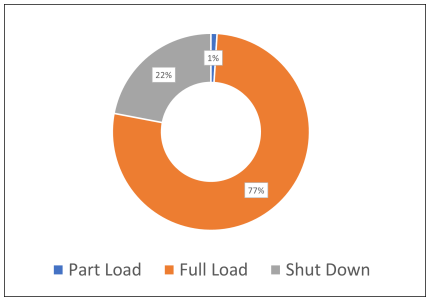

Figure 5.9: Allocation of modules into different operating modes

The plant was simulated using the DNI profile of Rajasthan and module allocation, hydrogen production were studied. The DNI data is recorded at a hourly frequency this means for each and every hour a decision has to be made for all 10 modules on which operating mode the module has to enter, this split of this decision is represented using the figure 5.4 and the varying DNI profile is shown in the figure 5.3. It should also be noted the storage is designed in such a way to produce power for 10 hours a day during hours of low sunshine. The figure 5.9 depicts the share at which decisions are made towards a particular mode. It is evident that the drawback of this mode is that the module goes into shutdown 22% of the time. It can aslo be seen that for this strategy the selection towards putting the modules in part load is $\sim$ 1% only. Performing cold shutdown and start up is dangerous for the stacks and this necessitates the presence of hot standby mode.

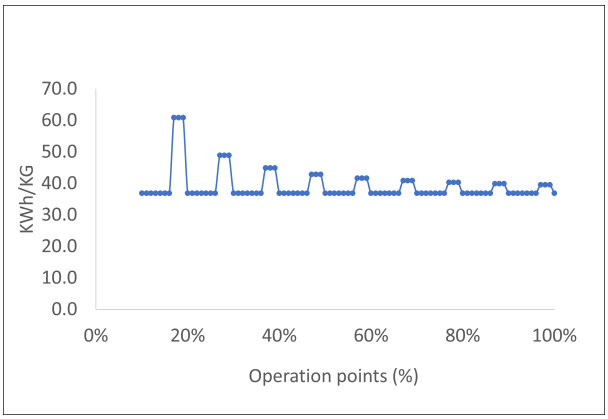

Figure 5.10: Specific energy consumption of the system using strategy-2

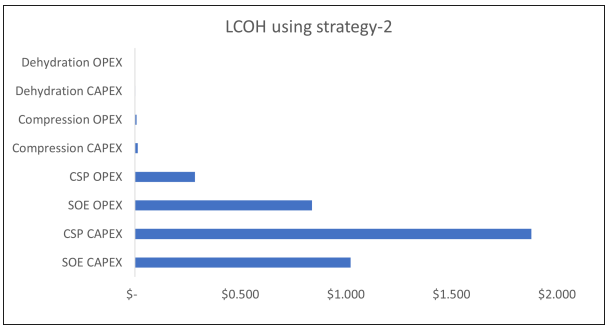

Figure 5.11: LCOH when using strategy-2

Table 5.2: LCOH when using strategy-2

Cost Component	Cost/Kg
SOE CAPEX	$1.022
CSP CAPEX	$1.879
SOE O&M	$0.839
CSP O&M	$0.284
Compression CAPEX	$0.015
Compression O&M	$0.008
Dehydration CAPEX	$0.002
Dehydration O&M	$0.001
LCOH	$4.051

It can be noted that the SEC for this strategy is less than that of strategy-1 5.10 this is because in this mode whenever power is consumed the power is used for useful process (i.e Hydrogen is being produced) and the spike in SEC is whenever a module gets fired in part load as operating in aprt load is inefficient compared to full load. The LCOH values is not extremely cheaper and and it is interesting to note that neither lesser SEC nor the higher shutdown time have a huge impact on the cost in this system.

5.3 Strategy-3: Full Load, Part Load & Hot Standby

Strategy-3 aims to combine both strategy-1 and strategy-2. Once again same parameters are studied with respect to the operation point. The relationship between power consumption and operation point ins represented in the figure 5.12. Very similar to strategy-2 the power consumption plots display a

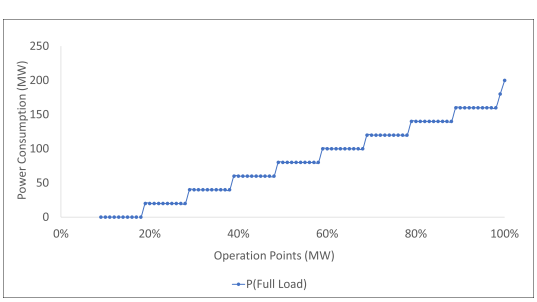

(a) Power consumption of modules in Full Load

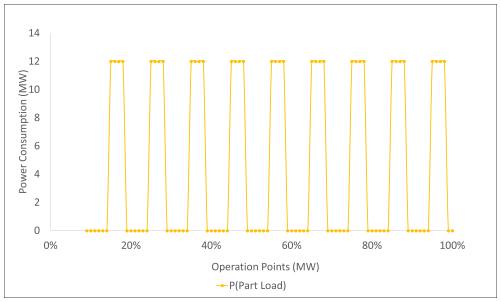

(b) Power consumption of modules in Part Load

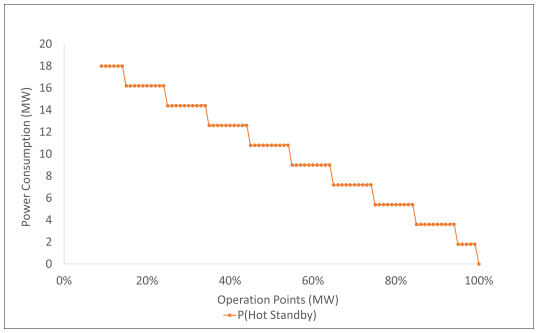

(c) Power consumption of modules in Hot Standby

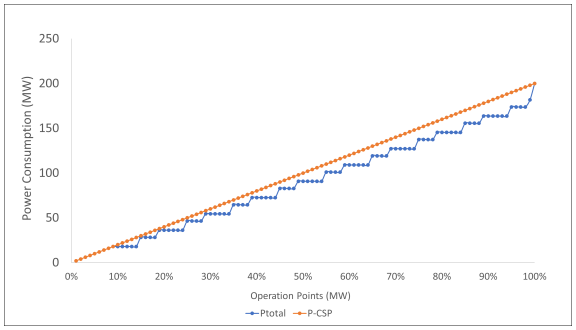

(d) Total Power consumption of modules

Figure 5.12: Power consumption of modules vs operation point

stepped curve, this is because of the way in which rules have been defined for the strategy. It can be noted from the rules for all values of power supply greater than the cutoff power a minimum power is reserved for putting all the modules in hot standby and this results in the stepped graph. We can also see for the part load power consumption there is cyclic jump.And the amplitude remains the same and corresponds to power consumption of one module in part load similar to strategy-2.The plant was simulated using the DNI profile of Rajasthan and module allocation, hydrogen production were studied. The DNI data is recorded at a hourly frequency this means for each and every hour a decision has to be made for all 10 modules on which operating mode the module has to enter, this split of this decision is represented using the figure 5.4 and the varying DNI profile is shown in the figure 5.3. It should also be noted the storage is designed in such a way to produce power for 10 hours a day during hours of low sunshine. The figure 5.15 depicts the share at which decisions are made towards a particular mode. From the figure 5.15 it can be seen the selection towards shutdown has reduced and is $\sim$ 9% only.

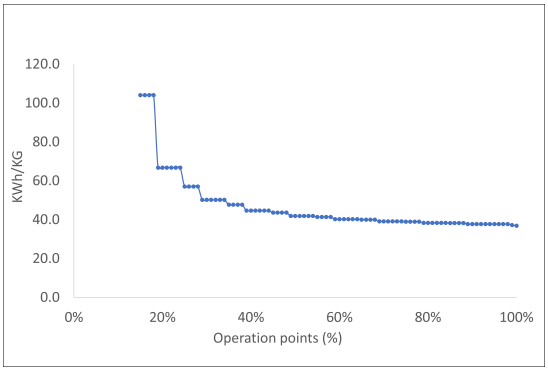

Figure 5.13: Specific energy consumption using strategy-3

The figure 5.13 represents the SEC while using strategy-3 and the trend is similar to that of strategy-1. The LCOH values and the split up are reported in the figure and table.

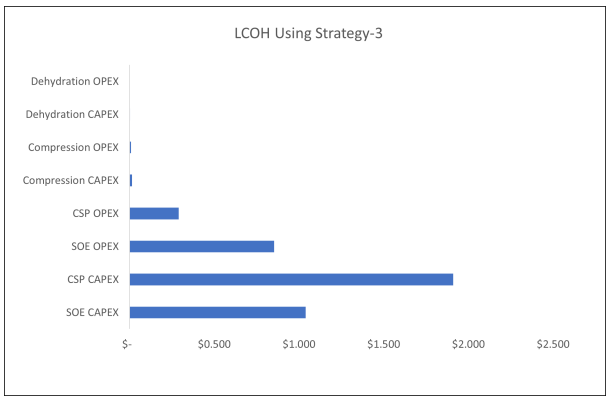

Figure 5.14: LCOH when using strategy-3

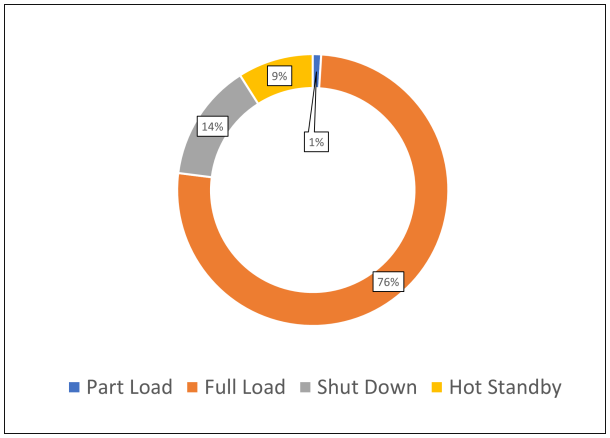

Figure 5.15: Allocation of modules into different operating modes

Table 5.3: LCOH when using strategy-3

Cost Component	Cost/Kg
SOE CAPEX	$1.040
CSP CAPEX	$1.910
SOE O&M	$0.854
CSP O&M	$0.289
Compression CAPEX	$0.015
Compression O&M	$0.008
Dehydration CAPEX	$0.002
Dehydration O&M	$0.001
LCOH	$4.118

5.4 Selection of suitable strategy

The important key performance indicators based on which selection of the strategy will be made are the LCOH, Power Consumption and the usefulness of the power consumed which is indicated by the Specific energy consumption. However, the degradation of the Electrolyzer modules also plays a important factor. Current degradation values of the technology are high since the technology is at low TRL level and using the current numbers would lead to extreme results. To tackle this problem the biggest contributor to the degradation, the number of start up/shut down events is considered as a proxy for degradation. The SEC

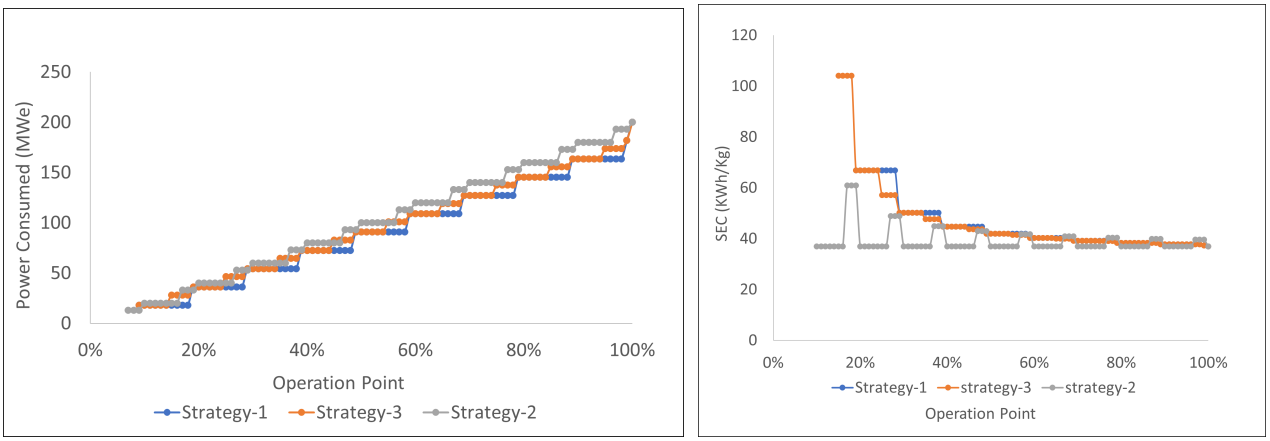

(a) Power consumption of all 3 strategies

(b) SEC of all 3 strategies

Figure 5.16: Comparison of the strategies based on power consumption and SEC

is lowest for the strategy-2, however it can be noted whenever the system gets into part load the SEC spikes and matches the other two strategies, the SEC for the strategy 1 and 3 are coincidental for most parts, at lower operation points strategy-3 is energy expensive and at higher operation points strategy-3 performs slightly better in comparison to strategy-1. In terms of power consumption strategy-1 has the lowest power consumption and highest is for strategy-2. The LCOH of all 3 strategies are listed in the table 5.4 and it can be seen that the values are similar for the 3 strategies and strategy-2 has the lowest LCOH.

Table 5.4: LCOH of all 3 strategies

LCOH Calculator	Strategy-1	Strategy-2	Strategy-3
SOE CAPEX	$1.043	$1.022	$1.040
CSP CAPEX	$1.917	$1.879	$1.910
SOE OPEX	$0.857	$0.839	$0.854
CSP OPEX	$0.290	$0.284	$0.289
Compression CAPEX	$0.015	$0.015	$0.015
Compression O&M	$0.008	$0.008	$0.008
Dehydration CAPEX	$0.002	$0.002	$0.002
Dehydration O&M	$0.001	$0.001	$0.001
LCOH	$4.134	$4.051	$4.118

The LCOH is studied as a function of SOE CAPEX and CSP CAPEX to understand the sensitivity of LCOH to these variables, both the CSP CAPEX and SOE CAPEX are varied approximately by 30% both positively and negatively. The LCOH values are not extremely different for the 3 strategies and fall in the same bandwidth of 3-6 $/Kg.

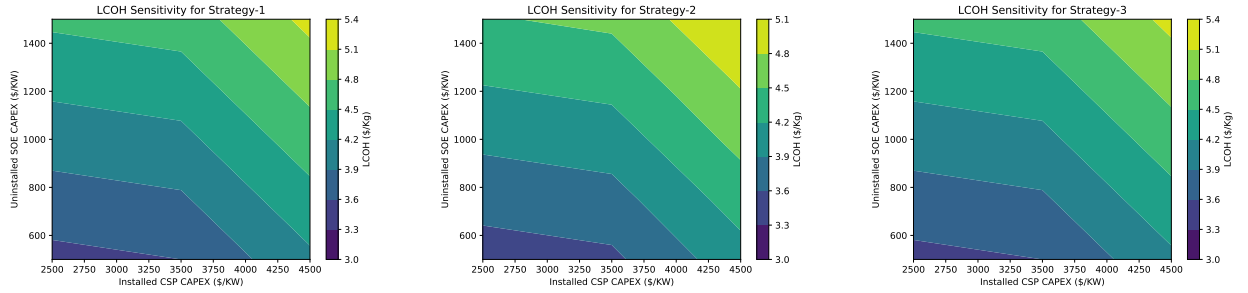

(a) LCOH Sensitivity for strategy 1 (b) LCOH Sensitivity for strategy 2 (c) LCOH Sensitivity for strategy 3

Figure 5.17: LCOH Sensitiviy towards changes in SOE CAPEX and CSP CAPEX

The start up/shut down events are represented in the figure 5.18, it can be seen while using the strategy-2 the startup and shut down events are more than that of the other strategies, this results in high degradation of the cells and damage to stacks due to prolonged cold shutdown times. In addition to this since the strategy-2 does not have hot standby mode, time to get the system back running is not immediate as there is a large thermal inertia associated with heating up the modules to operating temperature. For this reason selection of strategy-2 is not preferred. Strategy-3 is preferred as it gives the lowest LCOH, slightly better SEC values and it provides the option to have a part load operation.

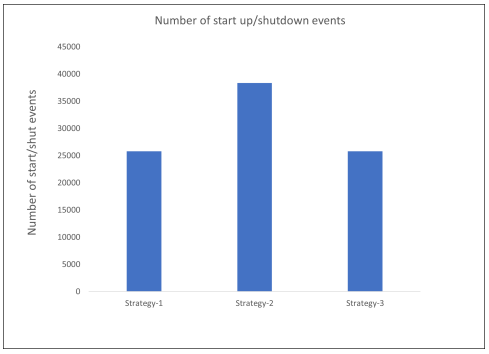

Figure 5.18: Start up shutdown events of all 3 strategies

Chapter 6

Conclusion & Recommendations

6.1 Conclusion

The objective of this work was to assess the technical and economic viability of integrating Solid Oxide Electrolyzer (SOE) and Concentrated Solar Power (CSP) systems. The study aimed to determine the competitiveness of the integration compared to existing technologies, design an integrated plant, examine the operation of a CSP-SOE plant, and analyze the economic aspects. These research questions were addressed to achieve these objectives.

The first research question addressed the business case for which CSP-SOE integration was competitive over current state-of-the-art technologies, and identified the high impact parameters for the integration. System level models were developed individually for CSP and SOE, and these models were combined to create a system-level model for the integrated plant. Sensitivity analysis was conducted to estimate the parameters with the highest impact on the cost of hydrogen. It was found that the capacity factor and CAPEX/KW of the CSP plant had the most significant influence on the cost of hydrogen. The analysis showed that the CSP+SOE integration outperforms the combination of Alkaline water electrolysis (AWE) with battery storage in achieving high capacity factors and lower costs. LCOH values below $5/kg were achieved, making the CSP+SOE integration more competitive for capacity factors greater than 0.35, particularly for large green hydrogen plants.

The second research question focused on building a plant to realize the identified business case. The required SOE and CSP power capacities of 200 MW were obtained from basic sizing. The plant scope was defined to ensure that the outlet dry hydrogen met the necessary quality and pressure standards. The SOE system was designed based on existing pilot plant modules. SOE modules with capacity of 20 MW each were implemented in Aspen. Different operation modes, such as Hot standby, Full Load, and Part Load, were studied, and their power consumption and hydrogen production were estimated. The Hydrogen post-processing section layout which included vapor-liquid separator, compressor, and Temperature swing adsorption (TSA) to achieve the required delivery pressure and quality of dry hydrogen were selected and designed. A thermal energy storage system (TES) with a capacity of 600 MWth for 10 hours was designed based on the availability of excess energy from solar radiation.

The third research question aimed to operate the plant efficiently to overcome intermittency. Even with an energy storage system, smart and effective operation strategies were crucial to reduce idle time. The SOE plant consisted of 10 systems, each with a capacity of 20 MW. Three proposed strategies for operating during intermittent energy production were compared based on economics, energy consumption, and degradation. After considering the power delivered from the CSP plant, decisions were made on how the 10 modules would be operated during each hour, i.e., determining the number of modules in full load, part load, and hot standby. The most effective strategy resulted in an LCOH of $4.1/kg for the designed plant, with the best-case price at $3/kg and the worst-case price at $5/kg.

6.2 Recommendations to Shell

1. It is crucial to conduct a detailed study on cost reductions in the CSP sector, particularly focusing on CSP CAPEX (capital expenditure). The current installed CSP plants have high CAPEX costs, which can hinder the competitiveness of green hydrogen produced from CSP plants. Additionally, it is essential to improve cost estimates for CSP plants at different scales, as the existing estimates are based on specific plant sizes, and the scalability of the economics is unclear. By addressing these issues, we can enhance the economics of CSP plants and ensure the competitiveness of green hydrogen in the market

2. The choice of Temperature Swing Adsorption (TSA) technology over other alternatives was based on its potential for heat integration from our CSP plant. However, it is imperative to conduct a detailed feasibility study to assess the practicality of implementing this integration. Additionally, it is essential to comprehend the effects of intermittencies arising from CSP plant operations and understand the turndown characteristics specific to TSA technology. By thoroughly investigating these aspects, we can gain valuable insights into the potential challenges and benefits.

3. Exploring the high-pressure operation of Solid Oxide Electrolysis (SOE) technology is crucial and suitable systems have to be developed to achieve this. Implementing high-pressure operation has the potential to significantly reduce the power requirements for compression. As a result, there will be a reduction in the capacity of the CSP plant and this reduction in capacity leads to a corresponding decrease in the Levelized Cost of Hydrogen (LCOH) for dry hydrogen production. By focusing on the development and optimization of high-pressure SOE systems, we can achieve more efficient hydrogen production, lower operational costs, and enhance the overall economic feasibility of CSP-based hydrogen generation

4. Within this thesis, the primary focus has been on the hydrogen (H2) production side from the electrolyzer. However, it is essential to recognize that in addition to H2, oxygen (O2) can also be obtained and potentially sold after undergoing certain gas processing. Therefore, it is highly recommended to conduct a thorough feasibility study to evaluate the viability of this business case. By examining the market potential for O2 and exploring strategies to make it competitive for sale, valuable insights can be gained. Understanding the market dynamics for O2 and its potential value will enable informed decision-making and allow for the optimization of revenue streams from the electrolyzer, considering both H2 and O2 production

Bibliography

[1] IEA. *IEA, Global hydrogen demand by sector in the Net Zero Scenario, 2020-2030, IEA, Paris*. 2022. URL: https://www.iea.org/data-and-statistics/charts/global-hydrogen-demand-by-sector-in-the-net-zero-scenario-2020-2030,%20IEA.%20License:%20CC%20BY%204.0 (visited on 10/26/2022).

[2] Walter H.Scholz. "Processes for industrial production of hydrogen and associated environmental effects". In: *Gas separation Purification* 7.3 (1993), pp. 131–139.

[3] IPCC. *Global warming of 1.5 °C*. 2018. URL: https://www.ipcc.ch/sr15/.

[4] IRENA. "Green Hydrogen - Guide to policy making". In: (2020).

[5] Hydrogen council. "Path to hydrogen competitive ness- cost perspective". In: (2020).

[6] KPMG. *The Hydrogen trajectory*. 2020. URL: https://home.kpmg/xx/en/home/insights/2020/11/the-hydrogen-trajectory.html.

[7] R.de.Levie. "The Electrolysis of water". In: *Electroanalytical Chemistry* 476 (1999), pp. 92–93.

[8] W.Kreuter. "Electrolysis: The important energy transformer in a world of sustainable energy". In: *International Journal of Hydrogen Energy* (1998), pp. 661–666.

[9] IEA. *Electrolysers, IEA, Paris*.

[10] O.Schimdt. "Future cost and performance of water electrolysis:An expert elicitation study". In: *International Journal of Hydrogen Energy* 42 (2017).

[11] L.M.Gandia, G.Arzamendi, and Pedro. *Renewable Hydrogen Technologies*. Elsevier, 2013.

[12] Coutanceau, S.Baranton, and Audichon T. *Renewable Hydrogen Technologies*. Elsevier, 2018.

[13] M.T.Islam. "A comprehensive review of state-of-the-art concentrating solar power (CSP)technologies: Current status and research trends". In: *Renewable and Sustainable Energy Reviews* (2018).

[14] Xu. "Prospects and problems of concentrating solar power technologies for power generation in the desert regions". In: *Renewable and Sustainable Energy Reviews* 53(c) (2016), pp. 1106–1131.

[15] Amita Ummadisingu and M.S. Soni. "Concentrating solar power – Technology, potential and policy in India". In: *Renewable and Sustainable Energy Reviews* 15.9 (2011), pp. 5169–5175. DOI: 10.1016/j.rser.2011.07.04. URL: https://ideas.repec.org/a/eee/rensus/v15y2011i9p5169-5175.html.

[16] Andreas Poullikkas, George Kourtis, and Ioannis Hadjipaschalis. "Parametric analysis for the installation of solar dish technologies in Mediterranean regions". In: *Renewable and Sustainable Energy Reviews* 14.9 (Dec. 2010), pp. 2772–2783. URL: https://ideas.repec.org/a/eee/rensus/v14y2010i9p2772-2783.html.

[17] Fausto Cavallaro. "Multi-criteria decision aid to assess concentrated solar thermal technologies". In: *Renewable Energy* 34.7 (2009), pp. 1678–1685. URL: https://ideas.repec.org/a/eee/renene/v34y2009i7p1678-1685.html.

[18] A.Mohamad. "Heat losses from parabolic trough collectors". In: *International journal of energy research* 38 (2013), pp. 20–28.

[19] SOLARPACES. *Parabolic Trough projects*. 2022. URL: https://solarpaces.nrel.gov/by-technology/parabolic-trough.

[20] Giovanni Manente, Sergio Rech, and Andrea Lazzaretto. "Optimum choice and placement of concentrating solar power technologies in integrated solar combined cycle systems". In: *Renewable Energy* (2016).

[21] SOLARPACES. *Power tower projects*. 2022. URL: https://solarpaces.nrel.gov/by-technology/power-tower.

[22] H. M. Müller-Steinhagen and Franz Trieb. "Concentrating solar power, - A review of the technology". In: 2004.

[23] SOLARPACES. *Linear fresenl reflectors*. 2022. URL: https://solarpaces.nrel.gov/by-technology/linear-fresnel.

[24] Ugo Pelay et al. "Thermal energy storage systems for concentrated solar power plants". In: *Renewable and Sustainable Energy Reviews* 79.C (2017), pp. 82–100. DOI: 10.1016/j.rser.2017.03.13. URL: https://ideas.repec.org/a/eee/rensus/v79y2017icp82-100.html.

[25] SOLARPACES. *Atacama I*. 2022. URL: https://solarpaces.nrel.gov/project/atacama-i-cerro-dominador-110mw-csp-100-mw-pv.

[26] SOLARPACES. *Aalborg*. 2022. URL: https://solarpaces.nrel.gov/project/aalborg-csp-brondersl ev-csp-orc-project.

[27] SOLARPACES. *Tooele army depot*. 2022. URL: https://solarpaces.nrel.gov/project/tooele-army-depot.

[28] SOLARPACES. *SOLARPACES*. 2022. URL: https://www.solarpaces.org/.

[29] Pawel Stempien J. "Solid Oxide Electrolyzer Cell Modeling: A Review". In: ().

[30] Meng Ni, Michael K.H. Leung, and Dennis Y.C. Leung. "Energy and exergy analysis of hydrogen production by solid oxide steam electrolyzer plant". In: *International Journal of Hydrogen Energy* 32 (18 Dec. 2007), pp. 4648–4660. ISSN: 03603199. DOI: 10.1016/j.ijhydene.2007.08.005.

[31] J. Sigurvinsson et al. "Can high temperature steam electrolysis function with geothermal heat?" In: *International Journal of Hydrogen Energy* 32 (9 June 2007), pp. 1174–1182. ISSN: 03603199. DOI: 10.1016/j.ijhydene.2006.11.026.

[32] Abdullah A. AlZahrani and Ibrahim Dincer. "Modeling and performance optimization of a solid oxide electrolysis system for hydrogen production". In: *Applied Energy* 225 (Sept. 2018), pp. 471–485. ISSN: 03062619. DOI: 10.1016/j.apenergy.2018.04.124.

[33] Karittha Im-orb et al. "Flowsheet-based model and exergy analysis of solid oxide electrolysis cells for clean hydrogen production". In: *Journal of Cleaner Production* 170 (Jan. 2018), pp. 1–13. ISSN: 09596526. DOI: 10.1016/j.jclepro.2017.09.127.

[34] Amin Mohammadi and Mehdi Mehrpooya. "Techno-economic analysis of hydrogen production by solid oxide electrolyzer coupled with dish collector". In: *Energy Conversion and Management* 173 (Oct. 2018), pp. 167–178. ISSN: 01968904. DOI: 10.1016/j.enconman.2018.07.073.

[35] Luca Mastropasqua et al. "Solar hydrogen production: Techno-economic analysis of a parabolic dish-supported high-temperature electrolysis system". In: *Applied Energy* 261 (Mar. 2020). ISSN: 03062619. DOI: 10.1016/j.apenergy.2019.114392.

[36] Dohyung Jang et al. "Techno-economic analysis and Monte Carlo simulation of green hydrogen production technology through various water electrolysis technologies". In: *Energy Conversion and Management* 258 (Apr. 2022). ISSN: 01968904. DOI: 10.1016/j.enconman.2022.115499.

[37] James T. Hinkley et al. "An analysis of the costs and opportunities for concentrating solar power in Australia". In: *Renewable Energy* 57 (Sept. 2013), pp. 653–661. ISSN: 09601481. DOI: 10.1016/j.renene.2013.02.020.

[38] T. Bouhal et al. *Technical feasibility of a sustainable Concentrated Solar Power in Morocco through an energy analysis*. Jan. 2018. DOI: 10.1016/j.rser.2017.08.056.

[39] Ephraim Bonah Agyekum and Vladimir Ivanovich Velkin. "Optimization and techno-economic assessment of concentrated solar power (CSP) in South-Western Africa: A case study on Ghana". In: *Sustainable Energy Technologies and Assessments* 40 (Aug. 2020). ISSN: 22131388. DOI: 10.1016/j.seta.2020.100763.

[40] AbdullahS. "Design of a 100 MW concentrated solar power Linear Fresnel plant in Riyadh, Saudi Arabia: A comparison between molten salt and liquid sodium thermal energy storage". In: *Energy Reports* 8 (Nov. 2022), pp. 697–704. ISSN: 23524847. DOI: 10.1016/j.egyr.2022.08.055.

[41] Javier Sanz-Bermejo et al. "Optimal integration of a solid-oxide electrolyser cell into a direct steam generation solar tower plant for zero-emission hydrogen production". In: *Applied Energy* 131 (Oct. 2014), pp. 238–247. ISSN: 03062619. DOI: 10.1016/j.apenergy.2014.06.028.

[42] M. Seitz et al. “Techno economic design of a solid oxide electrolysis system with solar thermal steam supply and thermal energy storage for the generation of renewable hydrogen”. In: *International Journal of Hydrogen Energy* 42 (42 Oct. 2017), pp. 26192–26202. ISSN: 03603199. DOI: 10.1016/j.ijhydene.2017.08.192.

[43] Manuel Gruber et al. “Power-to-Gas through thermal integration of high-temperature steam electrolysis and carbon dioxide methanation - Experimental results”. In: *Fuel Processing Technology* 181 (Dec. 2018), pp. 61–74. ISSN: 03783820. DOI: 10.1016/j.fuproc.2018.09.003.

[44] K. Schwarze et al. “Operational Results of an 150/30 kW RSOC System in an Industrial Environment”. In: *Fuel Cells* (Apr. 2019). DOI: 10.1002/fuce.201800194. URL: https://doi.org/10.10022Ffuce.201800194.

[45] Günter Schiller et al. *Solar heat integrated solid oxide steam electrolysis for highly efficient hydrogen production*.

[46] Ro. Peters et al. “Long-Term Experience with a 5/15kW-Class Reversible Solid Oxide Cell System”. In: *Journal of The Electrochemical Society* 168 (1 Jan. 2021), p. 014508. ISSN: 0013-4651. DOI: 10.1149/1945-7111/abdc79.

[47] Benjamin Munz and James Hays. “Concentrating Solar Trough Modeling: Calculating Efficiency”. In: *A Burns McDonnell Publication* (2009).

[48] Office of Energy efficiency renewable energy. *2030 Solar cost targets*. 2021. URL: https://www.energy.gov/eere/solar/articles/2030-solar-cost-targets.

[49] NREL. *KVK Energy Solar Project CSP Project*. 2022. URL: https://solarpaces.nrel.gov/project/kvk-energy-solar-project.

[50] SOLARPACES. *Concentrating Solar Power*. 2022. URL: https://atb.nrel.gov/electricity/2021/concentrating_solar_power.

[51] Andrés Rodriguez-Caviedes and Isabel C. Gil-García. “Multifactorial Analysis to Determine the Applicability of Wind Power Technologies in Favorable Areas of the Colombian Territory”. In: *Wind* 2 (2 June 2022), pp. 357–393. DOI: 10.3390/wind2020020.

[52] Arne Burdack et al. “Techno-economic calculation of green hydrogen production and export from Colombia”. In: *International Journal of Hydrogen Energy* 48 (5 Jan. 2023), pp. 1685–1700. ISSN: 03603199. DOI: 10.1016/j.ijhydene.2022.10.064.

[53] Valeria Juárez-Casildo, Ilse Cervantes, and R. de G. González-Huerta. “Solar hydrogen production in urban areas of Mexico: towards hydrogen cities”. In: *International Journal of Hydrogen Energy* 47 (70 Aug. 2022), pp. 30012–30026. ISSN: 03603199. DOI: 10.1016/j.ijhydene.2022.06.137.

[54] Alessandro Giampieri, Janie Ling-Chin, and Anthony Paul Roskilly. “Techno-economic assessment of offshore wind-to-hydrogen scenarios: A UK case study”. In: *International Journal of Hydrogen Energy* (2023). ISSN: 03603199. DOI: 10.1016/j.ijhydene.2023.01.346.

[55] Shell. “Study on adding energy storage system to AWE and PV green hydrogen system”. In: (2020).

[56] Jeith Lovegrove. *Concentrating Solar Power technology*. Woodhead publishing series in energy, 2021.

[57] Energy data.info. *Global Solar atlas*. 2022. URL: https://globalsolaratlas.info/map?c=28.362402,75.849609,5&a=68.071289,23.079732,68.071289,29.764377,77.255859,29.764377,77.255859,23.079732,68.071289,23.079732.

[58] Gavin Towler and Ray Sinnott. “Chapter 2 - Process Flowsheet Development”. In: *Chemical Engineering Design (Second Edition)*. Ed. by Gavin Towler and Ray Sinnott. Second Edition. Boston: Butterworth-Heinemann, 2013, pp. 33–101. ISBN: 978-0-08-096659-5. DOI: https://doi.org/10.1016/B978-0-08-096659-5.00002-X. URL: https://www.sciencedirect.com/science/article/pii/B978008096659500002X.

[59] Mohammad Reza Tahan. “Recent advances in hydrogen compressors for use in large-scale renewable energy integration”. In: *International Journal of Hydrogen energy* (2022).

[60] Nick Power. *Hydrogen refuelling stations and the role of gas compression technology*. 2022. URL: https://www.haskel.com/en-hu/blog/hydrogen-refuelling-stations-and-the-role-of-gas-compression-technology.

[61] Peter Huang. “Humidity Standard of Compressed Hydrogen for Fuel Cell Technology”. In: *ECS Transactions* 12.1 (May 2008), p. 479. DOI: 10.1149/1.2921574. URL: https://dx.doi.org/10.1149/1.2921574.

[62] Sunfire. *GREEN HYDROGEN FOR GREEN STEEL - SUCCESSFUL PROJECT COMPLETION WITH RECORD PRODUCTION RATES OF HIGHLY EFFICIENT ELECTROLYZER*. 2022. URL: https://www.sunfire.de/en/news/detail/green-hydrogen-for-green-steel-successful-project-completion-with-record-production-rates-of-highly-efficient-electrolyzer.

[63] Patrick Lovera. “Operational Modelling of High Temperature Electrolysis (HTE)”. In: (2006).

[64] Pegah Mottaghizadeh et al. “Process modeling of a reversible solid oxide cell (r-SOC) energy storage system utilizing commercially available SOC reactor”. In: *Energy Conversion and Management* 142 (2017), pp. 477–493. ISSN: 0196-8904. DOI: https://doi.org/10.1016/j.enconman.2017.03.010. URL: https://www.sciencedirect.com/science/article/pii/S0196890417302121.

[65] Marius Tomberg et al. “Operation strategies for a flexible megawatt scale electrolysis system for synthesis gas and hydrogen production with direct air capture of carbon dioxide”. In: *Sustainable Energy Fuels* 7 (2 2023), pp. 471–484. DOI: 10.1039/D2SE01473D. URL: http://dx.doi.org/10.1039/D2SE01473D.

[66] L.M. Robeson. “Polymeric Membranes for Gas Separation”. In: (2016). DOI: https://doi.org/10.1016/B978-0-12-803581-8.03297-5. URL: https://www.sciencedirect.com/science/article/pii/B9780128035818032975.

[67] Gavin Towler and Ray Sinnott. “Chapter 16 - Separation of Fluids”. In: *Chemical Engineering Design (Second Edition)*. Ed. by Gavin Towler and Ray Sinnott. Second Edition. Boston: Butterworth-Heinemann, 2013, pp. 753–806. ISBN: 978-0-08-096659-5. DOI: https://doi.org/10.1016/B978-0-08-096659-5.00016-X. URL: https://www.sciencedirect.com/science/article/pii/B978008096659500016X.

[68] Davies Pryce Bayley D. “Process applications of knitted mesh mist eliminators”. In: *Chemical Processing* 33 (1973).

[69] Gereunda. “How to size liquid-vapor separators”. In: *Chemical Engineering* (1981).

[70] Saeid Mokhatab, William A. Poe, and John Y. Mak. “Chapter 7 - Natural Gas Dehydration”. In: *Handbook of Natural Gas Transmission and Processing (Third Edition)*. Ed. by Saeid Mokhatab, William A. Poe, and John Y. Mak. Third Edition. Boston: Gulf Professional Publishing, 2015, pp. 223–263. ISBN: 978-0-12-801499-8. DOI: https://doi.org/10.1016/B978-0-12-801499-8.00007-9. URL: https://www.sciencedirect.com/science/article/pii/B9780128014998000079.

[71] Meyer. “Mercaptans removal with molecular sieves – options and reality”. In: GPA Europe Conference.

[72] Saeid Mokhatab, William A. Poe, and John Y. Mak. “Chapter 7 - Natural Gas Dehydration”. In: *Handbook of Natural Gas Transmission and Processing (Third Edition)*. Ed. by Saeid Mokhatab, William A. Poe, and John Y. Mak. Third Edition. Boston: Gulf Professional Publishing, 2015, pp. 223–263. ISBN: 978-0-12-801499-8. DOI: https://doi.org/10.1016/B978-0-12-801499-8.00007-9. URL: https://www.sciencedirect.com/science/article/pii/B9780128014998000079.